1. Award Information

Award Number: DE-EE0006063

Project Title: Pt-based Bi-metallic Monolith Catalysts for Partial Upgrading of Microalgae Oil

Project Period: 01/07/13 – 12/31/14 ***(No-cost Extension till 12/31/14)***

Recipient: Stevens Institute of Technology
Castle Point on Hudson
Hoboken, NJ 07030
13th Congressional District

Project Location: Stevens Institute of Technology

Technical Contact: Adeniyi Lawal (PI, Stevens), (201) 216-8241, alawal@stevens.edu

Partners: Valicor Renewables, LLC (formerly SRS Energy)
7400 Newman Blvd.
Dexter, Michigan 48130
Brian Goodall (Co-PI)
(734) 253-2873

Columbia University
500 West 120th Street
New York, NY 10027
Prof. Robert Farrauto (Co-PI)

2. No distribution limitations

3. Executive Summary

Valicor's proprietary wet extraction process in conjunction with thermochemical pre-treatment was performed on algal biomass from two different algae strains, Nannochloropsis Salina (N.S.) and Chlorella to produce algae oils. Polar lipids such as phospholipids were hydrolyzed, and metals and metalloids, known catalyst poisons, were separated into the aqueous phase, creating an attractive "pre-refined" oil for hydrodeoxygenation (HDO) upgrading by Stevens. Oil content and oil extraction efficiency of approximately 30 and 90% respectively were achieved.

At Stevens, we formulated a Pt-based bi-metallic catalyst which was demonstrated to be effective in the hydro-treating of the algae oils to produce 'green' diesel. The bi-metallic catalyst was wash-coated on a monolith, and in conjunction with a high throughput high pressure (pilot plant) reactor system, was used in hydrotreating algae oils from N.S. and Chlorella. Mixtures of these algae oils and refinery light atmospheric gas oil (LAGO) supplied by our petroleum refiner partner, Marathon Petroleum Corporation, were co-processed in the pilot plant reactor system using the Pt-based bi-metallic monolith catalyst. A 26 wt% N.S. algae oil/74 wt % LAGO mixture hydrotreated in the reactor system was subjected to the ASTM D975 Diesel Fuel Specification Test and it met all the important requirements, including a cetane index of 50.5. An elemental oxygen analysis performed by an independent and reputable lab reported an oxygen content of trace to none found. The successful co-processing of a mixture of algae oil and LAGO will

enable integration of algae oil as a refinery feedstock which is one of the goals of DOE-BETO. We have presented experimental data that show that our precious metal-based catalysts consume less hydrogen than the conventional hydrotreating catalyst NiMo Precious metal catalysts favor the hydrodecarbonylation/hydrodecarboxylation route of HDO over the dehydration route preferred by base metal catalysts, and consumes less hydrogen, if methanation can be mitigated. Our methanation data on Pt and Rh indicate effective suppression of methanation. Our data also show that our catalysts are less susceptible to coking; and unlike NiMo and CoMo, precious metal catalysts are not deactivated by water, a by-product of HDO of algae oil. Finally, our catalysts do not need to be sulfided to be active.

A rigorous techno-economic analysis of our process for commercial scale production of 10,000 barrels per day of hydrotreated algae oil, with nutraceuticals co-product claiming only 0.05% of the raw algae oil, indicates an estimated plant gate price of ~$10/gal. Sensitivity analysis shows that critical parameters affecting sale price include (1) algae doubling time (2) biomass oil content (3) CAPEX, and (4) moisture content of post extracted algae residue. Modest improvements in these areas will result in enhanced and competitive economics. Based on a life cycle assessment for greenhouse gas emission, we found that if algae oil replaced 10% of the US consumption, this would result in a CO2e reduction of 210,000 tons per day. Improving the drying process for animal feed by 50% would result in further significant reduction in CO2e

4. Project Accomplishments

The following are the major accomplishments of this project:

- Developed in-house at Stevens, reliable analytical methods for obtaining the fatty acid profile of algae oils, and hydrocarbon product distribution in hydrotreated products.
- Valicor's wet extraction technology produced algae oils from two strains of microalgae, Nannochloropsis Salina (N.S.) and Chlorella, with low levels of metals, mettaloids and polar lipids which otherwise would be poisons for hydrotreating catalysts.
- The pre-refined algal oil exceeded all the set analytical specs (Nitrogen, Sulfur and Phosphorus)
- Valicor achieved oil content and oil extraction efficiency of approximately 30 and 90% respectively for Nannochloropsis Salina, the workhorse algae of the industry
- Stevens designed, constructed and operated two reactor systems for the HDO of algae oils, one a low flow rate microreactor system (for catalyst screening) and the other, a flexible high flow rate, high pressure (pilot plant) reactor system capable of operating as either a trickle-bed reactor or a monolith reactor
- *Stevens evaluated 15 catalysts for HDO of algae oils, 13 in particulate form and 2 wash-coated on a monolith*
- Stevens formulated a Pt-based bi-metallic catalyst which was demonstrated to be effective in hydrotreating of algae oils to 'green' diesel.
- The Pt-based bi-metallic catalyst was washcoated on a monolith and used successfully in hydrotreating mixtures of algae oils and light atmospheric gas oil (LAGO) supplied by our petroleum refiner partner, Marathon Petroleum Corporation
- A 26 wt% N.S. algae oil/74 wt % LAGO mixture hydrotreated in the reactor system was subjected to the ASTM D975 Diesel Fuel Specification Test and it met all the important requirements, including a cetane index of 50.5. An elemental oxygen analysis performed by an independent and reputable lab reported an oxygen content of trace to none found.
- Our experimental data below show that our precious metal-based catalysts consume less hydrogen than the conventional petroleum refining hydrotreating catalyst NiMo
- Our experimental data below show that our precious metal-based catalysts are effective in mitigating methanation which otherwise would be consuming a significant amount of H_2

- We have shown below experimentally that our precious metal-based catalysts are less susceptible to coke formation in comparison to NiMo

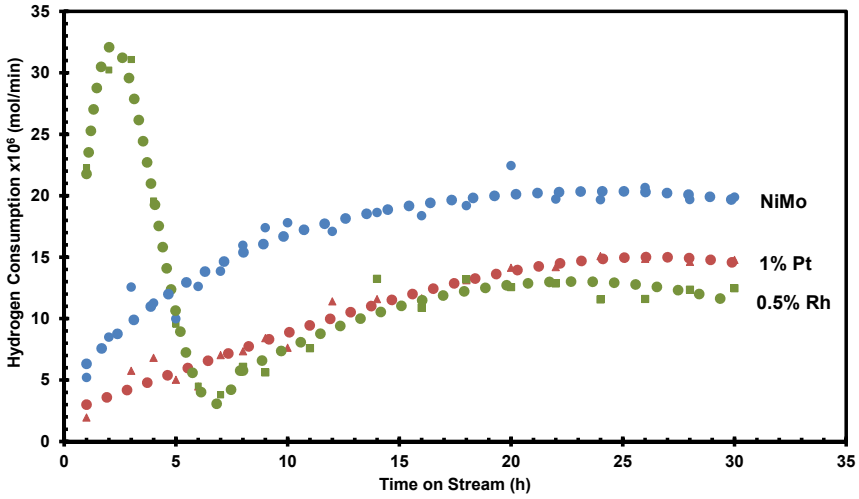

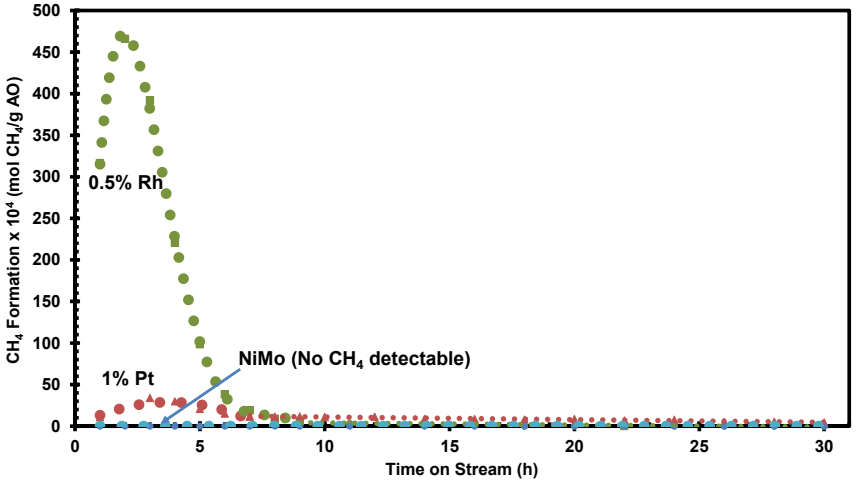

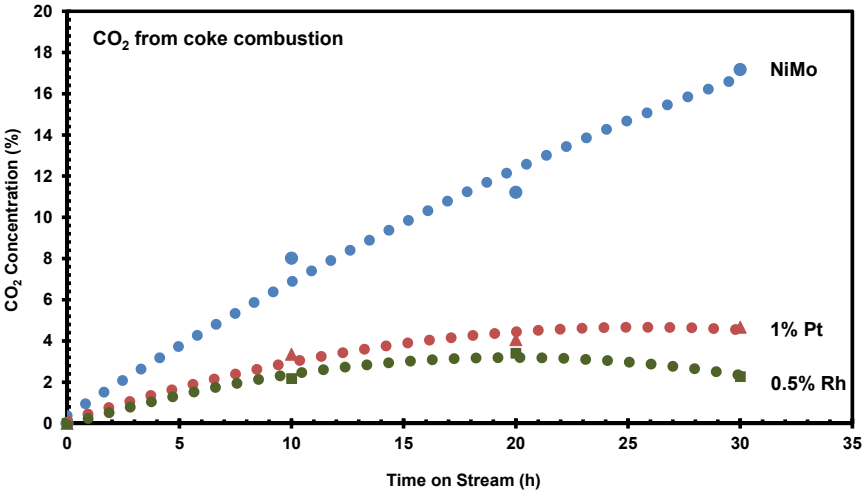

- Unlike NiMo and CoMo, precious metal catalysts are not deactivated by water, a by-product of HDO
- Unlike NiMo and CoMo, precious metal catalysts do not need to be sulfided to be active
- We secured a 'letter of intent' from Marathon Petroleum Corporation, the fourth largest refiner in the US stating their intent to work with us in the current, as well as the next phase of the project. This is an important award goal set by DOE-BETO.
- As a further demonstration of their commitment to the success of the project, MPC provided us with five gallons of refinery LAGO which was co-processed with algae oils. MPC also provided guidance on hydrotreating of algae oils
- We also secured a 'letter of intent' from Qualitas Health LLC on their interest to collaborate with us in the commercial scale growth and harvesting of microalgae
- Scoular Company expressed, in an email, their interest in working with us to evaluate the animal feed co-product from our integrated enterprise in the next phase of the project
- Completed a 'Techno-economic Analysis of Microalgae Production and Conversion into Refinery Ready Oil with Co-Product Credits
- Completed a study of the Life Cycle Assessment of our integrated process

5. Project Activities

Task 1: Chemical and Physical Characterization of Process Streams (Stevens & Valicor)

I. Summary

As indicated in Figure 1.1, there are four process streams involved in our hydro-deoxygenation process; two gas streams and two liquid streams, with each stream requiring its own characterization method. The gas stream, either feed or product was analyzed using GC-TCD while the hydrocarbons in the liquid product were identified and quantified via GC-FID. Elemental analysis (CHNS) was performed by Robertson Microlit Laboratories, LLC, Ledgewood NJ while oxygen analysis was carried out by MidWest MicroLab LLC, Indianapolis, Indiana. Valicor Renewables performed both acylglycerides and fatty acid analyses of the algae oil samples used in the project. Stevens also developed an analytical procedure based on a method provided by Synthetic Genomics Inc. to determine the fatty acid profile of both liquid feed and liquid product. New Jersey Food Lab (NJFL), an analytical lab with national reputation was used to confirm the fatty acid profile from Valicor, and Stevens when deemed necessary.

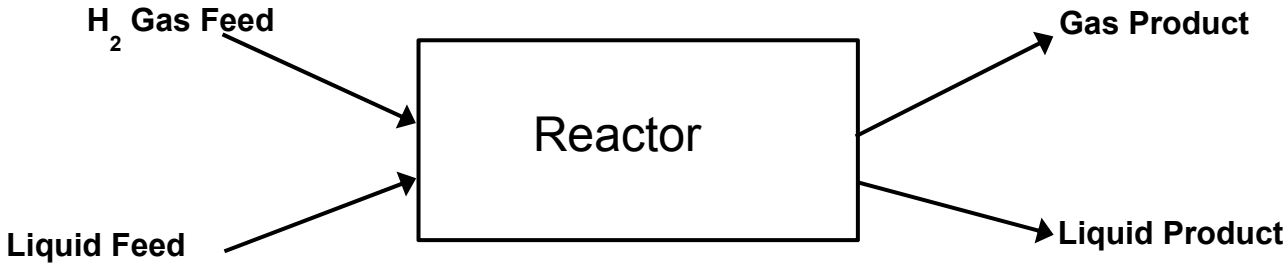

Figure 1.1: Process streams for the HDO of algae oil

II. Gas Feed and Gas Product Analysis

Although the gas feed for the hydro-treating experiments was pure hydrogen, H_2/N_2 mixture was used for catalyst reduction (see Task 3 below) and in the first few hours of the hydro-treating experiment, it was not unusual to detect N_2 in the product gas because it took quite some time for all the N_2 to be purged from the system during the hydro-treating experiment. In addition to H_2 and N_2, the gas product could contain other gases, namely CO, CO_2, and CH_4, which are products of hydro-treating (see Fig. 1.4 below). An analytical method was developed for detecting and quantifying all these gases. Gas stream, either the feed or the product, was analyzed and quantified using Shimadzu GC-14B with a thermal conductivity detector (TCD) and two capillary columns (MS-5A and HP-Plot Q). Calibration curves were prepared using standard mixtures of the gases at low molar composition of H_2 in conjunction with known metered gas mixtures at high molar composition of H_2. Propane (C_3H_8), although a product of hydrogenolysis (Fig. 1.4 below), was not included in the product analysis.

III. Elemental Analysis of Liquid Feed and Liquid Product

III.1. CHNSP Analysis of Nannochloropsis Salina Algae Oil

The CHNSP elemental compositional analysis of liquid streams was performed by Robertson MicroLit Laboratories, LLC (Ledgewood, NJ). All the algae oils processed in this project were supplied by Valicor Renewables, LLC. The project started with algae oil extracted from the Nannochloropis Salina (N.S.) algae strain, considered as the workforce of the algae industry. The results of the elemental analysis of the Nannochloropsis Salina algae oil are shown in Table 1.1 below.

Table 1.1: Elemental Analysis of Nannochloropsis Salina Algae Oil

C (wt %)	76.29
H (wt %)	11.22
N (wt %)	0.43
S (ppm)	2033
P (ppm)	246
O (wt %)	12.06

The oxygen content was obtained by difference, and this approach is usually reliable at high values of oxygen content. For accurate determination of oxygen content at low values (< 2wt%), we relied on the services of another analytical lab, MidWest MicroLab LLC, Indianapolis, Indiana which has developed a method capable of accurately determining oxygen content to levels as low as 0.3 wt%. The results are presented and discussed in Task 3 below.

III.2. Analysis of Metal Content of Chlorella Algae Oil

In addition to Nannochloropsis Salina, another commonly grown algae strain, Chlorella was processed for oil production in this project. The Chlorella biomass was provided by Arizona State University to Valicor, which used their wet hexane extraction platform (see Task 2 below) to extract the oil. The analyses of algae oils were expanded by Valicor to include metals. Measuring the metal content in the oil is important since they are potent catalyst poisons.

As can be seen in Table 1.2, Valicor's thermochemical pre-treatment process results in oil with dramatically lower metal levels than oil obtained by a wet hexane extraction without thermochemical pre-treatment. In particular, the phosphorous content decreased from 407 ppm to <0.2 ppm and the iron content decreased from 540 ppm to 0.6 ppm. The sulfur content declined by about 30%, but sulfur (like oxygen) is readily removed in the hydro-treating step. These data demonstrate that thermochemical pre-treatment helps to hydrolyze the bonds that attach fatty acids and glycerides to metal-containing groups, as would occur in phospholipids, for example. The acidic conditions of the pre-treatment step also help to dissolve other metals like iron into the water phase and away from the hexane-oil mixture. Overall, Valicor was very pleased with the enhanced extraction process and had begun implementation of scale up to larger quantities of oil using this extraction process. Indeed an acceptable oil for hydro-treating must contain less than 20ppm total metals and metalloids with iron and phosphorous being the major contaminants in these categories: As indicated in Table 1.2, iron and phosphorus total almost 1,000ppm in the native algae oil, but <0.8ppm in the Valicor extracted oil.

Table 1.2: Metal content in *Chlorella* oils extracted with and without Valicor's pre-treatment

Element	Units	Oil Sample

		Valicor pre-treatment + extraction	Low temp. bead milling + extraction
Phosphorus	Ppm	<0.20	407.0
Iron	Ppm	0.6	540.0
Sulfur	Ppm	84.8	120.0

IV. Compositional Analysis of Liquid Feed and Liquid Product

IV.1. Compositional Analysis of Nannochloropsis Salina (N.S.) Algae Oil

The analysis for glycerides content of Nannochloropsis Salina algae oil was performed by Valicor Renewables, LLC. The detailed composition as obtained by Valicor is given in Table 1.3 below:

Table 1.3: Composition of the Algae Oil

Fatty Acid	Monoacylglycerides, MAG (wt%)	4.41	
	Diacylglycerides, DAG (wt%)	4.56	
	Triacylglycerides, TAG (wt%)	29.23	
	Free Fatty Acid, FFA (wt%)	9.25	
		47.45	Total Fatty Acid (wt%)
	Chlorophyll a&b (wt%)	0.78	
	Carotenoids (wt%)	0.46	
Solvent	Hexane (wt%)	0.05	
	Water (wt%)	0.86	
	Total	49.6	Total Identified Compounds (wt%)

The water content of N.S. was determined by Karl Fischer (K-F) titration, and was performed by Robertson Microlit Laboratories. It should be pointed out that only 49.6 wt% of the microalgae oil was initially identified and quantified.

In an effort to account for the remainder of the Nannochloropsis Salina algae oil, at Stevens we carried out vacuum filtration on the oil and it was determined that about 11.8 wt% of the oil was solids, the biomass that was not removed during the oil extraction step. Further, an ash analysis by Robertson Microlit Laboratories showed a small amount of about 0.34 wt%, bringing to ~62 wt% all the components that had been accounted for. The remaining 38wt%, we suspected, was constituted in part by residual polar lipids which were not completely hydrolyzed. These polar lipids would include phospholipids, glycolipids and betaine lipids. These lipids ordinarily should be saponifiable, and should therefore be captured by fatty acid analysis but the fatty acid profile (see Section IV.2.1 below) did not appear to reflect their presence in significant amount. Based on the elemental analysis of the crude algae oil, the phospholipids content is not expected to be more than 1wt%. If the origin of the sulfur in the crude algae oil is the glycolipid SQDG (Sulfoquinovosyldiacylglycerol), then it is possible for the glycolipid content to be as high as 5%. Crude fat analysis by NJFL (New Jersey Food Lab), an internationally renowned lab for oil analysis gave 86 wt% which combined with the 50 wt% from fatty acid profile (see section IV.2.1 below), will indicate that about 36 wt% of the crude algae oil is ‘unsaponifiable,’ a value that is pretty close to 38 wt%, the portion of the oil that compositional analysis did not account for.

To investigate further if the unknown components were polar lipids, e.g. glycolipid SQDG, a sample of the algae oil was sent to a lab in Germany, Spectral Service AG which specializes in the use of NMR for lipid analysis. The sulfur content of our algae oil is 2033 ppm by weight which would imply a minimum of 2 wt% SQDG, an amount that must be visible in the 13C NMR. However, it was not detected thus prompting Spectral Service AG to conclude that the source of the sulfur was not organic. They also confirmed that the amount of polar lipids in our algae oil was very small (Phospholipds < 0.1 wt%, MGDG and DGDG not present in the spectra). However, they detected and quantified cholesterol and manitol. Combining all the results of the various analyses, the composition of the Nannochloropsis Salina algae oil is presented in Table 1.4.

Table 1.4: Oil Compounds in Algae Oil from Nannochloropsis Salina (w/w%)

• Monoacylglycerides	4.41
• Diacylglycerides	4.56
• Triacylglycerides	29.23
• Free Fatty Acids	9.25
Total Fatty Acids	47.45 wt%
• Cholesterol	~5.0
• Manitol (sugar alcohol)	~1-5
• Solids	11.8
• Chlorophyll a&b	0.78
• Carotenoids	0.46
Total solvent residues	0.05
Water content (KF titration)	0.86
• Unknown (Unsaponifiable Matter)	28.6 – 32.6 wt%

Based on all the results of the analyses, it was concluded that the 'unknowns' are not polar lipids but material that should be rightly classified as 'Unsaponifiable Matter.'

Our experience with the analysis of the glycerides content of Nannochloropsis Salina, and FAME analysis of both Nannochlorposis Salina and Chlorella indicates that different strains of algae produce oils with different glycerides content. The main advantage of N.S. over Chlorella is the high oil content achievable with N.S. but the oil from Chlorella has very high glycerides content, and unlike the oil from N.S. which is semi-solid and opaque at room temperature, the Chlorella algae oil is transparent and flows easily at room temperature. These factors need to be taken into consideration when selecting an algae strain for production of biofuel.

IV.2. FAME Analysis of Liquid Feed and Liquid Product

IV.2.1. FAME Analysis of Nannochloropsis Salina Algae Oil Feed

FAME (Fatty Acid Methyl Ester) analysis of N.S. algae oil was carried out with a GC-FID after sample derivatization. The sample derivatization (esterification) method was developed by Valicor Renewables, and the resulting fatty acid profile is shown in Table 1.5a.

Table 1.5a: Fatty Acid Profile (by Valicor)

Compounds	Relative Basis (w/w %)	Sample Basis (w/w %)
C14:0 Myristic	4.45	2.19
C14:1 Myristoleic	0.07	0.04
C16:0 Palmitic	24.76	12.21
C16:1n7 Palmitoleic	32.28	15.91
C16:2 Hexadecadienoic	0.00	0
C18:0 Stearic	0.83	0.41
C18:1 –cis Oleic	6.18	3.05
C18:1 –trans Vaccenic	2.23	1.1
C18:2 Linoleic	1.94	0.96
C18:3 Linolenic	0.09	0.04
C20:0 Arachidic	0.12	0.06
C20:1 Eicosenoic	0.07	0.03
C20:2n6 Eicosadienoic	0.78	0.38
C20:3n6 Homogamma Linolenic	0.00	0
C20:4n6 Arachidonic	2.91	1.43
C20:3n3 Eicosatrienoic	7.14	3.52
C20:4n3 Eicosatetraenoic	0.00	0
C20:5n3 Eicosapentaenoic	15.54	7.66
C22:0 Behenic	0.15	0.07
C21:5n3 Heneicosapentaenoic	0.09	0.05
C24 Lignoceric	0.21	0.1
C24:1 Nervonic	0.09	0.05
C22:4n6 Docosatetraenoic	0.00	0
C22:5n6 Docosapentaenoic	0.00	0
Other	0.07	0.04
	100.00	**49.30**

Valicor's fame analysis was confirmed by independent fame analysis carried out by NJFL at the instance of Stevens, and the results are shown below in Table 1.5b for comparison.

Table 1.5b: Fatty Acid Profile (by NJFL)

Fatty Acid Profile	C# : Dbl. Bonds	Relative Basis %	Sample Basis %
Caprylic	8:0	0.35	0.19
Capric	10:0	0.28	0.15
Lauric	12:0	0.35	0.19
Myristic	14:0	3.50	1.93
Myristoleic	14:1	0.17	0.10
Pentadecanoic	15:0	0.31	0.17
Palmitic	16:0	19.64	10.85

Palmitoleic	16:1	26.49	14.64
Hexadecadienoic	16:2	0.23	0.13
Heptadecanoic	17:0	0.25	0.14
Stearic	18:0	0.66	0.36
Oleic	18:1ω9	5.50	3.04
Oleic	18:1ω7	2.03	1.12
Linoleic	18:2ω6	1.34	0.74
Linolenic	18:3ω6	0.70	0.39
Octadecatetraenoic	18:4ω3	0.16	0.09
Eicosatrienoic	20:3ω6	0.13	0.07
Arachidonic	20:4ω6	2.61	1.44
Eicosapentaenoic (EPA)	20:5ω3	13.38	7.39
Docosapentaenoic	22:5ω6	0.09	0.05
Other	n/a	21.84	12.07
		100.00	**55.25**

The obtained fatty acid profile (from Valicor) in conjunction with the elemental analysis of the algal oil by Robertson Microlit Laboratories enabled us to calculate the elemental composition of the unidentified (or unsaponifiable) portion of the microalgae oil. The results are presented in Table 1.6 below:

Table 1.6: Elemental Composition of Identified and Unidentified Parts of N.S. Algal Oil

		Based on whole microalgae oil	Elemental composition with respect to the two parts of the algal oil
Fatty Acids	C	37.50%	49.16%
	O	5.86%	48.56%
	H	5.90%	52.57%
Un-identified	C	38.79%	50.84%
	O	6.20%	51.44%
	H	5.32%	47.43%

The table above indicates that the unidentified portion of algal oil has nearly the same elemental composition as the fatty acids, but with a slightly higher degree of unsaturation.

IV.2.2. FAME Analysis of Chlorella Algae Oil Feed

The algal biomass (from Chlorella) provided to Valicor by ASU was analyzed for its lipid content, and the oil extracted was analyzed to determine the fatty acid profile. Extracted algal oils were catalytically trans-esterified and analyzed by GC-FID to determine the identity of the lipids. FAMEs were identified based on retention time using a standard mix. The results were verified by an independent analytical lab (NJFL) and were found to be in ± 3% agreement. The total lipid content of the biomass was 33.5%. The fatty acid profile of the extracted oil as reported by NJFL is presented in Table 1.7 and corresponds to the lipid profile of the biomass.

Table 1.7: Fatty Acid Profile for Chlorella 1201.

Report: Stevens Institute Extraction		
Sample Source	ASU	
Strain Type	Chlorella	
Sample	**ASU Chorella Pre-Refined oil**	
Valicor Renewables	FAME Content (% of total FAMEs)	FAME content (wt.% in oil)
C14:0 Myristic	0.18	0.16
C14:1 Myristoleic	nd	nd
C 15:0 Pentadecylic	0.12	0.10
C 15:1 Pentadecenoic	nd	nd
C16:0 Palmitic	21.48	18.48
C16:1n7 Palmitoleic	2.58	2.22
C16:4 Hexadecatetraenoic	1.41	1.21
C 17:0 Heptadecanoic	0.22	0.19
C 17:1 Heptadecenoic acid	5.66	4.87
C18:0 Stearic	1.07	0.92
C18:1 cis/trans	30.16	25.95
C18:2 Linoleic	19.01	16.36
C18:3n6 gamma-linolenic acid	nd	nd
C18:3n3 alpha-linolenic acid	12.25	10.54
C20:0 Arachidic	0.18	0.16
C20:1n9 Eicosenoic	0.10	0.09
C20:2 Eicosadienoic	nd	nd
C20:3n6	nd	nd
C21:0 Heneicosanoic	nd	nd
C20:4n6 Arachidonic	nd	nd
C20:3n3 Eicosatrienoic	nd	nd
C20:5n3 Eicosapentaenoic (EPA)	nd	nd
C22:0 Behenic	nd	nd
C22:1 Erucic	0.08	0.07
C22:2 Brassic	nd	nd
C23:0 Tricosanoic acid	nd	nd
C24:0 Lignoceric acid	nd	nd
C22:6n3 Docosahexaenoic	nd	nd
C24:1n9 Nervonic	nd	nd
Other	5.48	4.27
% FAME in Oil	100.0	85.6

The total fatty acid content of 85.6 wt% (Table 1.7) for Chlorella algae oil should be compared to 55.25 wt% obtained by the same lab, NJFL, for Nannochloropsis Salina algae oil (Table 1.5b).

IV.2.3. FAME Analysis of Liquid Product

Identification and quantification of fatty acids in both the reactor feed and product solution are required for the calculation of lipids conversion. In order to facilitate the calculation of the lipids conversion from the experimental hydro-treating data, an in-house method needed to be developed at Stevens. Therefore, Stevens adapted for implementation a FAME analysis procedure provided to us by Synthetic Genomics Inc., using our existing lab equipment. For confidentiality reasons, the details of this procedure cannot be disclosed. Minor modifications were made to the procedure for microalgae oil samples based on experience and trial-and-error experiments. In this FAME analysis method, external standards were used for peak identification, and internal standards for derivatization efficiency check and quantification. Sample preparation is of vital importance to convert all lipids detectable by GC-FID and was evaluated by the mentioned derivatization efficiency. Two case studies are reported to illustrate the analysis.

IV.2.3.1. Development of GC-FID Method Using External Standards

All the GC-FID setting parameters are listed below:

GC: Varian 450GC
Column: SP2560 column (100 m x 0.25 mm x 0.20 μm)
Oven: 140 ^{o}C (5 min.), 4 ^{o}C/min. to 240 ^{o}C (30 min.)
Injector: 250^{o}C
Detector: FID, 280 ^{o}C
Carrier gas: Helium, Constant flow: 1.8ml/min
Injection: 1ul, 1:20 split

Due to the complexity of the fatty acid profile (FAP) of microalgae oils used in our lab, an SP-2560 capillary column (L×I.D. 100 m×0.25 mm, d_f 0.20μm) was selected for FAME analysis. This highly polar biscyanopropyl column was specifically designed for detailed separation of geometric positional (cis/trans) isomers of FAME, and it has been shown to be extremely effective for FAME isomer analysis.

Minor modifications were made to a GC-FID method provided by Supelco (ref. 1), to obtain better peak shape and resolution. These modifications mainly pertain to the adjustment of oven temperature program and carrier gas flow rate. Also, a 15-min column baking at 240 ^{o}C was added due to the existence of impurities in microalgae oil.

Three qualitative external standard solutions were used for retention time FAME identifications. Figure 1.2 shows the chromatogram of Food industry FAME mix solution from our Varian 450GC. Compared with the reference chromatogram provided by the manufacturer of FAME mix, Restek, analysis time was decreased by roughly 13 minutes without adversely affecting resolution. Also, peak shape and area integration were checked to confirm that the GC-FID system comprising both the instrument and software, was performing well. Table 1.8 shows the components in the Food industry FAME mix.

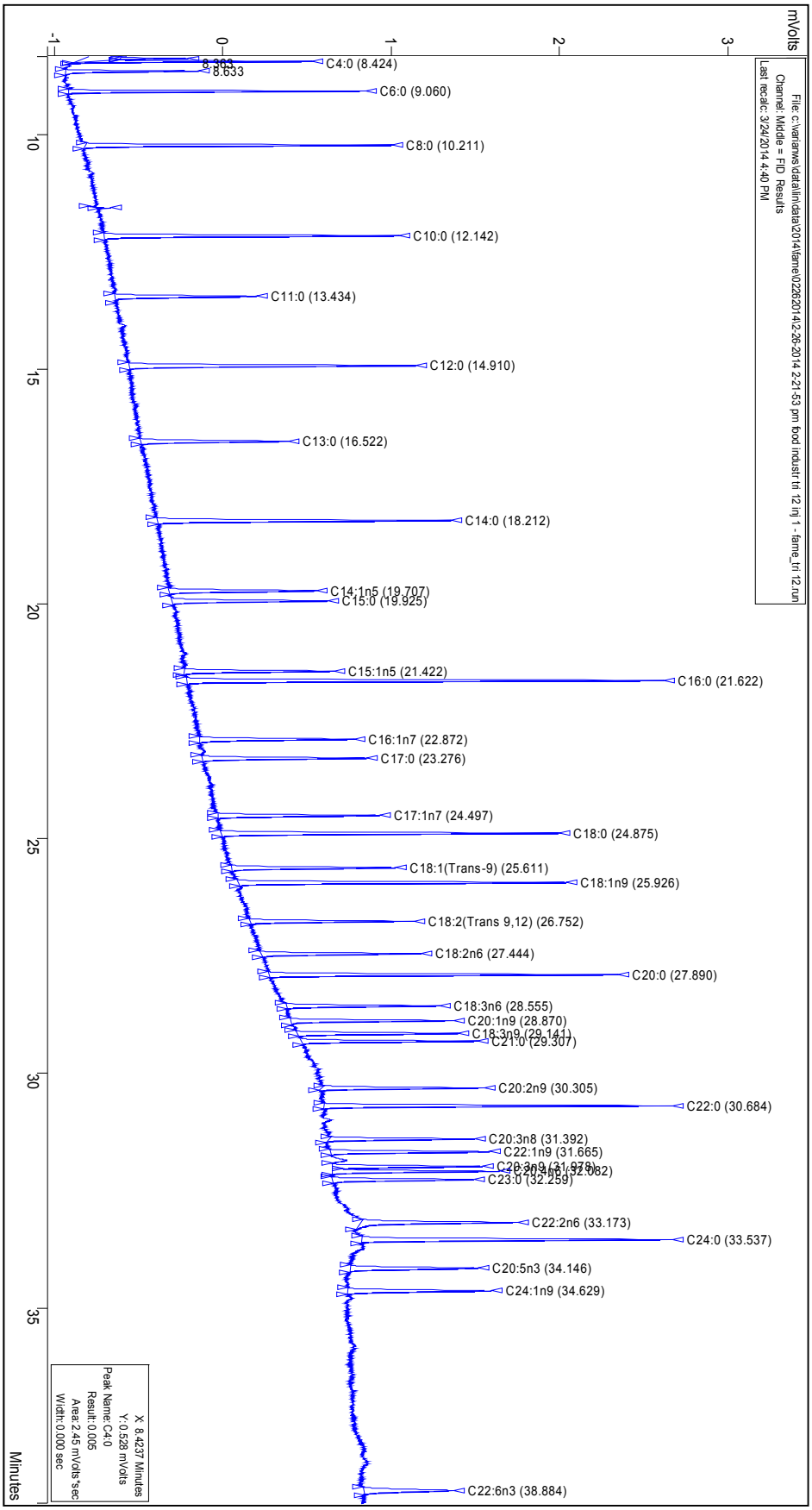
mVolts
-1
0
1
2
3
File: c:\varianws\data\in\data\2014\fame\022820142-26-2014 2-21-53 pm food industr tri 12 inj 1 - fame_tri 12.run
Channel: Middle = FID Results
Last recalc: 3/24/2014 4:40 PM
C4:0 (8.424)
8.363
8.633
C6:0 (9.060)
C8:0 (10.211)
C10:0 (12.142)
C11:0 (13.434)
C12:0 (14.910)
C13:0 (16.522)
C14:0 (18.212)
C14:1n5 (19.707)
C15:0 (19.925)
C15:1n5 (21.422)
C16:0 (21.622)
C16:1n7 (22.872)
C17:0 (23.276)
C17:1n7 (24.497)
C18:0 (24.875)
C18:1(Trans-9) (25.611)
C18:1n9 (25.926)
C18:2(Trans 9,12) (26.752)
C18:2n6 (27.444)
C20:0 (27.890)
C18:3n6 (28.555)
C20:1n9 (28.870)
C18:3n9 (29.141)
C21:0 (29.307)
C20:2n9 (30.305)
C22:0 (30.684)
C20:3n8 (31.392)
C22:1n9 (31.665)
C20:3n9 (31.978)
C20:4n6 (32.082)
C23:0 (32.259)
C22:2n6 (33.173)
C24:0 (33.537)
C20:5n3 (34.146)
C24:1n9 (34.629)
C22:6n3 (38.884)
10
15
20
25
30
35
Minutes
X: 8.4237 Minutes
Y: 0.528 mVolts
Peak Name: C4:0
Result: 0.005
Area: 2.45 mVolts*sec
Width: 0.000 sec

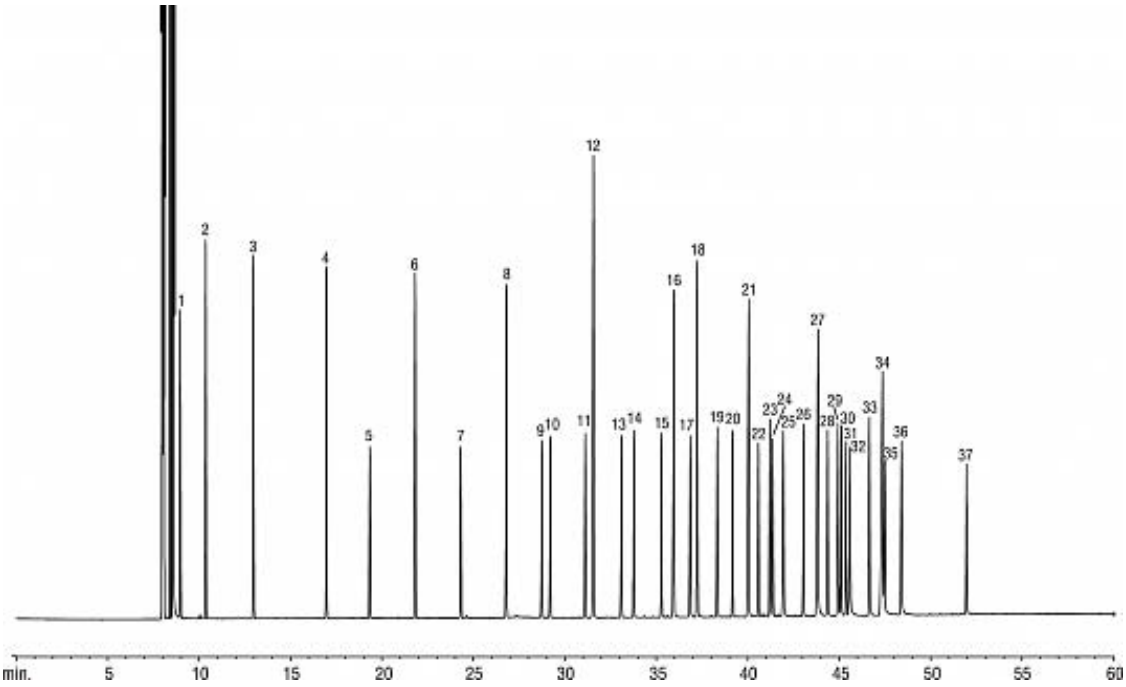

Figure 1.2: Chromatogram of Food Industry FAME mix from (a) our lab (b) reference: http://www.restek.com/chromatogram/view/GC_FF00649/prod::6098

Table 1.8: Composition of Food Industry FAME

Peak	FAME	Peak	FAME
1	C4:0 Methyl butyrate	20	C18:2 Methyl linoleate (cis-9,12)
2	C6:0 Methyl hexanoate	21	C20:0 Methyl arachidate
3	C8:0 Methyl octanoate	22	C18:3 Methyl γ-linolenate (cis-6,9,12)
4	C10:0 Methyl decanoate	23	C20:1 Methyl eicosenoate (cis-11)
5	C11:0 Methyl undecanoate	24	C18:3 Methyl linolenate (cis-9,12,15)
6	C12:0 Methyl laurate	25	C21:0 Methyl heneicosanoate
7	C13:0 Methyl tridecanoate	26	C20:2 Methyl eicosadienoate (cis-11,14)
8	C14:0 Methyl myristate	27	C22:0 Methyl behenate
9	C14:1 Methyl myristoleate (cis-9)	28	C20:3 Methyl eicosatrienoate (cis-8,11,14)
10	C15:0 Methyl pentadecanoate	29	C22:1 Methyl erucate (cis-13)
11	C15:1 Methyl pentadecanoate (cis-10)	30	C20:3 Methyl eicosatrienoate (cis-11,14,17)
12	C16:0 Methyl palmitate	31	C20:4 Methyl arachidonate (cis-5,8,11,14)
13	C16:1 Methyl palmitoleate (cis-9)	32	C23:0 Methyl tricosanoate
14	C17:0 Methyl heptadecanoate	33	C22:2 Methyl docosadienoate (cis-13,16)
15	C17:1 Methyl heptadecenoate (cis-10)	34	C24:0 Methyl lignocerate
16	C18:0 Methyl stearate	35	C20:5 Methyl eicosapentaenoate (cis-5,8,11,14,17)
17	C18:1 Methyl elaidate (trans-9)	36	C24:1 Methyl nervonate (cis-15)
18	C18:1 Methyl oleate (cis-9)	37	C22:6 Methyl docosahexaenoate (cis-4,7,10,13,16,19)

19	C18:2 Methyl linoleaidate (trans-9,12)		

IV.2.3.2. Sample Preparation (ref. 2)

The GC can be used to analyze fatty acids either as free fatty acids or as fatty acid methyl esters. There are two compelling reasons for analyzing free fatty acids as fatty acid methyl esters. First, in their free, underivatized form, fatty acids may be difficult to analyze because these highly polar compounds tend to form hydrogen bonds, leading to adsorption issues. Reducing their polarity through derivatization may make them more amenable for analysis. Second, to distinguish the slight differences in behavior exhibited by unsaturated fatty acids, the polar carboxyl functional groups must first be neutralized. This then allows column chemistry to perform separations by boiling point elution, and also by degree of unsaturation, position of unsaturation, and even the cis vs. trans configuration of unsaturation. Therefore, before the fatty acid group of lipids can be analyzed by GC, it is necessary to convert them to low molecular weight non-polar derivatives, such as methyl esters. Peak shape and resolution are greatly improved at the same time.

Based on the independent fatty acid profiles analyzed by NJFL and Valicor, three internal standards were chosen to check derivatization efficiency and validate component quantification. Negative control runs were done at different conditions to check purity of all chemicals used and ensure that there was no contamination by reaction vials, caps, stirring bars etc. The results showed that all supplies met the GC analysis requirement. Due to the high sensitivity of chromatographic analysis, only small amounts of material are required. Therefore, all analytes needed to be diluted according to their expected oil content to make the peak area of the main measured peak the same magnitude as that of the internal standard peaks.

A two-step reaction was conducted to convert all lipids and free fatty acids into FAME. The first step is transesterification of lipids. KOH in MeOH, and internal standards were added to diluted oil sample in a glass vial with PTFE cap. Magnetic stirring bar was added after vortex-mixing the solution. The glass vial was well sealed with Teflon tape. Then, the vials were heated for a period of time. If the reaction time was prolonged unduly or if too strong an alkaline solution was used, some isomerization of double bonds could occur. The second step is esterification of free fatty acids which requires the addition of BF3 in MeOH as catalyst. Reaction was carried out under heating and stirring. The Teflon tape used to seal the cap of the vial must be checked all the time to ensure that there was no leakage. When the vials cooled down to room temperature, heptane was added and the contents of the vials vortex-mixed for FAME extraction. Then, NaCl solution was added to enhance phase separation. By adding brine, the solubility of FAME in water would be decreased, and more FAME would partition into the organic phase, which would enhance the extraction efficiency. In addition, the salting out effect of brine helped to remove trace amounts of water and anything water soluble from the organic layer. Organic and aqueous layers with solids were separated efficiently by centrifuging the vials content. Then only the top layer of the organic phase was transferred to GC-vials for analysis.

IV.2.3.3. Data Analysis

As mentioned earlier, the internal standards were added to check the derivatization efficiency. Therefore, we performed the calibration of our GC-FID by preparing a mixture containing respective FAMES, and dissolving the mixture in heptane at 7 different concentrations, and the results of this calibration are shown below in Table 1.9:

Table 1.9: Calibration of Three Internal Standard-derived FAMEs.

FAME 1		FAME 2		FAME 3	
Conc. (g/g)	**Peak Area**	**Conc. (g/g)**	**Peak Area**	**Conc. (g/g)**	**Peak Area**
0.000982	330806	0.000976	356669	0.000983	384620
0.000335	109217	0.000565	201822	0.000922	357158
0.000872	284779	0.000314	107953	0.000598	223691
0.000590	193762	0.000867	312170	0.000319	120359
0.000423	137122	0.000762	260412	0.000877	338346
0.001186	382087	0.000407	136152	0.000595	223190
0.000798	258001	0.001134	386204	0.000311	115872

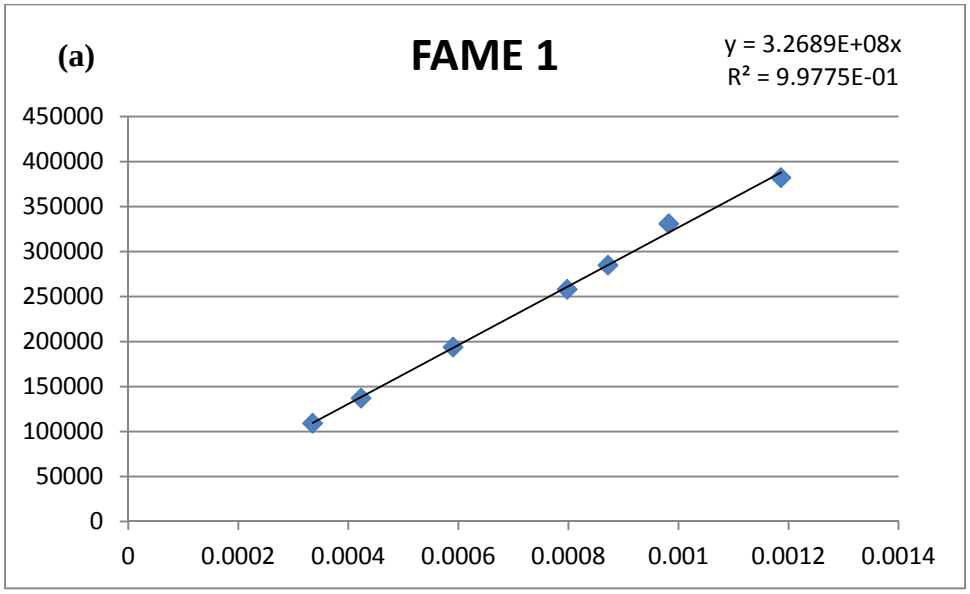

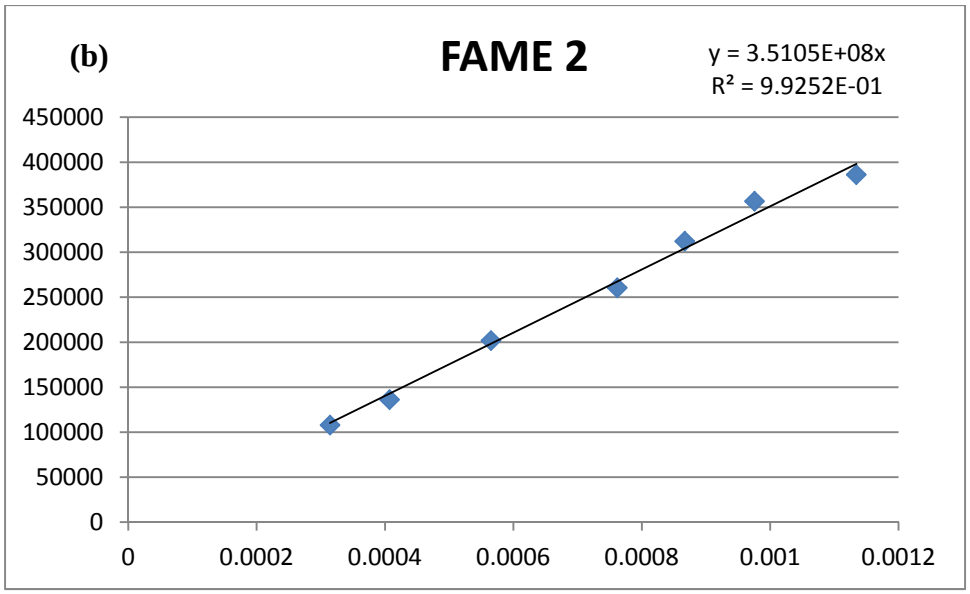

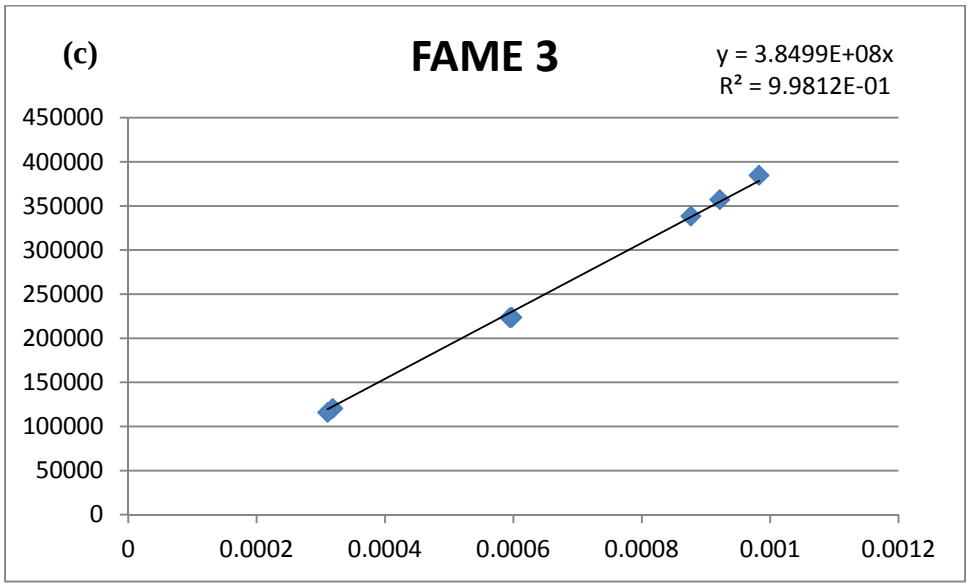

Figure 1.3: Calibration curves for the three internal standard-derived FAMEs

Single point internal standard, which was FAME 3, was used for FAME quantification due to the diverse nature of FAME. Since response factor is defined as the ratio between a signal produced by an analyte, and the quantity of analyte which produces the signal, the internal response factor can be similarly defined as below:

$$IRF = \frac{\frac{Area_{SC}}{Amount_{SC}}}{\frac{Area_{IS}}{Amount_{IS}}}$$

IRF : Internal Response Factor

IS : Internal Standard

SC : Specific Compound of Interest

Therefore,

$$\text{Amount}_{\text{SC}} = \frac{IRF_{SC} \times Area_{SC} \times Amount_{IS}}{Area_{IS}}$$

As shown in Fig. 1.3, the response factors of FAME 1, FAME 2, and FAME 3 are given by the slopes of the corresponding plots.

Table 1.10: Response factors of FAME 1, FAME 2, and FAME 3

Response Factor (RF)	
FAME 1	3.2689×10^{8}
FAME 2	3.5105×10^{8}
FAME 3	3.8499×10^{8}
Internal Response factor (IRF)	
FAME 1	0.8491
FAME 2	0.9118
FAME 3	1.0000

As reported in ref (3), the response factor of FAME increases as the number of carbon atoms increases. Based on these calibration data, we assumed a linear increase of IRFs with increase in carbon number; and the internal response factor of each FAME was thus calculated. It is necessary to perform this calibration each time a FAME analysis is undertaken. IRF tables need to be updated for each batch of FAME analysis.

IV.2.3.4. Case study I: Fatty Acid Profile of Nannochloropsis Salina Oil

An important parameter that should be used as a check on the reliability of the procedure is the relative amount of two compounds. We compare our preliminary results with FAP from Valicor and NJFL (New Jersey Food Lab) by comparing two adjacent FAMEs in Table 1.11. With the exception of C20:5n3, the values of the ratio are close for a majority of the FAMEs.

Table 1.11: Comparison of Fatty Acid Profile of Nannochloropsis Salina (Ratios of adjacent compounds are in second row)

	C14:0	**C16:0**	**C16:1N7**	**C18:1N9**	**C18: 2N6**	**C20:4N6**	**C20:5N3**
Valicor	2.19	12.21	15.91	3.05	0.96	1.43	7.66
		5.57534	1.30303	0.19170	0.31475	1.48958	5.35664

NJFL	1.93	10.85	14.64	3.04	0.74	1.44	7.39
		5.62176	1.34931	0.20765	0.24342	1.94595	5.13194
450GC	2791	16167	22139	5424	1512	4149	9832
		5.79255	1.36939	0.24500	0.27876	2.74405	2.36973

Because the area ratios were not within the theoretical value range, further improvement in GC calibration and modification of sample preparation needed to be explored.

IV.2.3.5. Case study II: Conversion Calculation

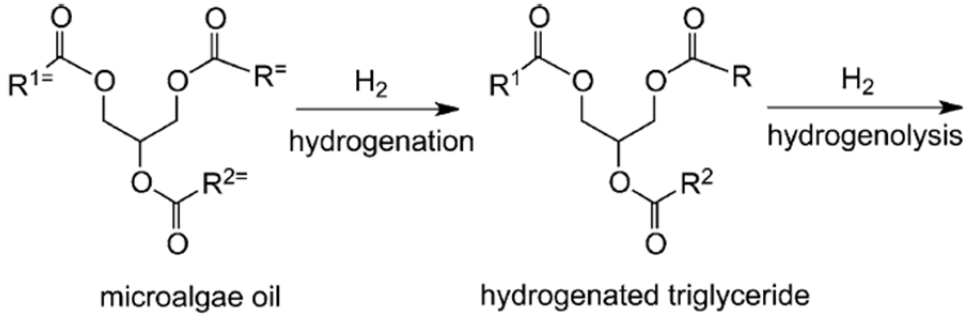

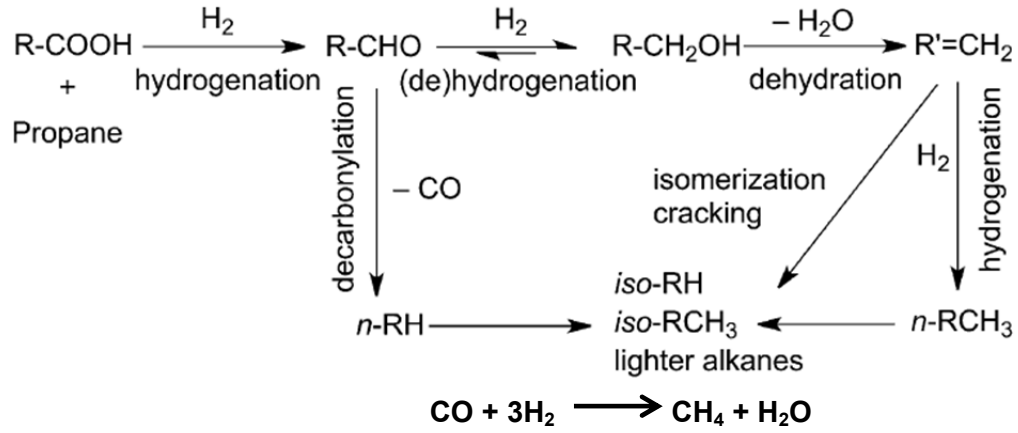

Figure 1.4: Reaction pathway of hydrotreating of triglycerides (ref. 4)

In the reaction pathway above (Fig. 1.4), the saturation of double bonds in the alkyl chain is fast, and the hydrogenolysis of saturated triglycerides is slower. The fatty acid hydrogenation step is the rate-limiting step. Therefore, we can assume fatty acids as the starting reactant, and the conversion calculated based on fatty acids. The product sample selected for conversion calculation has a hydrocarbon yield of 52.34%. As reported above (see Section IV.2.1), this yield is based on the saponifiable content of the algae oil. Three chromatograms are needed: (1) direct injection of product solution (2) feed solution after sample preparation (3) product solution after sample preparation. Whatever peaks appeared in the first chromatogram would not be fatty acids, and all the other peaks in the third chromatogram should be further compared with the second chromatogram. Then, peaks that did not change from the second to the third chromatogram were recognized as impurities or noise peaks. As a result, all FAME peaks were identified in both the second and third chromatograms and their areas integrated by the workstation automatically. The amount of each FAME was obtained by dividing each peak area

by its IRF listed in Table 1.10. Then the conversion was obtained as the difference in FAME amount between feed and product divided by the amount of FAME in the feed. The conversion for this particular sample was 62.08%. Again, this value was based on the saponifiable part of the algae oil. Compared with hydrocarbon yield of 52.34%, the 15.69% mass loss was mainly due to: (i) the loss of oxygen in transforming fatty acids into hydrocarbon, (ii) the gas product formation, and (iii) production of intermediates.

More work was done to improve the analysis thus enabling us to successfully determine the algae oil conversion for the performance study of the HDO of a mixture of Nannochloropsis Salina and dodecane as another case study (see Task 3 below).

IV.3. Liquid Product Analysis for Hydrocarbons

In Section IV.2.3 we presented an analytical method that we developed and implemented at Stevens for fatty acid profile analysis. The new method required that we modified our old GC-FID method for hydrocarbon quantification. Here, the new method is presented.

Based on the detailed fatty acid composition of the microalgae oil, the expected products of hydrodeoxygenation include C13-C24 alkanes, but with the C15-C20 alkanes as the more prominent components. Therefore, the liquid product mixture was analyzed by GC/MS and GC-FID. Using heptane as internal standard, six FID calibration curves were generated from 5 standards with respect to C15-C20 alkanes. The concentration ratio between analyte and internal standard was plotted on the horizontal axis while the peak area ratio was plotted on the vertical axis. Additional information generated from calibration was the retention time of each compound, with which we identified the peaks from the unknown samples. The unknown samples were quantified based on these calibration curves.

Due to the uncertainty about the presence of polar lipids in the algae oil, three modifications were made to liquid product analysis. Firstly, since the acyl groups in polar lipids were not discernible from the obtained fatty acid profile, heptane was not used as internal standard, in case it was one of the produced alkanes. Secondly, to minimize manual errors, the CP-8400 Auto-sampler was used for sample injection. Moreover, reproducibility test was done before each batch of sample analysis using a standard hydrocarbon mixture to ensure that the instrument was in good working order. Finally, C13 and C14 hydrocarbons were added to the alkane analysis. FID parameters are shown in Table 1.12.

Table 1.12: FID parameters

GC-FID			
Column	ZB-HT Capillary Column (30m×0.25mm×0.25um)		
Injector Temperature	250 ^{o}C		
Split Ratio	Splitless		
Column Flow	Constant Flow, 1ml/min		
Column Oven	Initial temperature (^{o}C)	Rate (^{o}C /min)	hold time (min)
	45		2
	300	10	7

Eight calibration curves, corresponding to C13 through C20 alkanes were generated by the GC software. The unit of horizontal axis is g HC/g sample, while the vertical axis is peak area.

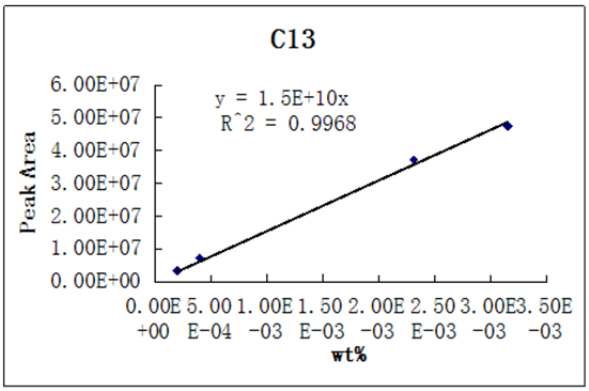

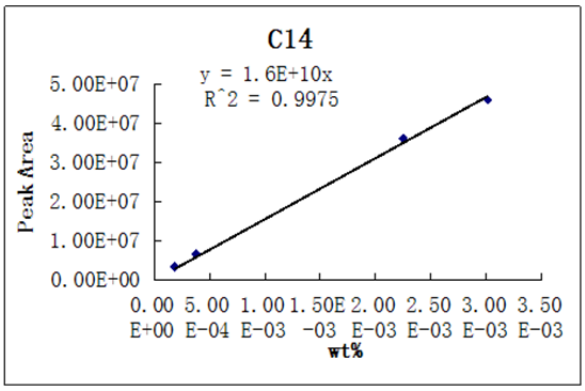

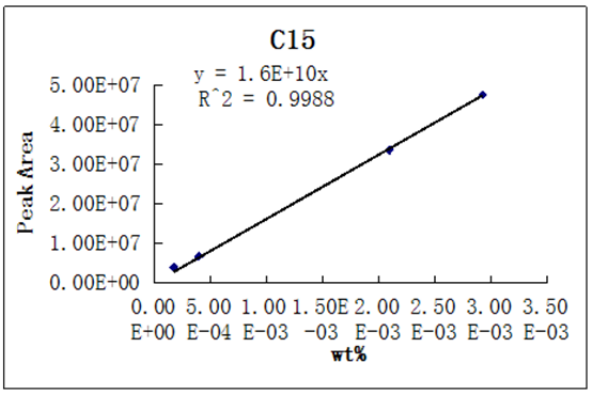

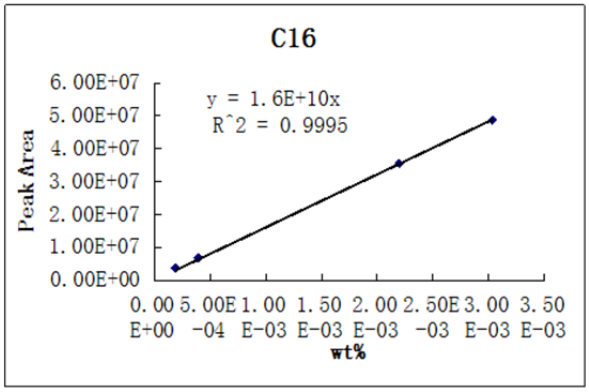

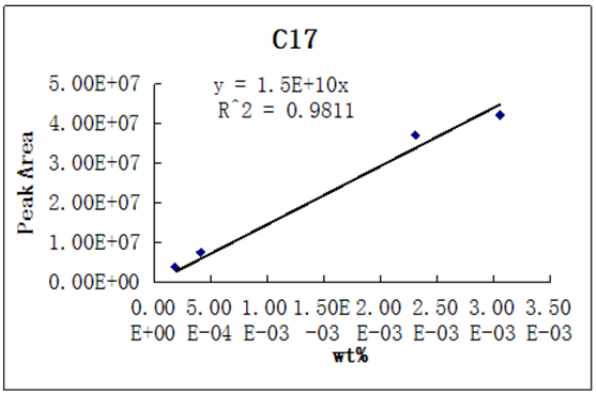

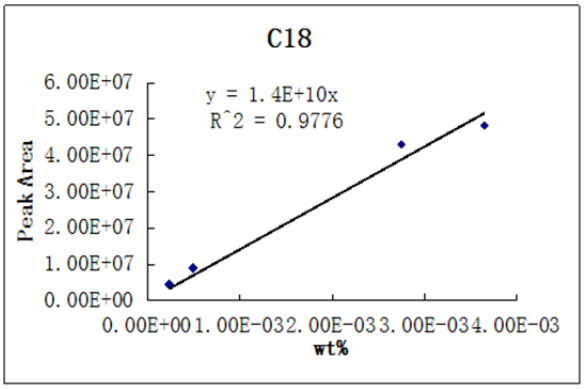

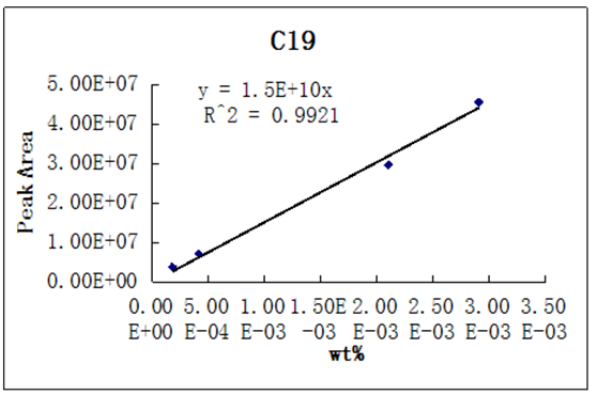

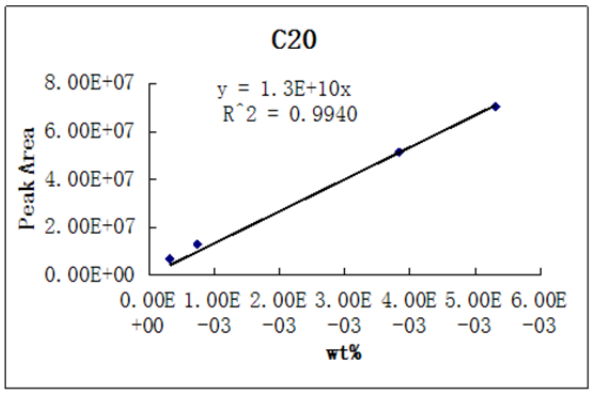

Figure 1.5: FID Calibration Curves for C13 – C20 Hydrocarbons

In the course of developing the new hydrocarbon quantification method, it was discovered that the non-polar capillary column, ZB-1HT, that we used in the past was not compatible with the fatty acids analysis procedure we developed at Stevens in Section IV.2.3. Therefore, it was replaced with a polar capillary column, SP-2560. We modified the hydrocarbon quantification method to ensure that the peaks of all the 8 targeted hydrocarbons were well separated, and the shapes well defined. All the GC parameters are as listed below:

GC: Varian 450GC
Column: SP2560 column (100 m x 0.25 mm x 0.20 μm)
Oven: 50 ^{o}C (1 min.), 15 ^{o}C/min. to 240 ^{o}C (5 min.)
Injector: 250^{o}C
Detector: FID, 240 ^{o}C
Carrier gas: Helium, Constant flow: 1.8ml/min
Injection: 1ul, 1:20 split

An analysis of a previous product sample was carried out with the new GC column, and the results are summarized in Table 1.13. The standard error was less than 0.4%, which indicated that the modified GC-FID system was reliable for hydrocarbon quantification.

Table 1.13: Confirmation of GC-FID Reproducibility

	Hydrocarbon Yield	Carbon Yield in Hydrocarbon
ZB-1HT	9.15%	10.21%
SP-2560	9.76%	10.89%
Standard Error	0.31%	0.34%

V. References

(1) http://www.sigmaaldrich.com/china-mainland/zh/analytical-chromatography/gas-chromatography/fatty-acid-methyl-ester/fame-capillary-columns/fame-mix-100m-sp2560.html

(2) AOCS lipid library: http://lipidlibrary.aocs.org/GC_lipid/04_deriv/index.htm

(3) F. Ulberth, R. G. Gaberning and F. Schrammel, Fame-ionization detector response to methyl, ethyl, propyl and butyl esters of fatty acids, JAOCS, vol. 76, November 2, 1999.

(4) B. Peng, Y. Yao, C. Zhao, J. A. Lercher, Angew. Chem. Int. Ed. 2011, Towards quantitative conversion of microalgae oil to diesel range alkanes with bifunctional catalysts.

Task 2: Extraction, Fractionation & Purification of Algal Oil (Valicor)

I. Summary

For this project, algae oil was extracted by Valicor Renewables from two microalgae strains, namely Nannochloropsis Salina (N.S.) and Chlorella, using their proprietary wet extraction technology. At the initial stage of the project, the N.S. algae biomass was provided to Valicor by CEHMM, New Mexico and later by Qualitas Health Inc., a nutraceutical company that became an industrial partner in this project upon invitation by Valicor. Qualitas now grows algae on a commercial scale in open raceway ponds in Texas. Valicor has also embarked on the establishment of a commercial algae farm in San Diego, California. The Chlorella algae biomass was provided to Valicor by Arizona Center for Algae and Technology Innovation (AzCATI) at Arizona State University. The algae oil extracted by Valicor was low in metals, mettaloids, and polar lipids that otherwise would cause catalyst deactivation during the hydrotreating process. Extraction efficiency as high as 90% was achieved.

II. Processing of Algae Biomass for Algal Oils

II.1. Nannochoropsis Salina from CEHMM, New Mexico

Nannochloropsis salina was grown and harvested in open ponds in Carlsbad, NM by CEHMM which is currently operating two 1/8th acre open raceway ponds and three 1/4th acre ponds with a maximum production capacity of nearly 1.4M liters of algal culture. To create the first fully integrated biorefinery at this facility, CEHMM partnered with Valicor Renewables to operate a patent pending (US2010/0233761; US2011/0086386) AlgaFrac™ algal oil extraction unit (Figure 2.1). The unit can process 100kg/day of biomass with a high lipid yield and low energy requirements. At the beginning of this project, 20 kg algal biomass (Nannochloropsis Salina) was grown in the open raceway ponds. The algal biomass was dewatered to 12% w/w by sequential chemical flocculation and centrifugation. Wet extraction of the algal biomass was performed using heat and chemical conditioning pretreatment step followed by a physical extraction with a non-polar solvent (hexane). The solvent was then recovered by distillation and recycled. During this process polar lipids such as phospholipids are hydrolyzed and metals, known catalyst poisons, are separated to the aqueous phase creating an attractive “pre-refined” oil for HDO upgrading. The aqueous phase is recycled back to supplement algae cultivation nutrients. At the initial stage of the project, a 1.2kg sample of the pre-refined oil was analyzed (see Task 1) and provided to Steven’s Institute for hydro-treating in Task 3. Later in the project, larger quantities of Nannochloropsis Salina oil, with the same target of low metals and high lipid, were made available to Stevens, which enabled the production in sufficient quantity for ASTM diesel testing, of a hydro-treated mixture of algae oil and refinery light atmospheric gas oil (LAGO) from Marathon Petroleum Corporation.

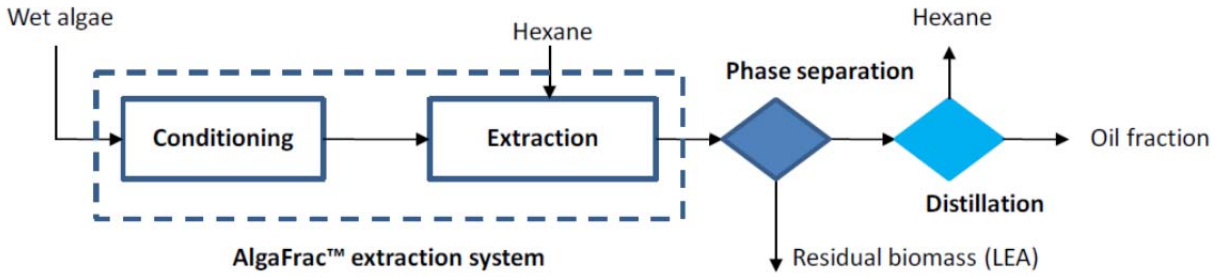

Figure 2.1: Schematic of AlgaFrac™ process

We obtained an oil extraction efficiency of greater than 80%. On the basis of many runs with this particular biomass over several years we see an extraction efficiency of around 83%. With multiple passes, we obtained efficiencies of >>90%. The actual extraction efficiency in commercial practice will be determined on the basis of oil value versus operating costs of multiple passes and/or longer residence times.

In batch operation we typically dispose of the spent water (since extractions occur remotely from the algae production facility), however in operation at an algae production facility the hexane is thoroughly stripped from the aqueous layer and the resulting water is utilized (with ZERO water discharge) as recycle water to the growth system or sent to anaerobic digestion (with lipid extracted biomass) depending on the bio-refinery configuration.

The oil that was supplied was suitable for first stage partial hydro-treating (N<1%, S<1% and P<0.1%, all in wt. percent). Elemental analysis was carried out by Stevens (see results in Task 1).

The pre-refined algal oil appeared to meet or exceed all the analytical specs we set ourselves (N, S, P)

Performance Metrics for Task 2

	Proposed	Achieved
Extraction Efficiency	80%	90%
Nitrogen	<1 wt%	0.43 wt%
Sulfur	<< 0.1wt%	0.2wt%
Phosphorus	<0.1wt%	0.025wt%

II.2. Chlorella from Arizona Center for Algae and Technology Innovation (AzCATI)

Another algae strain utilized in this project was Chlorella. Chlorella was grown and harvested by the Arizona Center for Algae and Technology Innovation (AzCATI) at Arizona State University which is currently operating flat-panel vertical PBRs, column PBRs, open raceway ponds and ARID Raceways for algae cultivation. Our previous experience with AzCATI biomass had identified a Chlorella, strain 1201, that through specialized culturing condition produces biomass with over 30% oil content. The Chorella biomass was provided to Valicor Renewables frozen in a 28% solids paste, and oil was extracted from the paste following the procedure outlined in Section II.1. above. A sample of the pre-refined oil was analyzed in Task 1 and provided to Stevens for hydro-treating. The amount of algal oil provided was sufficient for small scale catalysis evaluation. The performance metrics were similar to those obtained for Nannochloropsis Salina.

II.3. Commercial Scale Production of Nannochloropsis Oculata by Qualitas Health, LLC.

Towards the end of the fourth quarter of the project, Qualitas Health Inc. was brought in as a technical partner. Their letter, expressing their intent to participate in the project was submitted as part of a quarterly report. Qualitas Health is a privately-held company developing high-value vegetarian food supplements and pharmaceutical ingredients based on Omega-3 oils from a

sustainable algae source. For more information about Qualitas Health, visit their website at www.qualitas-health.com.

We intensively studied the biomass supplied by Qualitas Health. While studies on experimental, and academic, algae biomass can result in promising results (high lipid content for example) it is more practical and relevant to evaluate real-world, commercial algae biomass. Our partner Qualitas provides us exactly that – algae biomass that delivers an omega-3 product (AlmegaPL see www.almegapl.com) that is being launched commercially Q3 2014. The algae are grown on a 350 acre farm in Imperial, Texas with 12 acres of ponds currently in production, 64 acres by end of 2014. Hence this represents real biomass, produced at >4 tons per day part of which will be directed to our joint project.

One of the challenges with this biomass, and most others of practical application, is that extraction results in an oil comprising not only lipids such as triglycerides, but also polar lipids (such as phospholipids) and a high level of "unknowns". Since phosphorus in the form of phospholipids is a catalyst poison one of our goals was to hydrolyze these phospholipids and remove the phosphorus into the aqueous phase and remove it from the oil layer. Secondly we needed to understand the fate/role/composition of the "unknowns" and resolve this issue. If they are converted into fuel then the problem is minor (See the results of hydro-treating of a mixture of algae oil and LAGO in Task 3). If not, then they have to be eliminated from the extracted oil, preferably not extracting them in the first case.

To this end we ramped up efforts on a new extraction process which would deliver the lipids as a clean lipid fraction and leaving the remainder of the biomass as a "char" comprising carbonaceous material derived from the LEA (Lipid Extracted Algae) and the bulk of these unknowns. Furthermore we investigated a process which delivered all the lipids as a clean FFA (free fatty acid) fraction devoid of phosphorus.

We carried out both bench scale and pilot scale extraction studies with commercial Nannochloropsis Salina biomass from our partner Qualitas. Below are shown two examples of this work, a bench scale run using ethanol and a pilot scale run using hexane. As can be seen from the data, in both cases essentially quantitative extraction of the lipids (FAME yield) and the valuable EPA component were accomplished.

A liter of the hexane extracted oil (oleoresin) was supplied to Stevens for hydro-treating studies. A process involving filtration and acid degumming was used to create this high-quality crude algae oil for upgrading. This oil worked much better in hydro-treating than previous oils that were not filtered or degummed.

Benchtop

Qualitas Nanno - Precook Ethanol Extraction — **Date** 4/8/2014

Starting material for extraction:	280.0 g wet weight		Ethanol	1 L
	23.4% solids content (%AFDW)			
	65.4 g afdw		Extraction	See notebook 211 pg. 28 for details
				Acidic Precook - Ethanol Extraction
LEA	g wet weight			
	solids content (%DW)			
	0 g Dry weight			

Sample	Total FAME Content (Ash Free wt.% of biomass)	Total FAME present (g)	EPA Content (wt.% of biomass)	EPA Content of FAMEs (wt.%)	EPA Present (g)
Biomass Pre-Extraction	11.5%	7.52	0.7%	5.4%	0.46
Lipid Extracted Material	1.4%	0	7.2%	0.1%	0

Sample	Oil Obtained (g)	Oil Yield (wt.% of Ash Free biomass)	Total FAME Content (wt.% of oil)	Total FAME present in oil (g)	EPA Content of FAMEs (wt.%)	EPA Content of oil (wt.%)	EPA in oil (g)
Oil Pass 1	20.967	32.1	34.7%	7.28	5.5%	1.91%	0.40

Total FAME Yield (% of theoretical)	**97%**
Total ARA Yield (% of theoretical)	**87%**

Pilot

Qualitas Nanno - Gen 1 Hexane - Oleoresin shipped to Niyi — **Date** 4/10/2014

Starting material for extraction:	49.8 lbs wet weight		Hexane	140 lbs
	17.8% solids content (%AFDW)			
	8.9 lbs afdw		Extraction	Precook for 1 hr at 120C
	4020.9 g afdw			Process for 30 min @ 80 C
LEA	g wet weight			
	solids content (%DW)			
	g Dry weight			

Sample	Total FAME Content (Ash Free wt.% of biomass)	Total FAME present (g)	EPA Content (wt.% of biomass)	EPA Content of FAMEs (wt.%)	EPA Present (g)
Biomass Pre-Extraction	11.5%	462.40	0.7%	5.4%	28.15
Lipid Extracted Material	5.4%		3.2%		

Sample	Oil Obtained (g)	Oil Yield (wt.% of Ash Free biomass)	Total FAME Content (wt.% of oil)	Total FAME present in oil (g)	EPA Content of FAMEs (wt.%)	EPA Content of oil (wt.%)	EPA in oil (g)
Oil Pass 1	998.9	24.8%	49.8%	497.45	6.5%	3.24%	32.33

Total FAME Yield (% of theoretical)	**108%**
Total EPA Yield (% of theoretical)	**115%**

Isaac Berzin of Qualitas Health (Valicor's commercial partner, and together with Marathon Petroleum a partner for the present project) provided more high-EPA *Nannochloropsis Oculata* for extraction. Qualitas Health is a perfect partner for our project since they have the FIRST commercial phototrophic algae farm for omega-3 oils in the US (and the World) in Imperial, TX and guarantee us large volumes of biomass and oil as our project advances to pilot scale. **http://omega3.supplysideinsights.com/~/media/Files/Nutrition/Ebooks/2014/07/07_14SSO3_July%20Report_Secure.ashx**

Also, together with our partners at Qualitas Health, we are developing an extraction technology that produces a nutraceutical coproduct, EPA, and allows us to harvest the remaining low value lipids for conversion into fuels. Initial work towards this goal was executed with promising results. The practical separation of this valuable co-product and the "fuel lipids" would render

the resulting bio-refinery more economical and enable its commercial deployment – the ultimate goal of our joint endeavors.

In parallel with the above studies we turned our attention to HTC (high temperature carbonization) as developed by Dr. Levine from Valicor. Basically the algae paste is heated to around 200 – 230°C for a few minutes resulting in carbonization of the biomass affording a char which is very simple to de-water comprising a "char" in which is embedded the lipids. We have found that the lipids can be very simply recovered with a solvent wash. HTC results with our Qualitas Nannochloropsis Salina biomass are illustrated in the following figures:

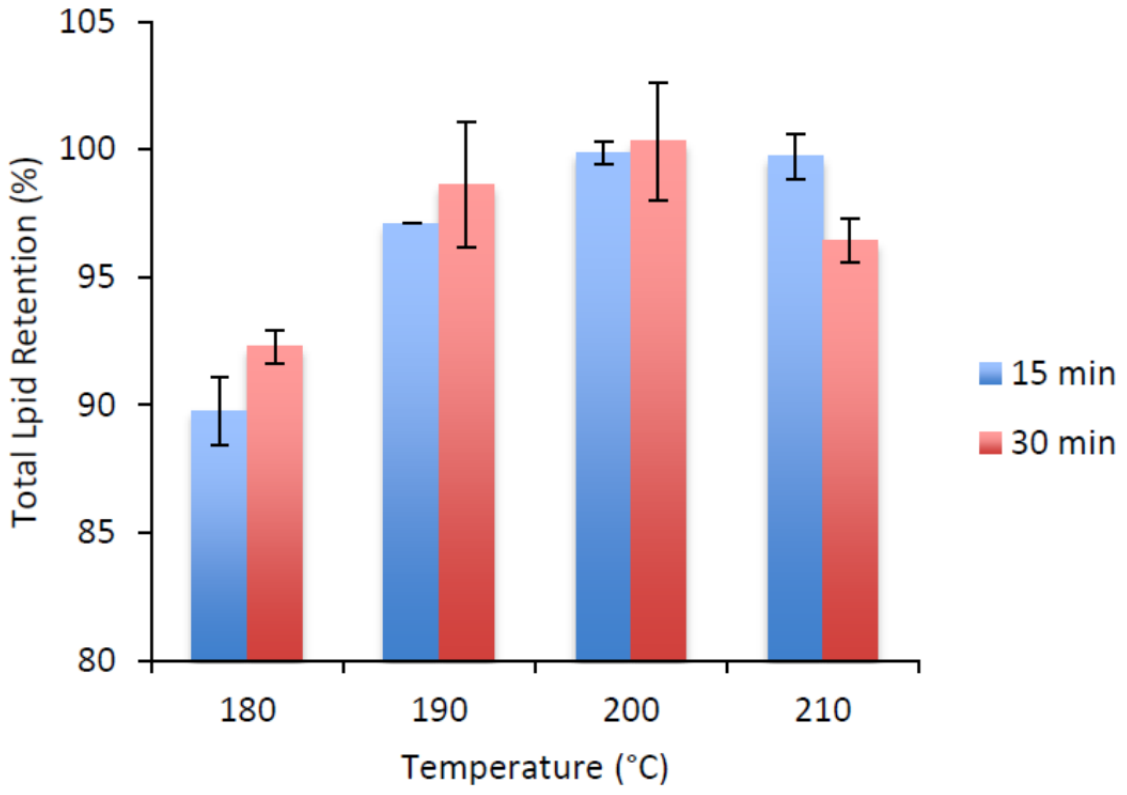

We are currently optimizing this process by investigating lipid recovery as a function of time, temperature, pH and other variables; some results being illustrated below:

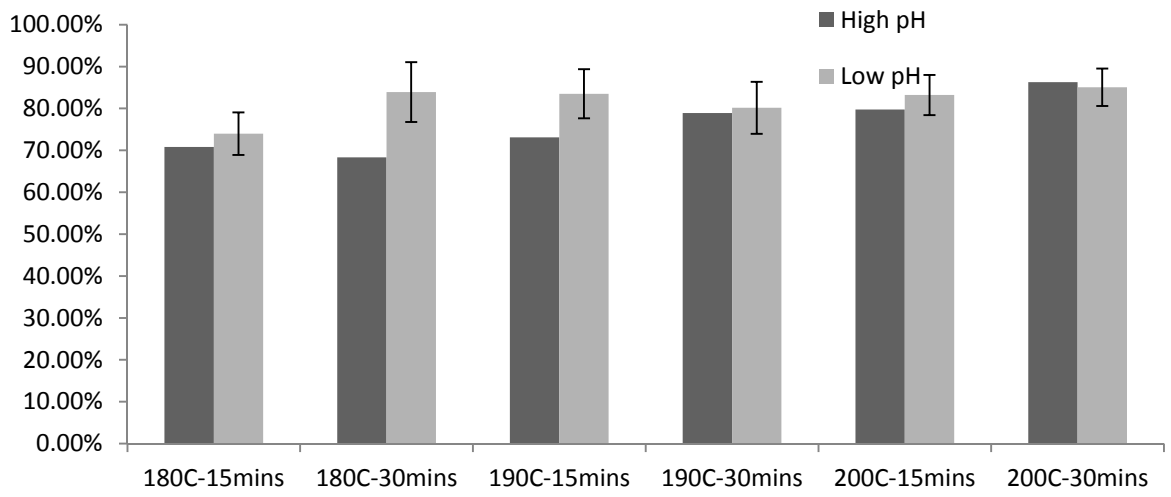

The benefits of this approach include simple dewatering, plus the delivery of light colored oil with low levels of unknowns.

III. Processing of Algae Biomass for Free Fatty Acids (FFAs)

We also pursued the concept of hydrolyzing the lipids to afford the product as FFA's from which one can separate out and isolate valuable components (such as EPA (omega-3)) and leave the remainder as a clean fraction ready for co-processing to diesel in a 5-15% blend with LAGO or VGO (Vacuum Gas Oil) or other diesel fractions to a 5-15% renewable diesel blend. Just how clean this fraction can be is shown in the following figure showing a high purity FFA product recovered by steam stripping of a crude Nannochloropsis Salina oil (the residual "unknowns" are shown in the small inverted bottle).

Task 3: Evaluation of Monolith Reactor for First Stage HDO of Algal Oil (Stevens & Columbia University)

I. Summary

In the first part of this task, an existing microreactor system was used for catalyst screening. Altogether, fifteen different catalysts, thirteen in ***particulate form***, including the conventional petroleum refining hydrotreating catalysts, sulfided NiMo and CoMo, and two washcoated on a monolith, were evaluated for their effectiveness for hydrodeoxygenation of microalgae oil. The effectiveness of a catalyst was measured by the hydrogen consumption and hydrocarbon yield. Mixtures of algae oil (N.S.) and hexane were used for catalyst screening. Temperature varied between 280 and 300^{o}C, and pressure was fixed at 500 psig. In the second part of the task, a performance study of hydrodeoxygenation of algae oil using sulfided NiMo, and two precious-metal based catalysts was conducted in the microreactor system but only the results for NiMo which have been published in a journal article are presented in details here. As of the time of submission of this report, a few of the results for the two precious metal catalysts were available for inclusion in the report while the detailed results were still being reviewed, and would be published in a journal article shortly thereafter. For the performance study, the hexane solvent was replaced by dodecane, and processing temperature varied between 300 and 360^{o}C while the pressure was fixed at 500 psig.

Based on the exhaustive catalyst evaluation, a Pt-based bi-metallic catalyst was identified to be the most effective catalyst for hydrotreating of algae oil. This catalyst was washcoated on a monolith using a coating procedure developed at Stevens. A high throughput high pressure pilot plant reactor system was designed and fabricated for evaluation of the monolith catalyst. A special sleeve was also fabricated that enabled the pilot plant reactor system to accept catalysts in particulate form. Both Nannochloropsis Salina and Chlorella algae oils were hydrotreated in this reactor system and the results are presented in the third part of this task. Because of the limited quantities of the algae oils, Canola oil was sometimes used as a surrogate for the algae oil. The processing temperature varied between 300 and 360^{o}C while the pressure was fixed at 700 psig. The pressure was selected based on the guidance from Marathon Petroleum Corporation (MPC), our petroleum refiner partner.

In the final part of this task, mixtures of algae oil and refinery light atmospheric gas oil (LAGO) supplied by MPC were co-processed in the pilot plant reactor system using the Pt-based bi-metallic monolith catalyst. Furthermore, a 26 wt% Nannochloropsis Salina algae oil/74 wt% LAGO mixture was hydrotreated in the reactor system in sufficient quantity for ASTM D975 Diesel Fuel Specification Test. The hydrotreated 'green' diesel met all the important properties including a cetane index of 50.5. The test was performed by SGS Herguth Laboratories, Inc., Vallejo, California. An elemental oxygen analysis on the same sample performed by MidWest MicroLab LLC, Indianapolis Indiana reported an oxygen content of trace to none found.

II. Catalyst Screening

Microreactors require small amount of catalyst and process feed therefore advantageous for catalyst screening. Their small size also makes process control easier compared to larger size conventional reactors. In consideration of these factors, we decided to use our existing microreactor system for catalyst evaluation which allowed us to concentrate on designing the high pressure, high throughput monolith reactor system while acquiring important reaction engineering data quickly from the microreactor system.

II.1. Preliminary Evaluation of Catalyst Performance

For the first stage of catalyst screening, only the single-metal Pt-based catalysts, namely 0.5wt% Pt, 5wt% Pt, and sulfided Ni/Mo, all supported on γ-alumina were selected for study in the microreactor. Throughout this project, sulfided Ni/Mo was used as a baseline catalyst for comparison with the Pt-based catalysts we proposed because it is the conventional hydrodesulfurization catalyst in the petroleum industry. The HDO reaction was conducted in continuous flow in a stainless steel 316 microreactor of length 12 cm and inner diameter of 775 μm. The reactor was packed with catalyst particles in the size range of 75 to 150 μm. The final reactor system would be based on a monolith catalyst and not a packed bed. The microreactor system was only used for evaluation of HDO on algal oil and catalyst screening. Once a promising catalyst was identified via catalyst screening in this section, the plan was to wash-coat such a catalyst on a monolith for exhaustive evaluation in the high pressure high throughput reactor system (see Section IV below). There are 4 criteria to be met by a catalyst for it to be effective for HDO of algal oil: it should promote: (1) Hydrogenolysis for C-O cleavage (2) Hydrogenation and (3) Decarbonylation and Decarboxylation but suppress Methanation. The hydration route consumes more hydrogen than the decarbonylation/decarboxylation route if methanation is suppressed. ***Hydrogen consumption and carbon yield*** in liquid product were the two measures used for evaluating catalyst performance.

II.1.1. H_2 Consumption

Nannochloropsis Salina algae oil of 1.0% (w/v) and 5.0% (w/v) concentrations in n-hexane were used as the liquid feed. The liquid was pumped by a HPLC pump at a rate of 0.05 ml/min. while H_2 and N_2 gases, supplied from separate cylinders, were metered through mass flow controllers and then mixed together. The inlet H_2 gas flow rate was 10.0 sccm and N_2 gas flow rate was 5.0 sccm. The gas mixture was contacted with the liquid reactant stream at a T-junction before entering the reactor. The microreactor was placed in a furnace and the reaction temperature was 283^{o}C while the pressure was set at 500 psig.

Hydrogen consumption was determined by analyzing the outlet gas stream using Shimadzu GC-14B with a thermal conductivity detector (TCD) and two capillary columns (MS-5A and HP-Plot Q). The N_2 gas feed was used to determine H_2 consumption. The injector temperature was set at 25^{o}C and detector temperature at 220^{o}C. The oven temperature was programmed as shown in Table 3.1.

Table 3.1: GC oven temperature programming

Initial temperature (^{o}C)	Rate (^{o}C /min)	Final Temperature (^{o}C)	Hold time (min)
60			13.5
	25	160	6.5

Calibration lines for N_2 and H_2 were obtained from four different gas mixtures with known compositions. These calibration lines are shown in Fig 3.1.

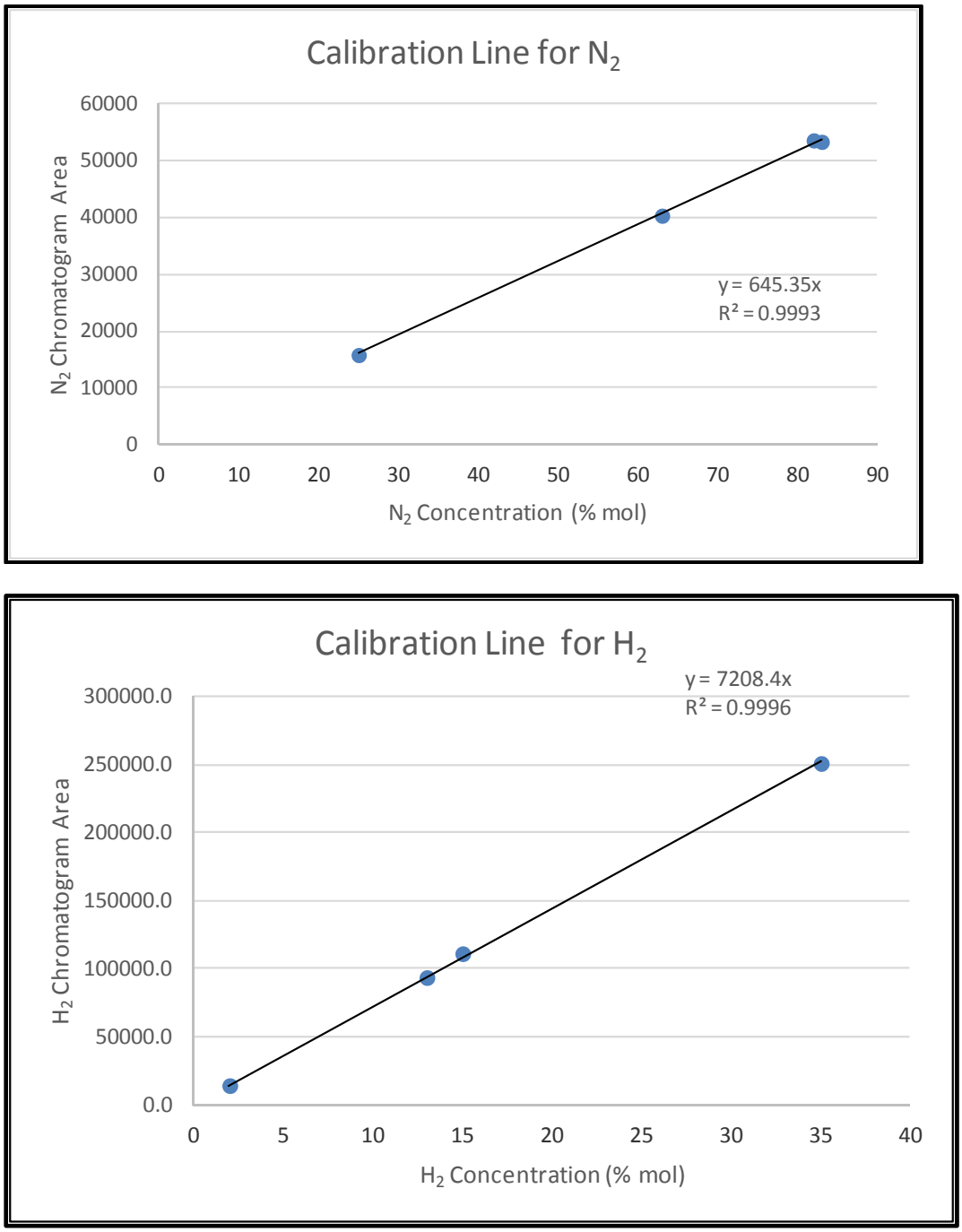

Fig 3.1: Calibration Lines for N_2 and H_2

The hydrogen consumption was normalized with the theoretical amount of H_2 required to hydrodeoxygenate the algae oil. The mass fraction of triglyceride in the algae oil was determined to be 0.475 (see Task 2). Microalgae oil has an average molecular weight of 862 (Sanchez et al., 2012). Depending upon the average number of C=C double bonds per fatty acid chain in the triglyceride, the moles of H_2 required to hydrodeoxygenate one mole of triglyceride will vary. Based on the analysis of the triglycerides in the algae oil in Task 2 above, approximately 6 moles of H_2 are required to hydrodeoxygenate each fatty acid chain (i.e., 18

moles of H_2 per mole of triglyceride). The results of the gaseous product analyses with different catalysts follow.

Table 3.2A shows the results obtained using the sulfided Ni-Mo catalyst and an inlet algae oil concentration of 1% (w/v) in n-hexane. The experimental results show that the actual H_2 consumption was much higher than the theoretical consumption based on triglycerides content in the algae oil. Some H_2 might have been consumed by the non-triglyceride portion of the algae oil. The results in the table show that H_2 consumption was less than 4% of the H_2 fed, which was very low as a percentage of the hydrogen feed. The measurement error would be more pronounced for this low consumption and might have affected the observed ratio of H_2 consumed to the theoretical hydrogen requirement.

Table 3.2A: Results of Algae Oil HDO Experiment using sulfided Ni-Mo Catalyst and 1%(w/v) Algae Oil in n-Hexane

Run Time (min)	Outlet H_2 Flow Rate (sccm)	Outlet Total gas flow Rate (sccm)	H_2 Consumption (as % of inlet)	Ratio of H_2 consumed to theoretical H_2 required based on triglycerides only
30	9.76	15.40	2.5	2.24
60	9.74	15.49	2.7	2.37
90	9.68	15.26	3.2	2.86
120	9.63	16.02	3.8	3.39

To reduce the error in measurements, we performed HDO experiments with 5% (w/v) of the algae oil in n-hexane (where the theoretical requirement of hydrogen consumption would be 5 times that of 1% solution, with other variables remaining the same) using 0.5wt% Pt supported on γ-alumina. Table 3.2B shows the results obtained.

Table 3.2B: Results of Algae Oil HDO Experiment using 0.5wt% Pt on γ-alumina and a feed of 5% (w/v) algae oil in n-hexane

Run Time (min)	Outlet H_2 Flow Rate (sccm)	Outlet Total gas flow Rate (sccm)	H_2 Consumption (% of inlet)	Ratio of H_2 consumed to theoretical H_2 required based on triglycerides only
30	9.31	16.66	6.9	1.23
60	9.28	16.69	7.2	1.29
90	9.39	16.83	6.0	1.07
120	9.23	16.61	7.7	1.38

The results show that the hydrogen consumption is more than 100% of the theoretical H_2 required based on the triglycerides only. The excess hydrogen might have been consumed by compounds in the non-triglyceride portion of the algae oil. To determine total theoretical H_2 requirement for the hydrodeoxygenation reaction, the H_2 requirement for the portion of the oil which contains non-triglyceride molecules needed also to be known. It should also be noted that the outlet gas flow rate was more than the combined inlet gas flow rate (under standard

conditions) which might be due to the presence of n-hexane in the outlet gas and some gaseous products (e.g. C_3H_8) in the outlet stream.

II.1.2. Carbon Yield

The second measure for evaluating catalyst performance was carbon yield. The parameters in Table 1.12 above, in conjunction with the GC-FID were used to determine the hydrocarbon yields. The total carbon content in Nannochloropsis Salina microalgae oil is 72.69wt% as obtained from elemental analysis, therefore the carbon yield in the hydrocarbon product can be calculated thus:

$$\text{Carbon Yield}_{\text{Based on total carbon in Microalgae oil}} = \frac{\sum_{13}^{20}\left(\frac{12n}{14n+2}\times\frac{m_{C_nH_{2n+2}}}{1g\ \text{AO}}\right)}{\left(\frac{0.7629g}{1g\ \text{AO}}\right)}$$

Similarly, from the fatty acid profile, the total carbon content in lipids is 37.5wt%, therefore the corresponding carbon yield is:

$$\text{Carbon Yield}_{\text{Based on total carbon in lipids}} = \frac{\sum_{13}^{20}\left(\frac{12n}{14n+2}\times\frac{m_{C_nH_{2n+2}}}{1g\ \text{AO}}\right)}{\left(\frac{0.375g}{1g\ \text{AO}}\right)}$$

Three catalysts were evaluated by measuring the carbon yield in the liquid product. Both the liquid and gas products were analyzed by GC-FID and GC-TCD respectively. The feed was 1g Nannochloropsis Salina microalgae oil dissolved in 100ml of n-hexane (i.e., 1 % (w/v)). The process conditions were the same as in the previous section except that the reaction temperature was varied. In addition to the microreactor, the batch reactor was also used to enable higher pressure operation since the microreactor system was limited to a maximum of 500 psig. However, it was difficult to collect gas samples, and reuse the powder catalysts in the batch reactor. A comparison of the results is summarized in Table 3.3 below:

Table 3.3: Summary of Liquid Analysis Results

	Reaction conditions		Carbon Yields [wt%]	
			Based on Total Carbon in Microalgae Oil	Based on Total Carbon in Lipids
Microreactor	NiMo	250 °C,500psi (2hrs)	9.31%	18.95%
		300 °C,500psi (2hrs)	21.42%	43.57%
	0.5wt% Pt	250 °C,500psi (2hrs)	10.93%	22.24%
		300 °C,500psi (2hrs)	25.53%	51.94%
	5wt% Pt	300 °C,500psi (2hrs)	21.32%	43.38%

Batch Reactor	NiMo	300 ^{o}C,1000psi (2hrs)	34.39%	69.95%

From this table, it can be concluded that Pt supported on γ-alumina is as good as sulfided Ni/Mo catalyst. Higher temperature and pressure expectedly increased the carbon yield. In consideration, the reactor system to be used for the evaluation of the monolith catalyst had been designed to operate at higher temperature and pressure (~ 2500 psi). In the GC/MS results of the liquid product, fatty acid and fatty acid ethyl ester (FAEE) peaks were found only in the sulfided Ni/Mo product which indicated possible C-C cleavage, an undesirable step in the catalytic HDO process.

II.2. Catalysts Evaluation for HDO of Nannochloropsis Salina Algae Oil

Altogether, eight different catalysts were evaluated for hydrotreating of Nannochloropsis Salina algae oil, all in particulate form. Catalyst performance was measured by carbon yield in the liquid product or hydrogen consumption normalized with algae oil feed. In this section, the results obtained from the following four catalysts are presented:

- **0.5wt% Pt**
- **1.0wt% Pt/1.0wt% Sn**
- **1.0wt% Pt/10.0wt% Mo and**
- **1.0wt% Pt**

all supported on γ-Al_2O_3. The catalyst screening as described in Section II.1, was conducted in a microreactor constructed from 316 SS tubing of length 12 cm and inner diameter 775 μm. The reactor was packed with catalyst particles in the size range of 75 to 150 μm. All fresh catalysts were first reduced before making any reaction run, using pure H_2 at a reactor temperature of 295^{o}C and pressure of 500 psig. The reactor feed was 11.6% (w/w) algae oil dissolved in hexane, which was obtained after filtering the 13.2% solution through VWR 410 filter paper. The feed was pumped by an HPLC pump at a rate of 0.05 ml/min. Hydrogen and nitrogen gases, supplied from separate cylinders, were metered through mass flow controllers and then mixed together in a T-junction. In most of the experiments, the H_2 flow rate was 5 sccm while that of N_2 was 2.5 sccm. A few preliminary runs were conducted using 10 sccm H_2 and 5 sccm N_2 but the results are not reported here. The nitrogen was used as a tracer gas to determine H_2 consumption. The gas mixture was contacted with the liquid reactant stream at a T-junction before entering the reactor. The mixture could also be made to bypass the reactor to release pressure from the system in case of reactor clogging. Pressures at the inlet and outlet of the microreactor were measured by pressure transducers. The microreactor was placed in a furnace. The reaction temperature was 295^{o}C while the pressure was set at 500 psig for all the experimental runs. Liquid product samples were collected for analysis from the sampling port located downstream of the reactor. The outlet gas stream was sent to a Shimadzu GC-14B GC equipped with a thermal conductivity detector (TCD) and capillary column (HP-Plot Q) for analysis. At the end of each experimental run, the reactor was flushed with nitrogen at a reactor temperature of 400^{o}C for at least one hour. This was done to prevent any operational problems, such as reactor clogging, during the run that followed.

Typically, after running the experiment for some time, the catalyst would be observed to be undergoing deactivation as indicated by reduced H_2 consumption and higher pressure drop across the reactor bed. It was assumed that coke formation was one of the sources of

deactivation and when catalyst deactivation occurred, the bed was combusted using a mixture of 80% N_2 and 20% air with the reactor temperature of 600^oC. Mixture of nitrogen and air, instead of air alone was used to minimize sintering of the catalyst and also prevent phase transformation of catalyst support from γ- to α-alumina. Carbon dioxide concentration in the combusted gas was used as an indication of the extent of completion of catalyst regeneration.

II.2.1. Carbon Yield

The liquid products from three Platinum-based catalysts were analyzed by GC-FID and the results are given in Table 3.4 below. Due to the blockage of the reactor when the 1wt% Pt/1wt% Sn was used (see Section II.2.2.2. below), no liquid sample was collected.

For the fresh single-metal Pt catalyst, when the Pt loading increased from 0.5 wt% to 1 wt%, the corresponding increase in carbon yield was 28.3%. 60 mg of 0.5wt% Pt catalyst was required to fill the microreactor while the corresponding value for the 1wt% Pt was 35 mg. The values of the effective mass of active metal are 0.3 and 0.35 mg for the 0.5 wt% Pt and 1wt% Pt respectively. The difference of 0.05 mg or 16.67% was thus consistent with the observed increase in carbon yield.

The first time a catalyst was to be evaluated, it was reduced with H_2 before the experiment was conducted. Subsequently, if the catalyst was to be re-used, reduction was not necessary. When the catalyst began to show signs of deactivation, as indicated by a reduction in catalyst activity of about 30% relative to fresh catalyst and increased pressure drop across reactor, catalyst regeneration was performed. It was assumed that one of the main causes of catalyst deactivation was coke deposition. Therefore, the regeneration process involved passing dilute air (4% O_2 and 96% N_2), a mixture of air and N_2 over the catalyst at about 600^oC to combust the coke while monitoring the CO_2 in the outlet gas. The regeneration process was assumed completed when there was no measurable amount of CO_2 in the effluent gas. According to the results of Table 3.4, the carbon yield tended to show an increase upon catalyst combustion, lending credence to the assumption that coking was one of the main mechanisms for catalyst deactivation. The activity of the single metal Pt catalyst was restored by combustion, and in many cases, enhanced compared to that of fresh catalyst.

Compared with the 1wt% Pt catalyst, the 1wt% Pt/10wt% Mo bimetallic catalyst generally produced lower carbon yields. This implies that the second metal, Mo, did not enhance the Pt activity, rather, it decreased the original activity of Pt. Moreover, studies reported in the literature suggest that, in hydrotreating, Mo enhances the dehydration route to HDO, which may consume more hydrogen per unit of hydrocarbon produced than the decarbonylation route, the route postulated to be favored by Pt. In consequence, for the same hydrogen consumption, lower amount of hydrocarbons will be produced by the Pt/Mo bimetallic catalyst. Therefore, it can be concluded that Mo is not a good promoter for hydrocarbon production unless it can be demonstrated that more oxygen is removed from the algae oil even at reduced hydrogen consumption.

Table 3.4 Summary of Liquid Analysis

Reaction Conditions	Carbon Yield [wt%] in the form of C13 to C20 HCs	
	Based on Total Carbon in	Based on Total Carbon in Lipids

		Microalgae Oil	
0.5wt% Pt	Fresh	14.91%	30.19%
	*6hr	17.46%	35.38%
	*33hr	16.81%	34.05%
	*62hr	16.82%	34.05%
	*65.5hr	17.09%	34.67%
	*67.5hr	15.56%	31.43%
	*76hr	15.48%	31.32%
	*79.5hr	18.63%	37.72%
1wt% Pt	Fresh	19.16%	38.74%
	*6hr	20.83%	42.21%
1wt% Pt/10wt% Mo	Fresh	14.37%	29.10%

Notes:

[a] Reaction Conditions: Microalgae Oil (1.0g), Hexane (10ml), 0.5wt% Pt/Al_2O_3 (60mg), 1wt% Pt/Al_2O_3 (35mg), 1wt% $Pt/10wt\% Mo/Al_2O_3$ (55mg), H_2(333psi at 300℃), N_2(167psi at 300℃). Liquid flow rate 0.05ml/min, WHSV (5 – 7.5 1/hr.)

[b] * Combustion before each experimental run.

II.2.2. Hydrogen Consumption

II.2.2.1. 0.5wt% Pt

The amount of this catalyst that could be packed into the microreactor was 60 mg. With the 0.5wt% Pt on γ-Al_2O_3 catalyst the H_2 consumption was found to average around 1.3 X 10^{-2} g of hydrogen per g of algae oil. This H_2 consumption corresponds to about 39% of the theoretical H_2 requirement, assuming that all the oil contains neutral lipids and can be hydrodeoxygenated fully following the hydrodeoxygenation route of the reaction pathways proposed by Kubicka and Kaluza, (Kubicka and Kaluza, 2010. If however, the hydrodecarbonylation route is followed, the percentage of the experimental H_2 consumption to the theoretical requirement would be much higher, 87%, since the hydrodecarbonylation route requires much lower H_2 than the hydrodeoxygenation route if methanation is successfully suppressed. Since the actual reaction pathway is expected to be a combination of the two pathways, our experimental H_2 consumption would be between 39 and 87% of the theoretical requirement.

Figure 3.2 shows the catalyst performance over time. Initially, the catalyst activity as measured by H_2 consumption was quite high and remained high for some time but after an on-stream time of about 7.5 hours, the activity decreased significantly. We continued with the experiment for many more hours but with intermittent reduction of the catalyst bed with H_2. The low activity data are not shown in Fig. 3.2. The catalyst activity did not show any improvement and eventually the reactor was clogged and nothing was flowing through it, forcing a shut-down. We presumed an association between catalyst deactivation and reactor clogging, and that both were due to deposition of coke on the catalyst. Initially, we attempted the regeneration of the catalyst by passing a mixture of 45 sccm N_2 and 5 sccm air through the reactor with the reactor temperature maintained at 260^{o}C. The gas mixture could not flow through the reactor. Since little or no gas was flowing through the reactor, the reactor temperature was then increased to 436^{o}C and the combustion gas started flowing through the reactor. The first attempt at catalyst regeneration was carried out using these operating conditions. Combustion was assumed completed when no carbon dioxide was detected in the outlet combustion gas. Mixture of nitrogen and air was used in the combustion instead of air alone to minimize any sintering of the

catalyst (active metal and support) or phase transformation of the catalytic support. After this first combustion, the catalyst almost regained its original activity. Subsequently whenever we observed deactivation, we combusted the coke in the catalyst bed using 40 sccm N_2 and 10 sccm air in conjunction with a reactor temperature of 600°C. The higher combustion temperature and higher air to nitrogen ratio were needed to complete the combustion within a reasonable time while mitigating damaging thermal effects on the catalyst. For every catalyst regeneration step (shown in Figure 3.2), outlet combustion gas was analyzed for the presence of carbon dioxide.

Figure 3.3 shows a typical chromatogram of the combustion outlet gas when carbon dioxide was present. Typically, at the optimized operating conditions of 80% N_2 and 20% air and reactor temperature of 600°C, presence of carbon dioxide in the combustion gas lasted for about 30-60 minutes after regeneration was begun. The combustion was completed when no carbon dioxide was detected for a few successive measurements.

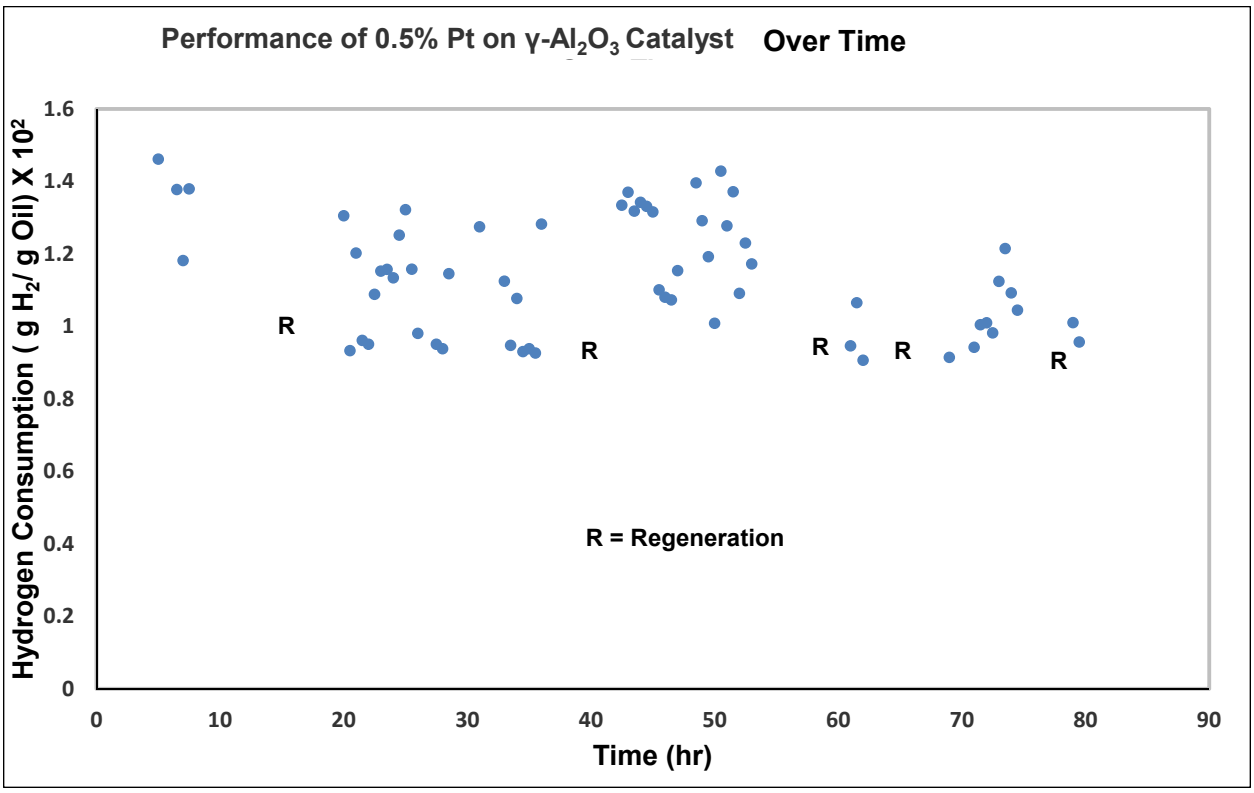

Figure 3.2: Performance of 0.5wt% Pt on Alumina over time (11.6 wt% algae oil in hexane flow rate =0.05 ml/min, inlet 5 sccm H_2, 2.5 sccm N_2, 295°C reaction temperature, 500 psig total pressure)

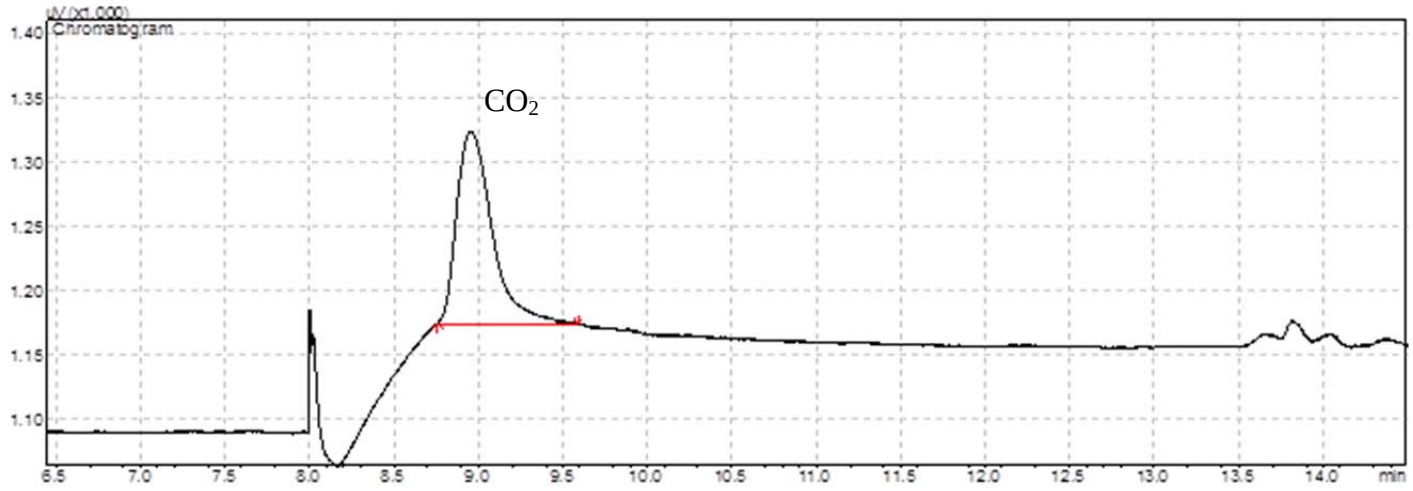

Figure 3.3: Presence of carbon dioxide in the combustion gas indicating coke formation in catalyst bed.

After combustion, the activity of the catalyst was found to be similar to that of the fresh catalyst. We regenerated this catalyst a few times and every time the catalyst was restored to close to its original activity. We operated the reactor with this catalyst for a total on-stream duration of about 80 hours. As shown in Fig. 3.2, at around 60 hours of on-stream time, we had very few steady state data. This is due to the fact that we had to change the back pressure regulator twice, and the new back pressure regulators did not control the reaction pressure properly. This resulted in wide pressure fluctuations which in turn resulted in big changes in gas and liquid slug lengths in the microreactor. Consequently, the catalyst activity was found to be very low and these low values are not reported in Fig. 3.2. When the operating conditions were properly controlled, from the data of Fig. 3.2 the catalyst was regenerated successfully many times. Even after a steady state was attained for each run, the H_2 consumption varied slightly from one measurement to the other. This variation can be attributed to the change in the ratio of gas and liquid slug lengths through the microreactor with time, probably due to some small fluctuations in operating conditions in the system.

II.2.2.2: 1.0wt% Pt/1.0wt% Sn

For this catalyst, the amount that could be packed into our microreactor was 39 mg. It appeared that the catalyst was not mechanically as strong as the 0.5wt% Pt on γ-Al_2O_3 catalyst. In our first attempt to run a reaction using the catalyst, the catalyst bed was clogged completely after 30 minutes. The clogging might be due to attrition of the catalyst particles. However, in our second attempt, using another fresh catalyst from the same batch, we could conduct the reaction but the H_2 consumption was quite low (<0.003 g of hydrogen/g algae oil) compared to that of 0.5wt% Pt catalyst, and we decided to discontinue the use of this Pt/Sn bimetallic catalyst.

II.2.2.3. 1.0wt% Pt/10.0wt% Mo

The amount of catalyst that we could pack into the microreactor was 40 mg. Its performance, in terms of H_2 consumption, was found to be somewhat lower than the 0.5wt% Pt on γ-Al_2O_3 catalyst. This is consistent with the data on carbon yield in liquid products presented in Section II.2.1. This catalyst was also prone to clogging, possibly due to attrition. We discontinued with this catalyst, but we planned to re-evaluate it in the future.

II.2.2.4: 1.0wt% Pt

For this catalyst, the amount that could be packed into the microreactor was 35 mg. The performance of this catalyst, in terms of H_2 consumption, was very similar to that of the 0.5wt% Pt on γ-Al_2O_3 catalyst. With 35 mg of this catalyst, a similar amount of H_2 was consumed as with 60 mg of the 0.5wt% Pt catalyst. We regenerated the catalyst after the catalyst began to show signs of deactivation. We then started the reaction again, however, after passing the reactant gas-liquid mixture for just over an hour through the reactor, the catalyst bed clogged completely, possibly due to attrition of the catalyst. We packed another reactor with the same amount of fresh catalyst, and performed another experimental run. The new reactor also performed similarly to the previous one in terms of H_2 consumption. After the catalyst began to show signs of deactivation, the catalyst bed was combusted and we made another experimental run with the regenerated catalyst. This time, even though there was increased pressure drop across the reactor, the reactor did not clog and we could complete the experimental run. The activity of the catalyst after regeneration was found to be similar to that of fresh catalyst.

In this section, the results of the hydrogen consumption from the four remaining catalysts are discussed. The catalysts are:

- **0.5wt% Pt/10wt% Mo**
- **10wt% Mo**
- **Sulfided NiMo and**
- **0.5wt% Rh**

all supported on γ-Al_2O_3. The reaction temperature and pressure for all the results presented in this section are 300^{o}C and 500 psig respectively. All other process conditions remained the same as for the first four catalysts.

II.2.2.5. Short Duration (~ 8 hours) Catalyst Activity Study

The activity of the catalysts for short duration run-time of approximately eight hours as measured by the hydrogen consumption is in the following order:

0.5wt% Rh (56 mg) > 0.5wt% Pt (60 mg), 1wt% Pt (30 mg) > Sulfided Ni-Mo (45 mg)

0.5wt% Pt (60mg), 1wt% Pt (30 mg) > 10wt% Mo (41mg)

0.5wt% Pt (60mg), 1wt% Pt (30 mg) > 0.5wt% Pt/10wt% Mo (60mg)

II.2.2.6. Long Term Catalyst Activity Study on Sulfided Ni-Mo and 0.5wt% Rh

Reaction runs using Ni-Mo and Rh catalysts were conducted over a long period of time to test catalyst stability. When appreciably reduced (20% or more) hydrogen consumption was observed during experimental run-time, the catalyst bed was assumed deactivated and it was subsequently regenerated by combustion with air, diluted with nitrogen (80% N_2-20% air). Both catalysts were found to regain activity close to their original values after the regeneration. Figures 3.4 and 3.5 show the catalyst activity over time.

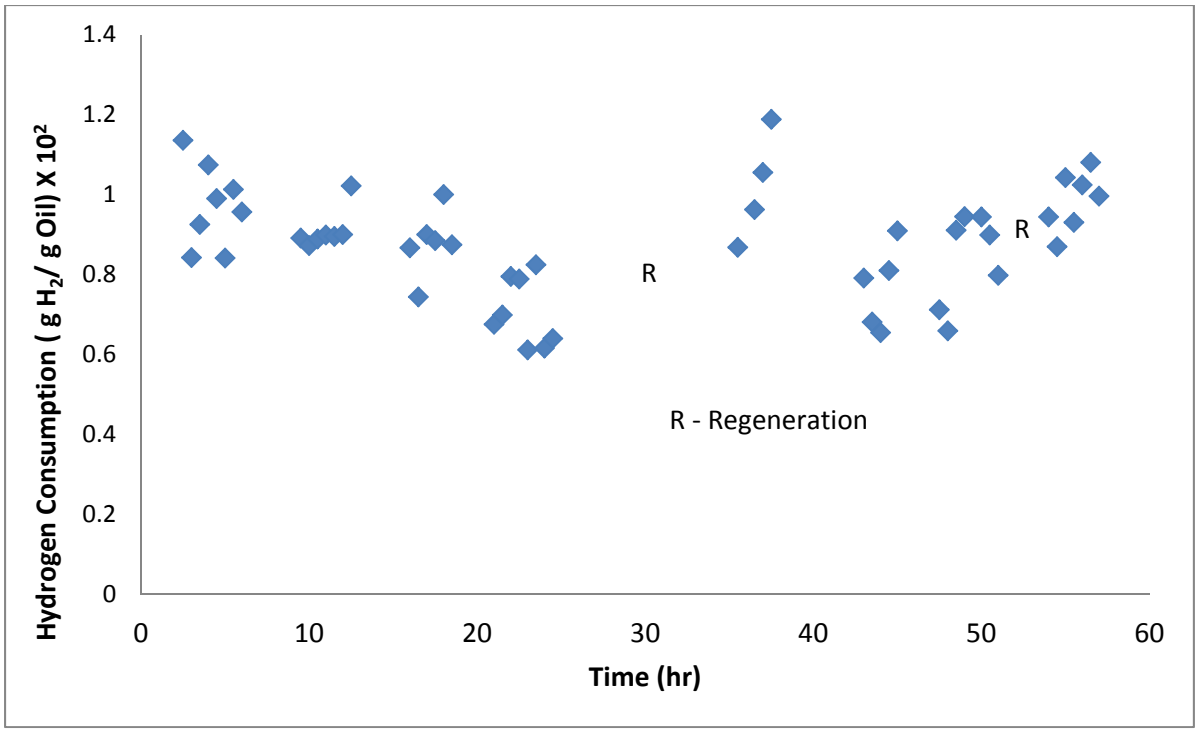

Figure 3.4: Performance of Sulfided Ni-Mo supported on γ-Al_2O_3 over time

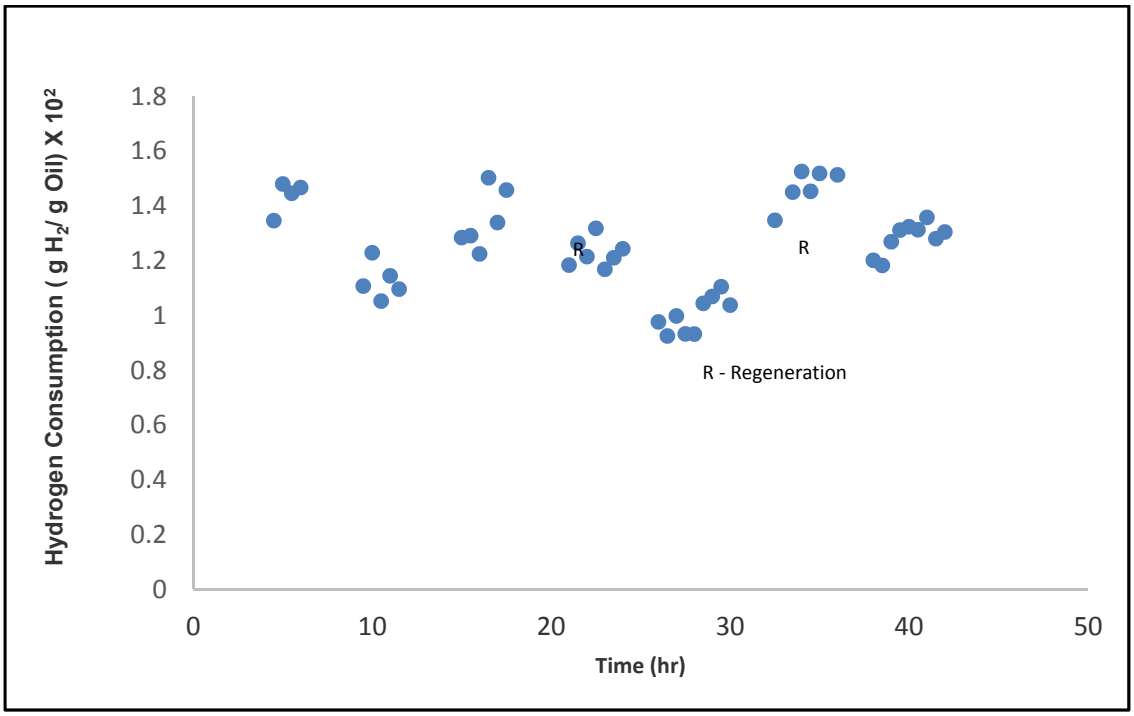

Figure 3.5: Performance of 0.5wt% Rh supported on γ-Al_2O_3 over time

II.2.2.7. CO_2 Measurements during Combustion

During combustion, the CO_2 chromatogram areas in the combustion gases were measured. Figure 3.6 shows the CO_2 chromatogram area data as a function of on-stream run-time for the two above mentioned catalysts along with the 0.5wt% Pt catalyst reported in Section II.2.2.1. It was assumed that more CO_2 chromatogram peak area was obtained when more coke was present in the catalyst bed. It appears from these data that the Ni-Mo catalyst formed the highest amount of coke for same on-stream running time while Rh catalyst produced the least amount of coke amongst these three catalysts.

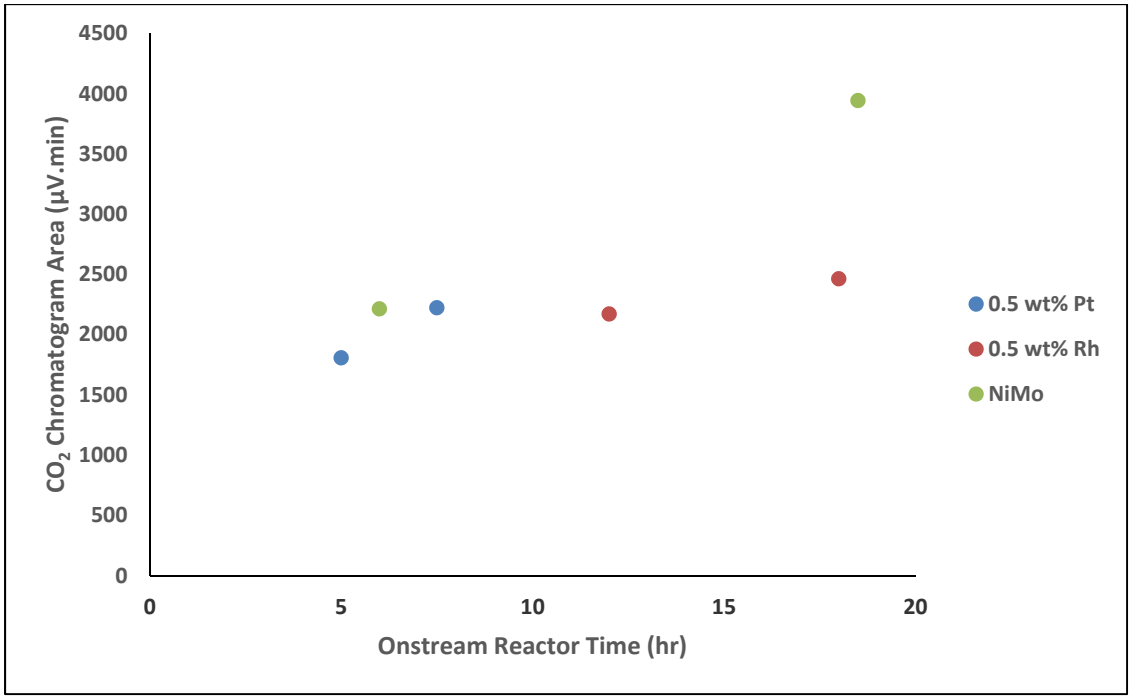

Figure 3.6: CO_2 chromatogram area with different catalysts during combustion

II.3. Performance Study of Precious Metal Catalysts for HDO of Chlorella Algae Oil and Canola Oil

The three catalysts evaluated in this section are:

- **0.5wt% Pt,**
- **0.5wt% Rh, and**
- **0.5wt% Pt/0.5wt% Rh.**

The carbon yield in the liquid product was used as a measure of the catalyst performance. A 1.5% (w/w) solution of the oils in hexane solution was prepared and fed into the microreactor system at a rate of 0.05ml/min by a single piston HPLC pump. The oil concentration in this section is lower than that in Section II.2. because both Chlorella algae oil and Canola oil has a higher concentration of C18 fatty acid than Nannochloropsis Salina and the amount of catalyst

in the microreactor, with its fixed volume, was not sufficient to hydrodeoxygenate the two oils. The amount of acylglycerides in both Chlorella algae oil and Canola oil are also significantly higher than that in Nannochloropsis Salina. At higher than 5 % (w/w) solution of either of the two oils, solids presumably unconverted fatty acids were formed in the microreactor thus causing reactor clogging. It should be pointed out that, compared with the microalgae oils that were used in the project (Chlorella and Nannochloropsis Salina), Canola oil has a higher lipids (acylglycerides) content, and was used as a clean lipids source to shed some light on the influence of the unidentified components in the microalgae oil.

All reaction runs described below were carried out at 500psig pressure using pure H_2 at a temperature of 300^oC. All fresh catalysts were reduced before making an experimental run. Reduction conditions were kept the same for each catalyst: 500psig pressure of H_2 at a flow rate of 50sccm and at a temperature of 300^oC for 2 hours. As a means of regenerating used catalysts, diluted air (96% N_2, 4% O_2) was used for catalyst combustion at 650^oC, and a GC-TCD was used to monitor the amount of CO_2 produced during combustion. The combustion was assumed completed when no CO_2 was detected in the exit gas.

To minimize contamination from previous experimental runs, the entire system was cleaned before each experimental run by pumping hexane at 5ml/min for 5 minutes. The liquid feed valve was closed after hexane pumping was stopped to prevent gas backflow into the HPLC pump. N_2 at 120 psig was used to flush out all the hexane from the system only downstream of the liquid feed valve. As a result, there would be residual hexane in the tubing line between the HPLC pump and liquid feed valve. Because of this residual hexane, the first-hour liquid samples were usually dilute, resulting in apparently lower hydrocarbon yield upon analysis of the liquid product samples.

II.3.1. Experimental Process Parameters

In addition to temperature and H_2 partial pressure, other process parameters such as Liquid Hourly Space Velocity (LHSV), Gas Hourly Space Velocity (GHSV), and Weight Hourly Space Velocity (WHSV) affect reactor performance in gas-liquid heterogeneous reactions. The LHSV is defined as the ratio of hourly volume of the liquid feed processed over the volume of the reactor which for all the data reported below was calculated based on empty bed. In consideration of the lower limit on the flow rate permissible by the HPLC pump, the liquid flow rate could not be reduced below 0.05 ml/min without significant loss of accuracy. Therefore, to vary the LHSV, in one set of experiments, reactors of three different IDs but of the same length were used. In order to keep the amount of catalyst in the bed the same, glass beads were used as inert, as needed. The catalyst was well mixed with glass beads before being packed into the microreactor to ensure that the catalyst was well dispersed along each reactor. In another set of experiments, the LHSV was changed by configuring two reactors of the same ID in parallel while keeping the flow rate constant at 0.05 ml/min. The WHSV is similarly defined as ratio of hourly volume of liquid feed over the catalyst weight while the GHSV is defined as the ratio of gas hourly volumetric flow rate over the reactor volume. The length of the reactor for all the experimental runs was 12cm. All reported GHSV values were calculated at standard temperature (273.15K) and pressure (1 atm.). The process conditions and process parameters for Canola oil and Chlorella oil are provided in Tables 3.5 and 3.6 respectively.

Table 3.5: Experimental Process Conditions and Parameters for Canola Oil

LHSV	54.80 h^{-1}	10.36 h^{-1}	1.52 h^{-1}

GHSV	54820.15 h^{-1}	10362.98 h^{-1}	1522.78 h^{-1}
ID of reactor	0.03”	0.069”	0.18”
Process Conditions	Gas Feed: H_2, 50sccm; Temperature: 300^oC; Pressure: 500 psig; WHSV: 0.55 g oil/hr/g catalyst		

Table 3.6: Experimental Process Conditions and Parameters for Chlorella Oil

LHSV	54.80 h^{-1}	27.4 h^{-1}
GHSV	54820.15 h^{-1}	27410.07 h^{-1}
WHSV	0.6 (g oil/hr/g catalyst)	0.3 (g oil/hr/g catalyst)
Number of reactors	1	2 (in parallel)
Process Conditions	Gas Feed: H_2, 50sccm; Temperature: 300^oC; Pressure: 500 psig; ID of Reactor: 0.03”	

II.3.2. Carbon Yield Analysis

The microreactor system had a pressure limit of 500 psig, therefore for safety reasons total process pressure should not exceed this value. In order to conduct experiments at 500psig H_2 partial pressure, the N_2 flow had to be set to zero. In the absence of internal standard, such as N_2, the flow rates of the gas product components could not be reliably quantified by GC-TCD. Therefore, no hydrogen consumption data were obtained for the experiments reported in this section, and only the liquid product was analyzed by GC-FID.

Using the same method described in other sections of this report, the desired products, (C13-C20 alkanes), were well separated and their peaks appeared between 19 and 39 minutes with increasing boiling point, an indication of number of carbon atoms in the hydrocarbon molecules. The difference in the retention time between two adjacent alkanes was around 2.3~2.5min. Applying this to the 6 to 19 minutes retention time range on the gas chromatograph, smaller carbon number alkanes were found, which could only have been produced via cracking of higher molecular weight oxygenates.

Furthermore, to confirm the analytical results, four of the liquid product samples were quantified by another GC-FID independently, and the result of the comparison was as follows:

	Sample 1	Sample 2	Sample 3	Sample 4
Deviation	1.39%	6.83%	1.27%	-0.08%

The small deviation between the results from two independent GC-FID systems did confirm the accuracy of the reported analytical data.

II.3.3. Results and Discussion

II.3.3.1. Catalyst Evaluation

The fatty acid profile of canola oil that follows here shows that it is composed of only even carbon number lipids.

Fatty Acid Profile of Canola Oil (wt%) (http: ftp://ftp.fao.org/es/esn/food/bio-10t.pdf)					
C16:0	C18:0	C18:1	C18:2	C18:3	C20:1
4.1	1.8	63.0	20	8.6	1.9

However, when quantifying the C13-C20 alkanes in the liquid products, odd number hydrocarbons with much larger concentration than even number of hydrocarbons were obtained for all the three precious metal catalysts. The reverse was the case for the sulfided NiMo catalyst. Therefore, it can be concluded that although hydrodeoxygenation, hydrodecarboxylation and hydrodecarbonylation all occur to some degree in each experimental run, the base metal catalyst NiMo has a higher selectivity to the hydrodeoxygenation route, while, precious metal catalysts prefer the hydrodecarboxylation or hydrodecarbonylation routes, which involve the loss of one carbon to produce CO_2 or CO. From the perspective of hydrogen economics, the pathway in which oxygen is removed by producing CO_2 or CO is favored, as long as other hydrogen-consuming reactions are suppressed. This is one of the motivations for selecting precious metal catalysts for study.

Figure 3.7 shows the performance of the three different precious metal-based catalysts over time for hydrotreament of canola oil. As mentioned earlier in section II.3, the low carbon yield of the first-hour product is due to the dilution of the hydrocarbon product by residual hexane in the process line. Therefore, except for the first-hour result, carbon yield can be considered as a measure of catalyst activity.

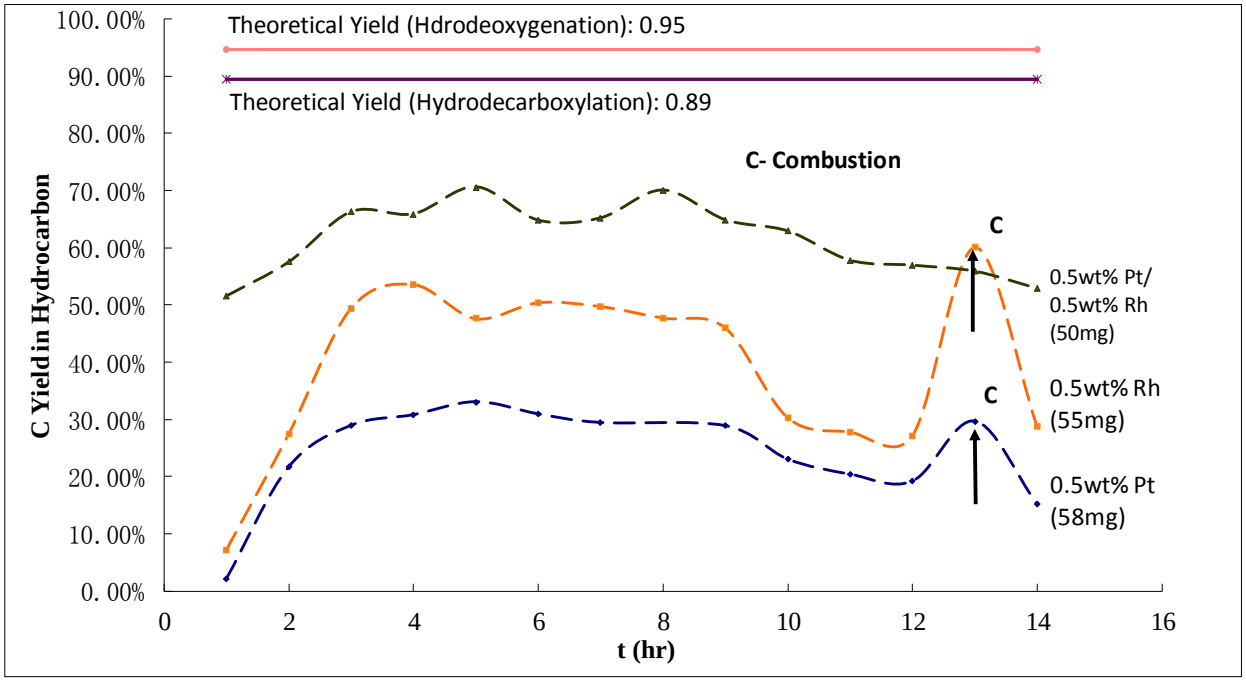

Figure 3.7: Evaluation of the performance over processing time of three different catalysts (1.47wt% canola oil in hexane, T=300^{o}C, liquid flow rate=0.05ml/min, H_2 flow rate=50sccm, H_2 pressure=500psig, LHSV=54.80 h^{-1} and GHSV=54820.15 h^{-1}).

All three catalysts appear to maintain a stable activity with no sign of deactivation for the first 9 hours, with an average carbon yield of 30.3% for Pt, 49.2% for Rh and 66.8% for Pt/Rh. The higher carbon yield of the bimetallic catalyst may be due to the fact that it has twice the number of active sites as the monometallic catalysts. Therefore, to study the synergy effect of the two metals, more experiments would need to be performed where the number of active sites will be kept approximately the same for all the catalysts. Between 9 and 12 hours, the carbon yield of the bimetallic catalyst decreases less rapidly than that of the monometallic catalysts, which indicates that the bimetallic catalyst is more resistant to deactivation.

In each of the experiments, combustion was carried out after running the reaction for 12 hours, and it appeared to have a larger influence on the monometallic catalysts, especially Rh, than on the bimetallic catalyst. Although combustion seemed to restore the initial activity of the catalyst, it did not appear to maintain this activity for a significantly long time as deactivation continued after combustion. Also, no CO_2 was detected in the combustion gas which indicated that coking was not the primary deactivation mechanism for these catalysts when used for hydrotreating of canola oil.

The bimetallic, best-performing catalyst was selected for evaluation with the microalgae oil from chlorella, and figure 3.8 shows the effect of the presence of nonsaponifiable chemical species on the hydrocarbon yield. Compared with the Chlorella oil, which has about 14wt% (see Task 1 above) nonsaponifiable oxygenates, the carbon yield of canola oil is higher and more stable. It can be observed that, with chlorella oil, the catalyst deactivated more rapidly after 8 hours suggesting that unidentified oxygenates were responsible for deactivation. In contrast, the gradual decrease of catalyst activity for canola oil may indicate a different origin for catalyst deactivation. We speculate that the deactivation probably arises from a different sort of oxygenates, the reaction intermediates, namely fatty acids, fatty alcohols, fatty aldehydes and fatty esters. The catalysts will be most susceptible to deactivation by fatty esters because of their much longer chain lengths. Regardless of the source of oxygenates responsible for catalyst deactivation, an effective catalyst regeneration process should be focused on removing the oxygenates but the developed process technology should ensure that oxygenates are not irreversibly adsorbed on the catalysts.

II.3.3.2. Effect of Liquid Hourly Space Velocity (LHSV)

As stated earlier in this section of the report, for the experiments on the effect of LHSV, both the liquid and gas flow rates were kept unchanged because the liquid flow rate on the HPLC pump could not be reduced further without incurring significant errors in liquid feed rate. By varying the reactor ID, both LHSV and GHSV decreased in the same ratio, while the WHSV remained unchanged. If the reaction is kinetically-controlled, a higher carbon yield should be expected in the larger ID reactor due to the longer contacting time of reactants with catalysts. However, comparing the average carbon yield at steady state (Figure 3.9), the larger ID reactor does not show a better performance. Reduction of the GHSV results in reduction of convective mass transfer. In conclusion, this reaction is not kinetically controlled but mass transfer-limited.

In consideration of the observation that oxygenates may be responsible for catalyst deactivation, a two-hour reduction was performed with 1/8” and 1/4” OD reactors. After the reduction (run-time greater than 7 hours), the catalyst activity rose to even a higher value than

the prior, 7th hour value, but dropped to the steady state level. This result suggests that reduction can help to remove some of the adsorbed oxygenates from the catalyst surface. Still, more experiments need to be done in the future to develop an effective catalyst regeneration strategy.

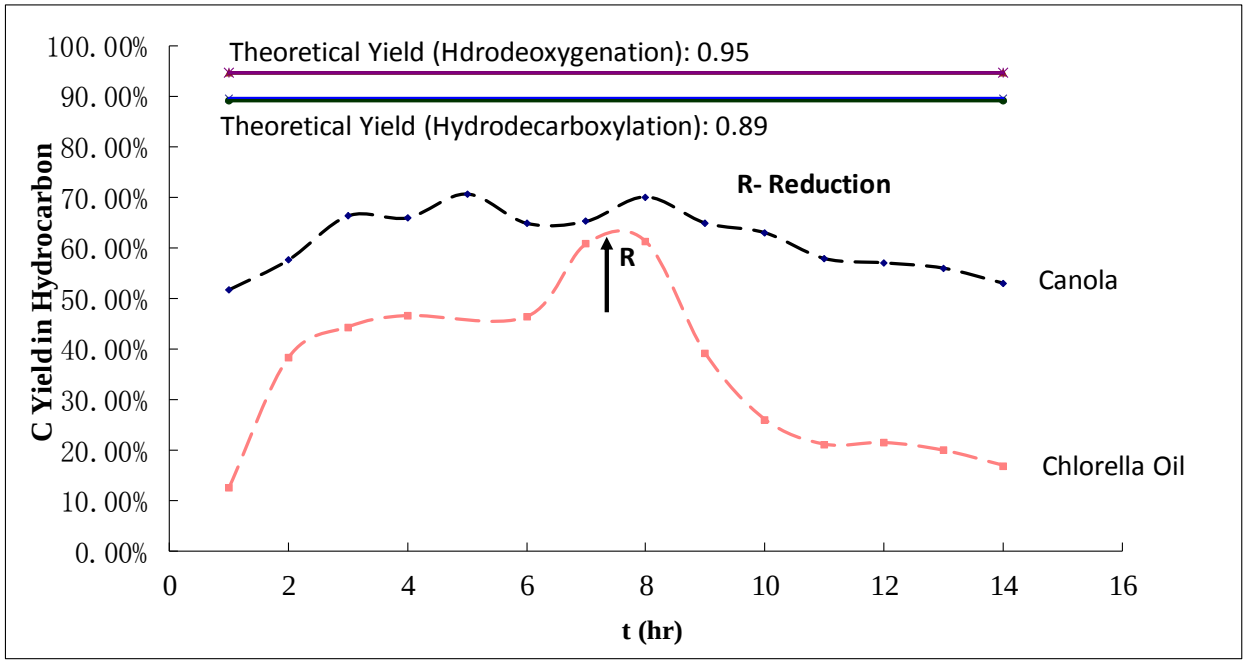

Figure 3.8: Effect of nonsaponifiable compounds on the carbon yield (0.5wt% Pt/ 0.5wt% Rh. 1.47wt% oil in hexane=300°C, liquid flow rate=0.05ml/min, H_2 flow rate=50sccm, H_2 pressure=500psig, LHSV=54.80 h^{-1} and GHSV=54820.15 h^{-1}).

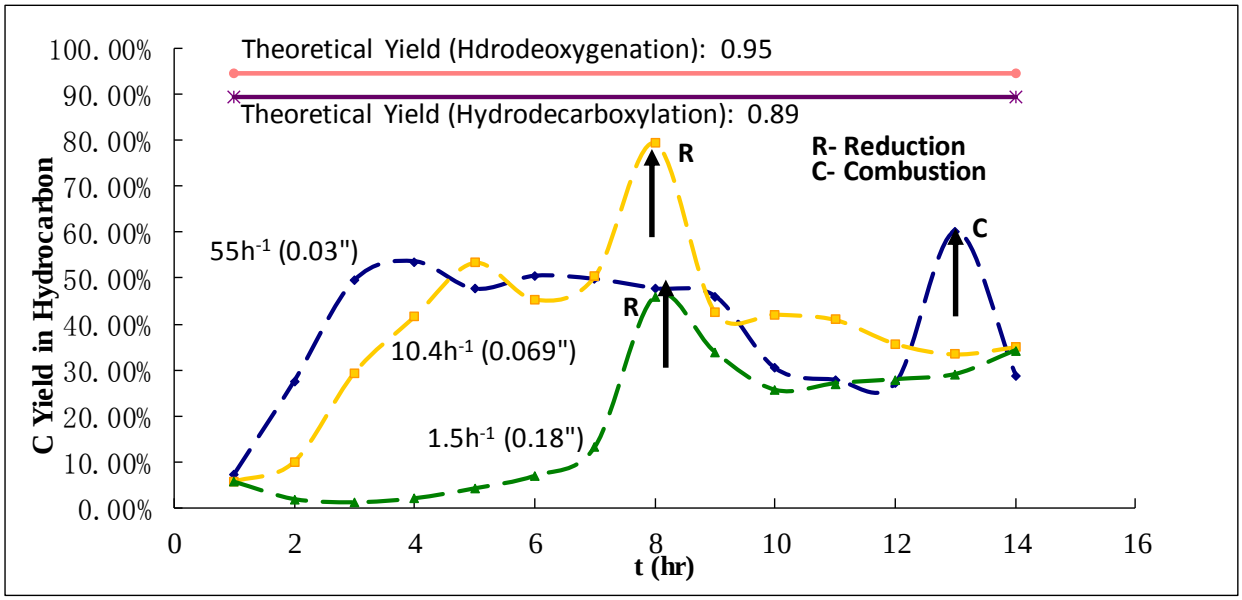

Figure 3.9: Effect of LHSV on the carbon yield (0.5wt% Rh, 1.47wt% canola oil in hexane, T=300°C, H_2 flow rate=50sccm, H_2 pressure=500psig).

Another method we used to change the LHSV was to keep the liquid flow rate the same but use two reactors of the same inner diameter in parallel. Since the amount of catalyst used was now double that of the standard single reactor, WHSV was decreased. However, no carbon yield increase was observed with the parallel reactor arrangement (Figure 3.10), which again confirmed that the reaction was mass transfer-controlled.

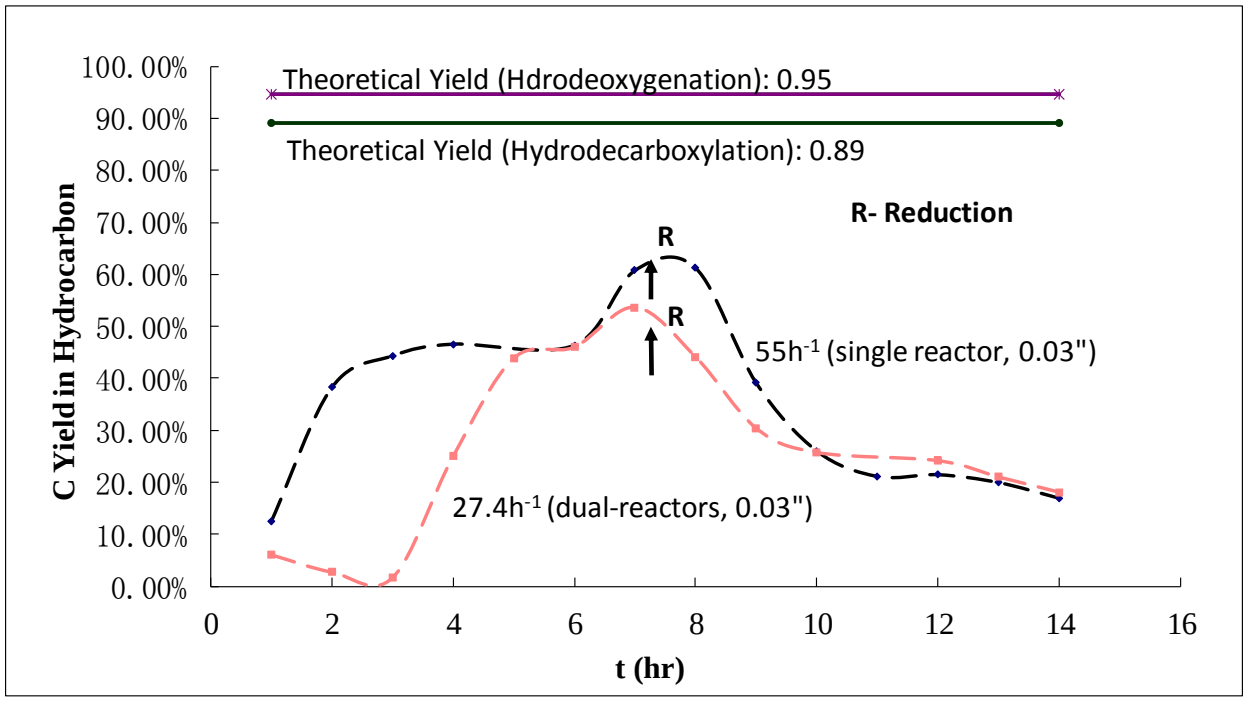

Figure 3.10: Effect of LHSV on the carbon yield (0.5wt% Pt/ 0.5wt% Rh. 1.47wt% chlorella oil in hexane,T=300°C, H_2 flow rate=50sccm, H_2 pressure=500psig).

II.3.3.*3.* Effect of Gas Hourly Space Velocity (GHSV)

Figure 3.11 shows the performance of the single reactor for two values of GHSV. The GHSV was changed by increasing the H_2 molar flow rate from 50 sccm to 100 sccm while keeping all the other process parameters the same. Although higher GHSV led to a higher initial activity and less rapid change in catalyst activity, however, the average activity from the 100sccm result is not better than that from the 50sccm result. We will need more experimental runs to determine the existence of an optimum gas flow rate

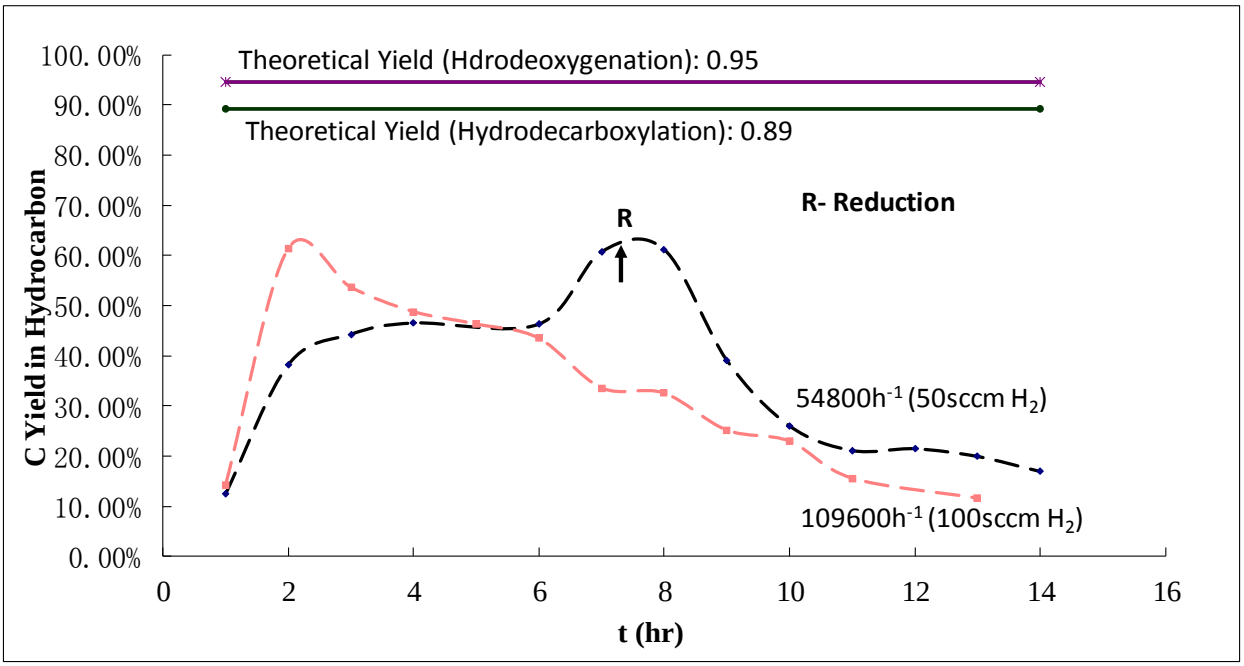

Figure 3.11: Effect of GHSV on the carbon yield (0.5wt% Pt/ 0.5wt% Rh. 1.47wt% chlorella oil in hexane, T=300°C, H_2 pressure=500psig, LHSV=54.80 h^{-1} and WHSV=0.6 g oil/hr/g catalyst).

II.4. References

Kubicka, D. and Kaluza, L., 'Deoxygenation of Vegetable Oils over Sulfided Ni, Mo and NiMo Catalysts', Applied Catalysis A: General 372 (2010) pp 199-208.

Sánchez, A., Maceiras, R., Cancela, A. and Rodríguez, M., 'Influence of *n*-Hexane on *in Situ* Transesterification of Marine Macroalgae', *Energies, 5*, 243-257 (2012).

III. Performance Study of HDO of Nannochloropsis Salina on Pre-sulfided NiMo in a Microreactor

A performance study of HDO of Nannochloropsis Salina algae oil using pre-sulfided NiMo catalyst (supported on γ-alumina) was conducted in the microreactor system to investigate the influence of process variables and parameters. The effect of reaction temperature, liquid hourly space velocity (LHSV), gas hourly space velocity (GHSV) and reaction pressure on C13 to C20 hydrocarbon yield, carbon yield and ratio of even number carbon hydrocarbon to odd number carbon hydrocarbon was investigated.

III.1. Effect of Process Variables and Parameters on Performance

The performance study initially focused on the effects of process conditions on carbon yield in the liquid product, the hydrocarbon yield, and the ratio of even numbered carbon hydrocarbon to odd numbered carbon hydrocarbon. The performance study was subsequently extended to include the effects of process parameters on the conversion of microalgae oil. The conversion of algae oil was indirectly measured through the conversion of the fatty acids produced in the hydrogenation/hydrogenolyisis steps of hydrotreating, and all the information related to conversion calculation is detailed in Section IV.2 of Task 1 above.

III.1.1. Temperature

Figure 3.12 shows the performance of the reactor under three different reaction temperatures and high LHSV (54.80 h^{-1}) value. Apparently, 280^{o}C is too low for this hydrotreating process. When the temperature increases from 310 to 360^{o}C, although the temperature effect is negligible during the first four hours, subsequently the stability of the reactor performance correlates with reaction temperature. At 360^{o}C, there is no sign of reduction in the carbon yield for seven hours. We suspect that at elevated temperatures, it may be difficult for the oxygenates to adsorb on the catalyst surface. As shown in Fig. 3.12a and 3.12b, a high reaction temperature can help to maintain catalyst life and activity.

From Fig. 3.12c, it can be observed that the HC (2n)/ HC (2n-1) ratio increases as temperature increases from 280 to 310^{o}C, but thereafter becomes less sensitive. For the overall hydrotreating reaction, hydrodeoxygenation appears to be favored at higher temperatures. According to Arrhenius' equation, the larger the activation energy, the more temperature sensitive the reaction is. Therefore, it can be concluded that, under the experimental conditions, the activation energy of hydrodeoxygenation is lower than that of hydrodecarbonylation or hydrodecarboxylation.

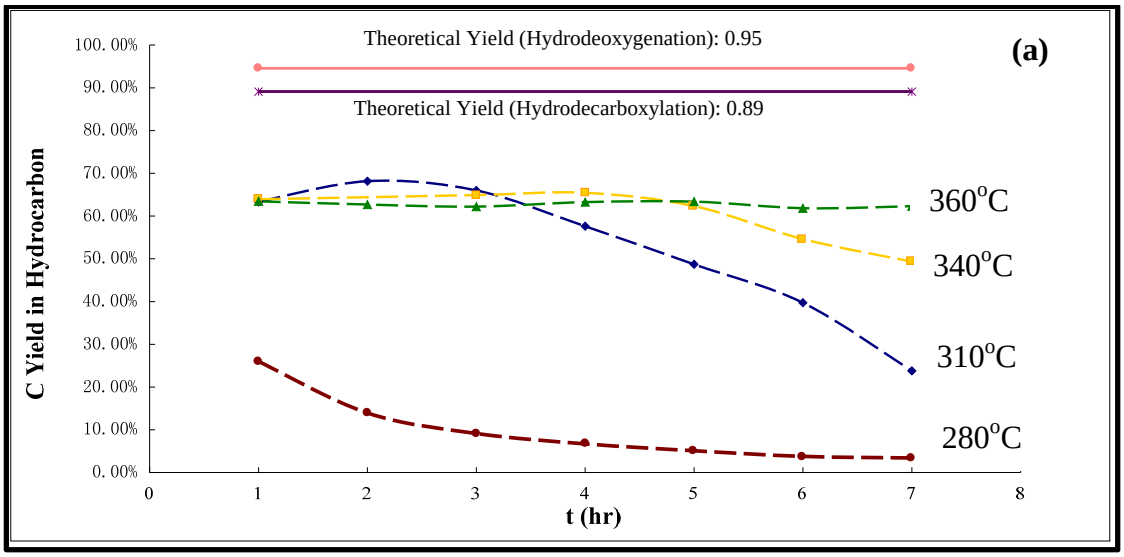
(a)
Theoretical Yield (Hydrodeoxygenation): 0.95
Theoretical Yield (Hydrodecarboxylation): 0.89
360°C
340°C
310°C
280°C
C Yield in Hydrocarbon
t (hr)

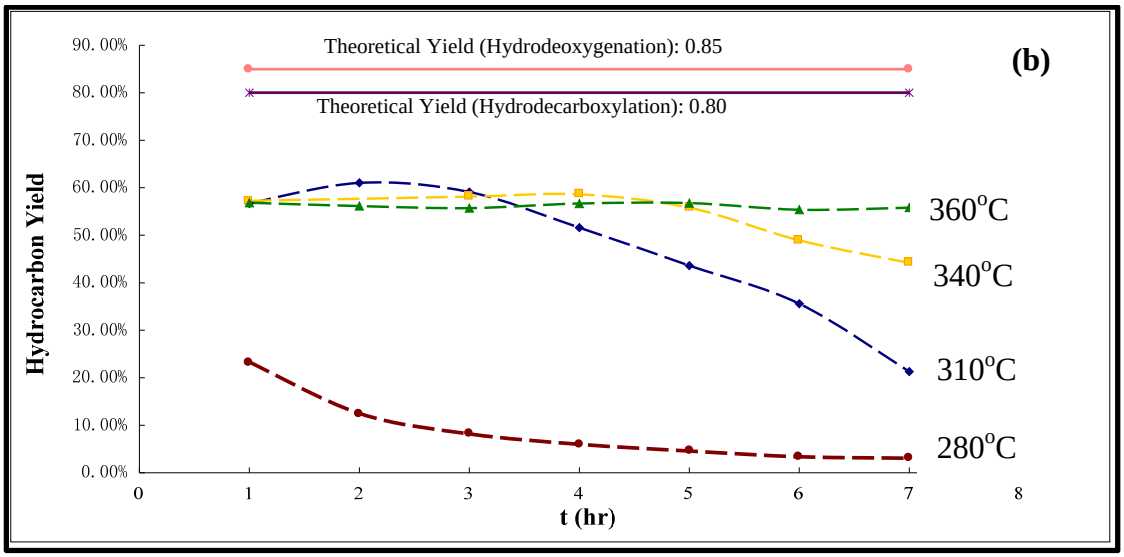
(b)
Theoretical Yield (Hydrodeoxygenation): 0.85
Theoretical Yield (Hydrodecarboxylation): 0.80
360°C
340°C
310°C
280°C
Hydrocarbon Yield
t (hr)

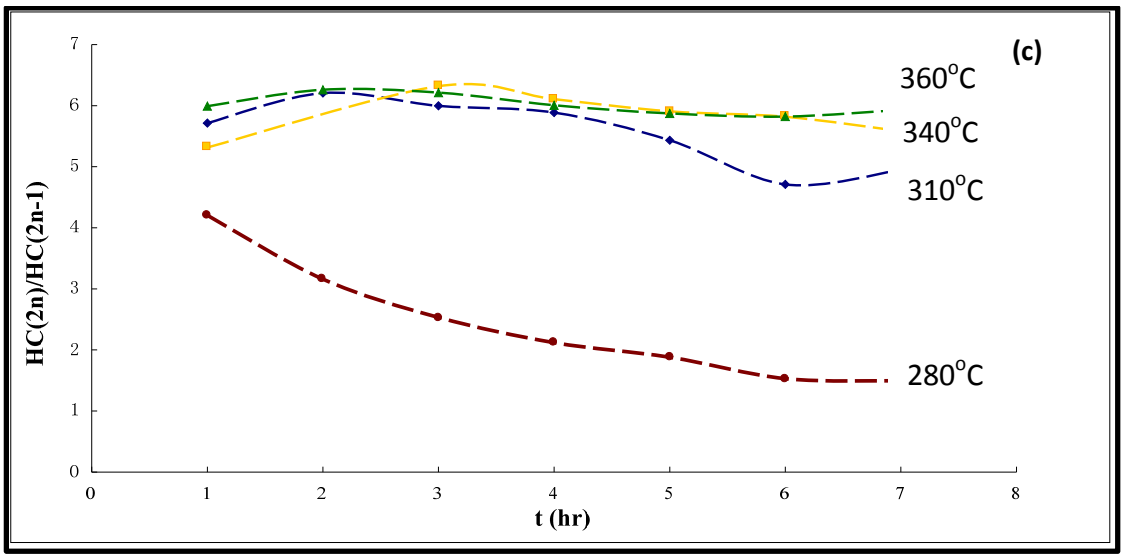
(c)
360°C
340°C
310°C
280°C
HC(2n)/HC(2n-1)
t (hr)

Figure 3.12: Effect of reaction temperature on (a) carbon yield in hydrocarbon , (b) hydrocarbon yield, and (c) ratio of even number carbon hydrocarbons to odd number carbon hydrocarbons (Presulfided NiMo, 1.32wt% Nannochloropsis Salina oil in Dodecane, H_2 pressure=500psig, liquid flow rate=0.05ml/min, LHSV=54.80 h^{-1}, GHSV=54,820 h^{-1}).

Based on the performance study data on carbon yield and hydrocarbon yield, the hydrocarbon yield of the 2nd hour sample was usually the highest, which indicated the highest catalyst activity. The change in the yield from the 2nd hour to the 3rd hour is an indication of the deactivation trend of the catalyst. Therefore, the 2nd and 3rd hour samples were selected for conversion calculation. These selected liquid product samples were first derivatized and then analyzed following the FAME quantification procedure for conversion calculation presented elsewhere in this report (Section IV.2 of Task 1 above). To some extent, the conversion of algae oil to fatty acids is always higher than the hydrocarbon yield value. Therefore, we can conclude that the hydrotreating of fatty acids to alkanes is slower than the hydrogenation/hydrogenolysis steps, and is considered the rate-determining step in the overall reaction.

The conversion of algae oil as measured by unreacted fatty acids over NiMo catalyst supported on γ-alumina as a function of reaction temperature is depicted in Figure 3.13. The conversion at 310°C and higher is over 95%, with an average of 97%, and is much higher than that at 280°C. The decline of conversion with time is smaller at higher temperatures, even negligible at 360°C. However, at 280°C, conversion decreases by 4.2% within one hour of reaction. This shows that 280°C is too low a temperature to obtain a significantly high value for conversion, as well as for maintaining the catalyst activity. At elevated reaction temperatures (> 310°C), catalyst activity is shown to be higher and more stable.

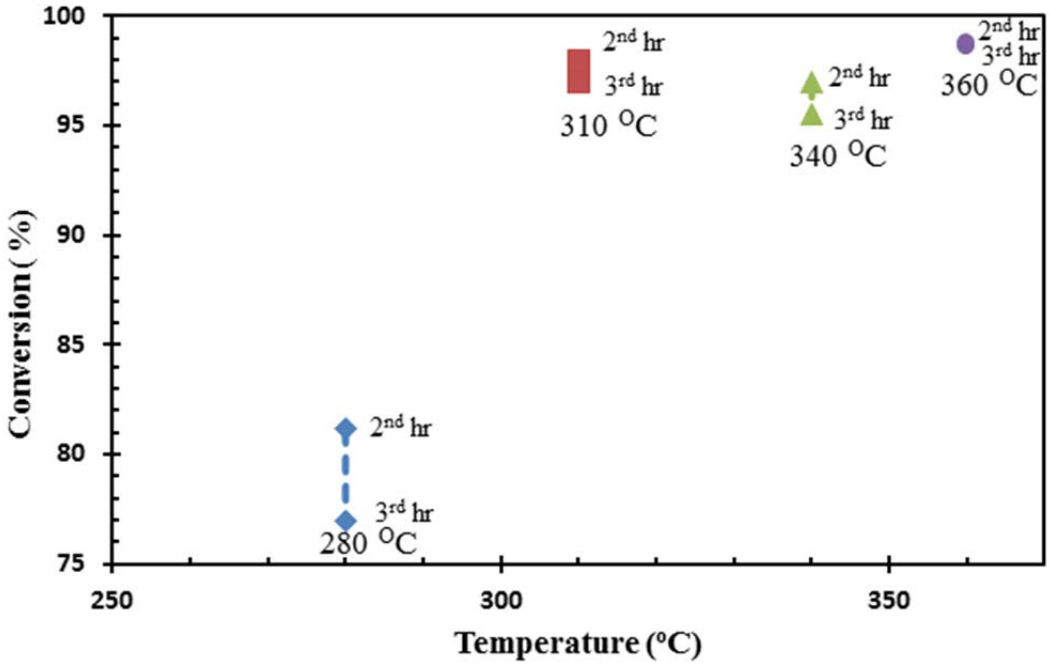

Figure 3.13: Effect of reaction temperature on microalgae oil conversion based on measured fatty acids (Presulfided NiMo, 1.32wt% Nannochloropsis Salina oil in Dodecane, H_2 pressure=500 psig, liquid flow rate=0.05ml/min, LHSV= 54.80 h^{-1}, GHSV=54,820 h^{-1}).

III.1.2. Pressure

The effect of reaction pressure on reactor performance is shown in Fig. 3.14. Two pressure transducers were used to measure the pressure, one at the inlet and the other at the outlet of the reactor. During the reaction, we manually adjusted the back pressure regulator, located at the exit of the reactor, to control the reaction pressure at set value. According to Fig. 3.14 (a) & (b), the initial catalyst activity is not affected by reaction pressure. However, the reaction pressure has obvious positive effect on the stability of the catalyst activity with time. The observed deactivation can be explained by the formation of higher amount of oxygenate intermediates at low reaction pressure, which will speed up the rate of catalyst deactivation.

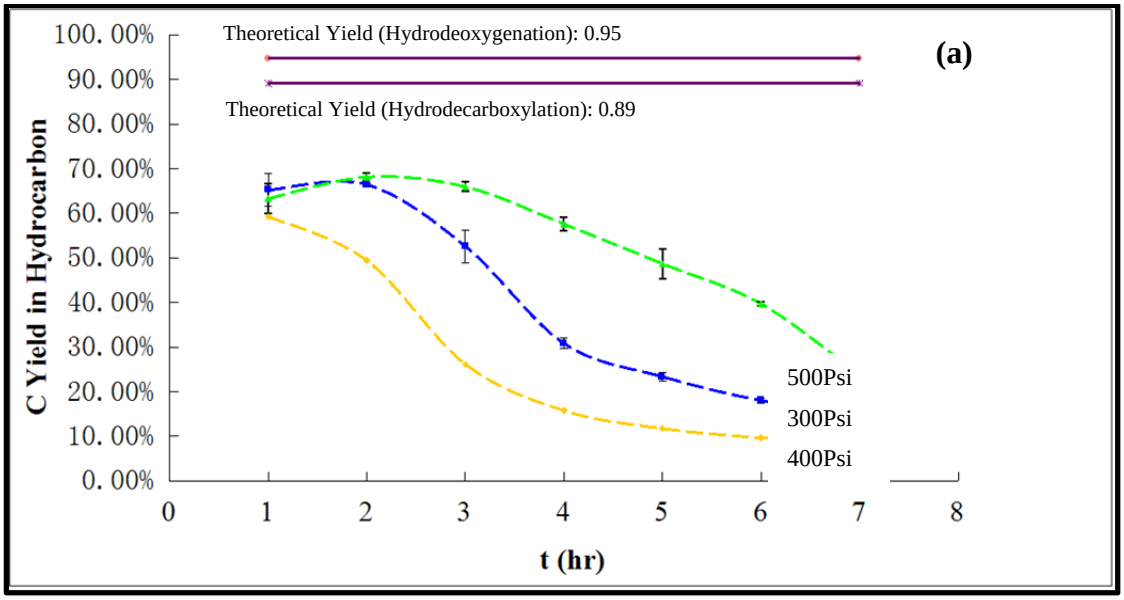

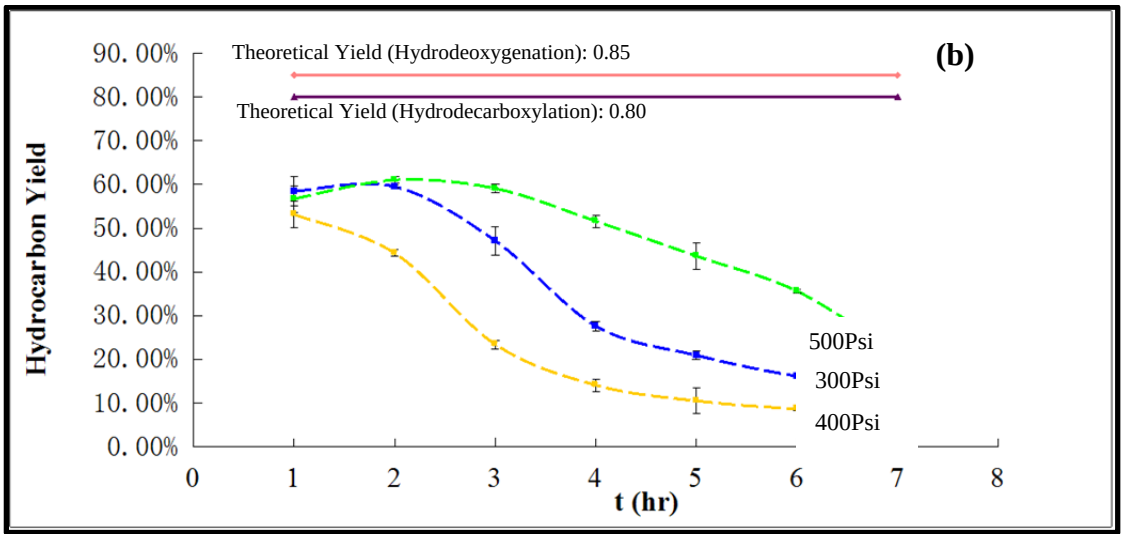

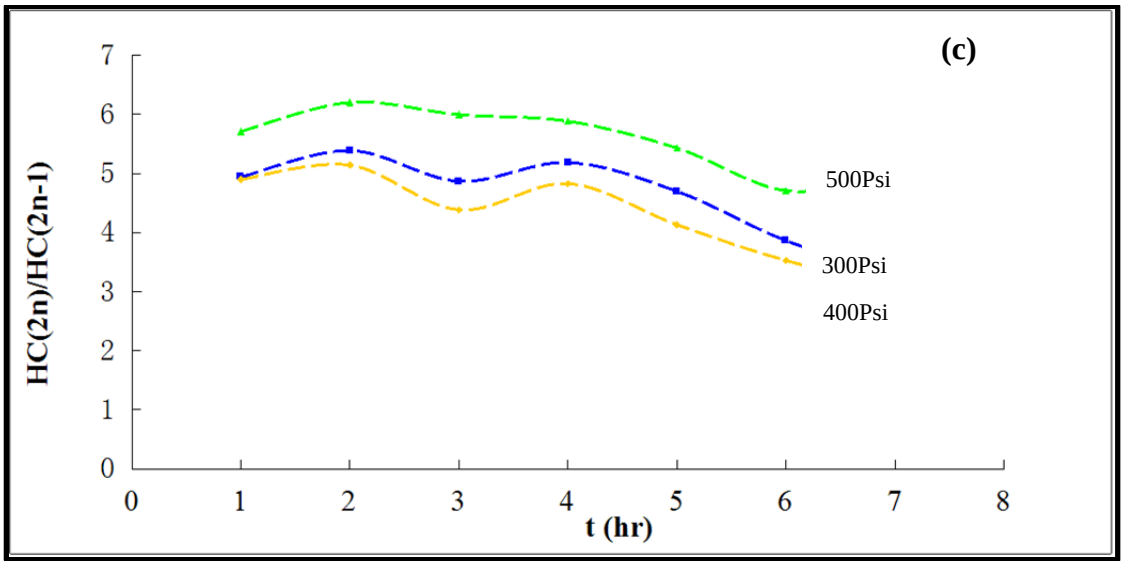

Figure 3.14: Effect of reaction pressure on (a) carbon yield in hydrocarbon, (b) hydrocarbon yield, and (c) ratio of even number carbon to odd number carbon hydrocarbon (Presulfided NiMo, 1.32wt% Nannochloropsis Salina oil in Dodecane, T=310°C, liquid flow rate=0.05ml/min, LHSV=54.80 h^{-1}, GHSV=54,820.15 h^{-1}).

From Fig. 3.14 (c), it can be concluded that reaction pressure has no influence on the ratio HC (2n)/ HC (2n-1) ratio. However, the value of this ratio follows the same trend as the product yield, which again confirms the association between catalyst selectivity and activity.

The conversion data in Figure 3.15 show that pressure has negligible effect on initial catalyst activity. At the pressure of 400 psig, the conversion decreased by 3% within one hour of reaction, but not much decrease is observed at pressures of 300 psig and 500 psig. This reflects the effect of hydrogen partial pressure. At 400 psig reaction pressure, although pure hydrogen was fed into the reactor, non-negligible amounts of propane, water, carbon monoxide, carbon dioxide and methane were produced. The formation of these gases will decrease the hydrogen partial pressure, which will reduce the catalyst activity rapidly. However, at 300 psig the production of gases is reduced compared to that at 400 psig, and will therefore have less effect on hydrogen partial pressure. At 500 psig, although these gases are produced at a high rate, the hydrogen partial pressure is high enough to maintain the catalyst activity.

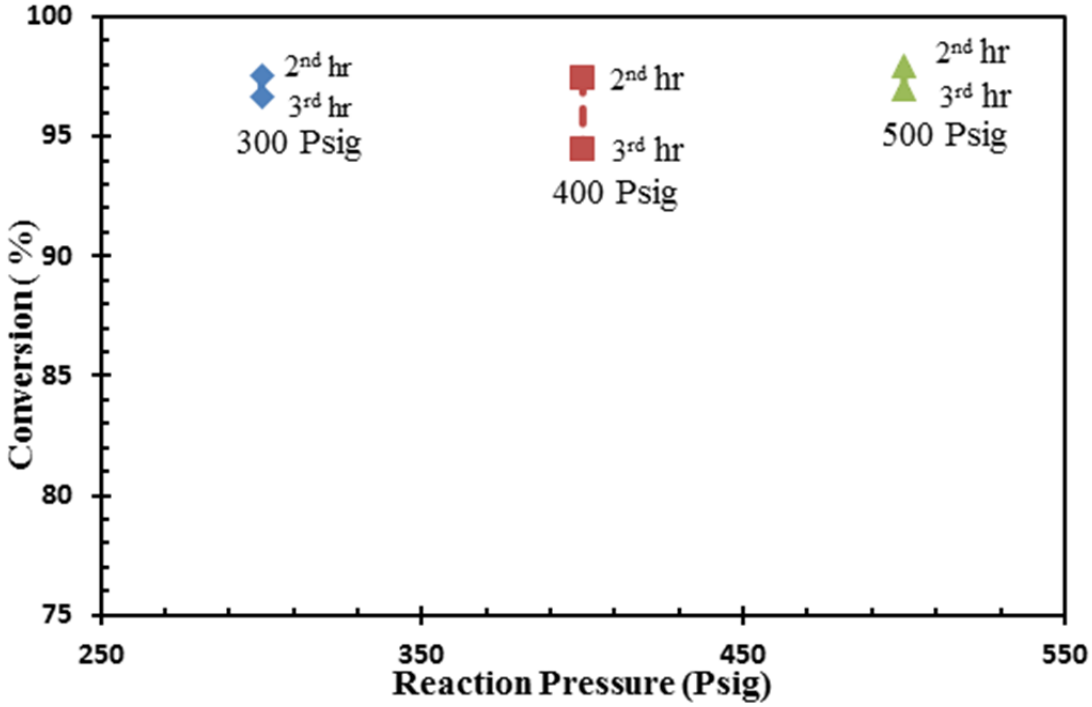

Figure 3.15: Effect of reaction pressure on microalgae oil conversion based on measured fatty acids (Presulfided NiMo, 1.32wt% Nannochloropsis Salina oil in Dodecane, T=310°C, liquid flow rate=0.05ml/min, LHSV=54.80 h^{-1}, GHSV=54,820 h^{-1}).

III.1.3. Liquid Hourly Space Velocity (LHSV)

The LHSV is usually conveniently varied by changing the liquid flow rate, however in the case of the microreactor system, the liquid flow rate is so small (0.05 ml/min) that lowering it further will incur significant error from the HPLC pump. Syringe pumps are accurate in this low flow rate range but are not capable of operating at the high pressures required for hydrotreating. Therefore to vary the LHSV, the reactor ID was changed. However, to keep the GHSV constant, the gas flow rate was adjusted based on the reactor volume while the WHSV was kept constant by using the same amount of catalyst in all the experiments, i.e., 50mg of NiMo catalyst. When using the reactor with large ID, catalyst was pre-mixed with glass beads (90 microns) before being packed into the microreactor.

According to Fig. 3.16a, during the first three hours of reaction, the carbon yield was higher at higher LHSV (shorter residence time), which indicates that the reaction was not kinetically-controlled. After three hours, the carbon yield at the higher LHSV continues to decline, while the performance of the reactor with larger ID (lower LHSV) remains stable. An obvious reason is that to keep the same GHSV in the larger ID reactor, the gas flow rate was also increased proportionately as the decrease in LHSV. The increase in gas flow rate increases the shear stress which should lead to the enhancement of mass transfer in the T-mixer. As a result, a stable Taylor flow pattern with shorter liquid slug was created inside the reactor at the larger gas flow rate, and a better mass transfer was obtained. This experiment shows that for this hydrotreating reaction, mass transfer should be improved to obtain high carbon yield in hydrocarbon. The hydrocarbon yield follows the same trend as the carbon yield as shown in Fig. 3.16b. Please refer to relevant sections of Task 3 for the definitions of carbon yield in hydrocarbon, hydrocarbon yield, and other parameters.

As described in the section on the effect of temperature, under the experimental conditions studied, the NiMo catalyst provided by Albemarle favors the hydrodeoxygenation route over the hydrodecarboxylation or hydrodecarbonylation route. Hence more even-numbered carbon alkanes are produced in comparison to odd-numbered carbon alkanes, for a ratio of HC (2n)/ HC (2n-1) larger than 1. As shown in Fig 3.16c, at lower LHSV, this ratio is relatively higher, and similar to the carbon and hydrocarbon yield, much more stable. We can conclude that the hydrodeoxygenation route is more mass transfer controlled than the hydrodeoxygenation or hydrodecarbonylation route. If the desired product is alkanes with even number of carbon atoms, in addition to the catalyst selection, mass transfer enhancement should also receive significant consideration.

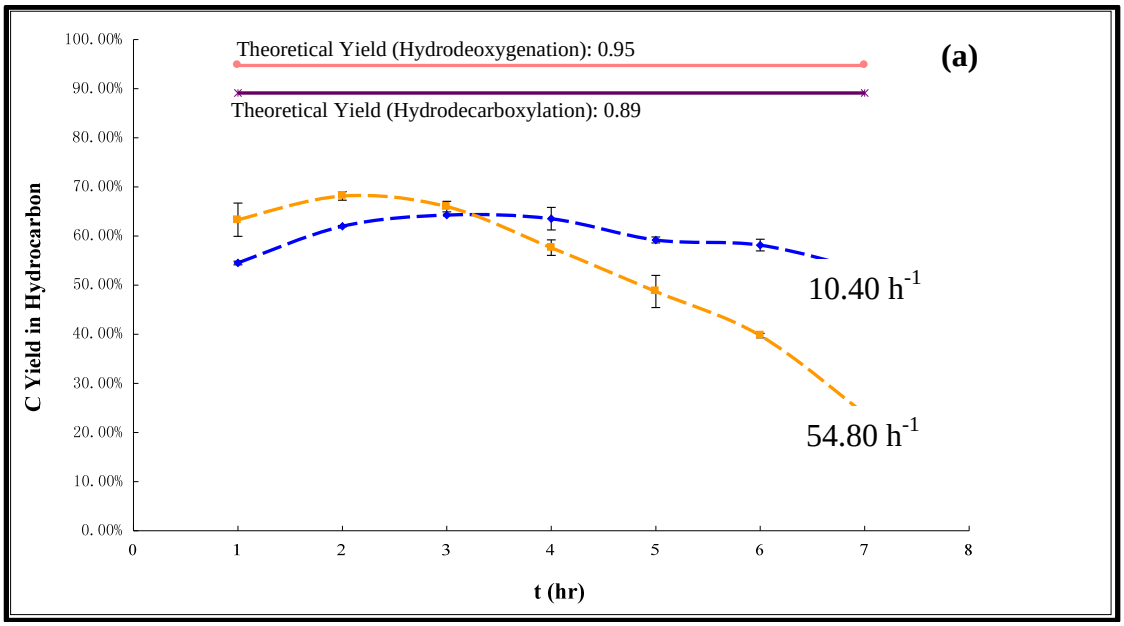

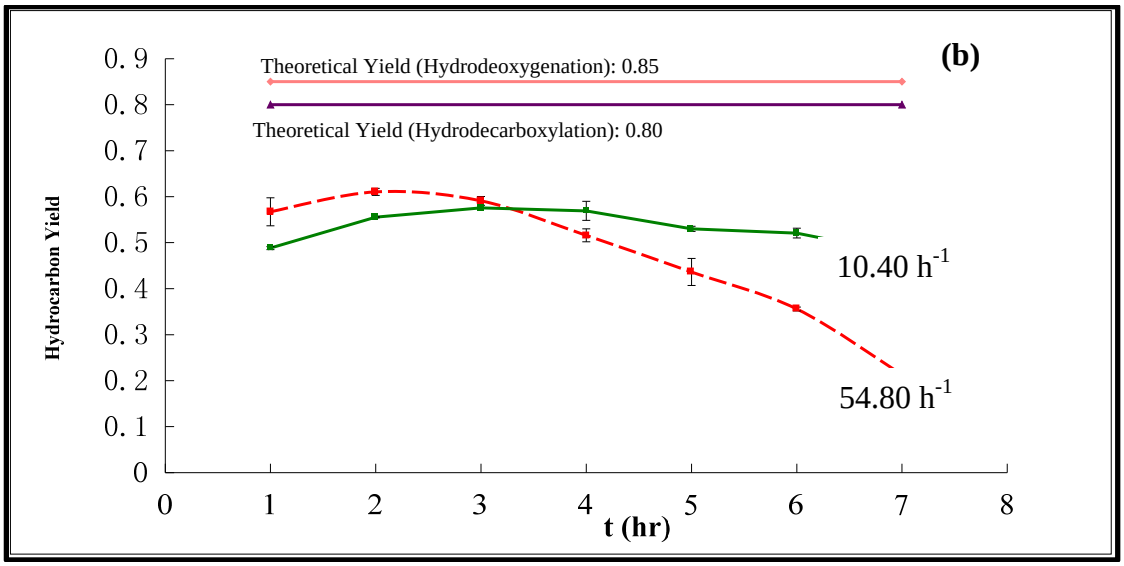

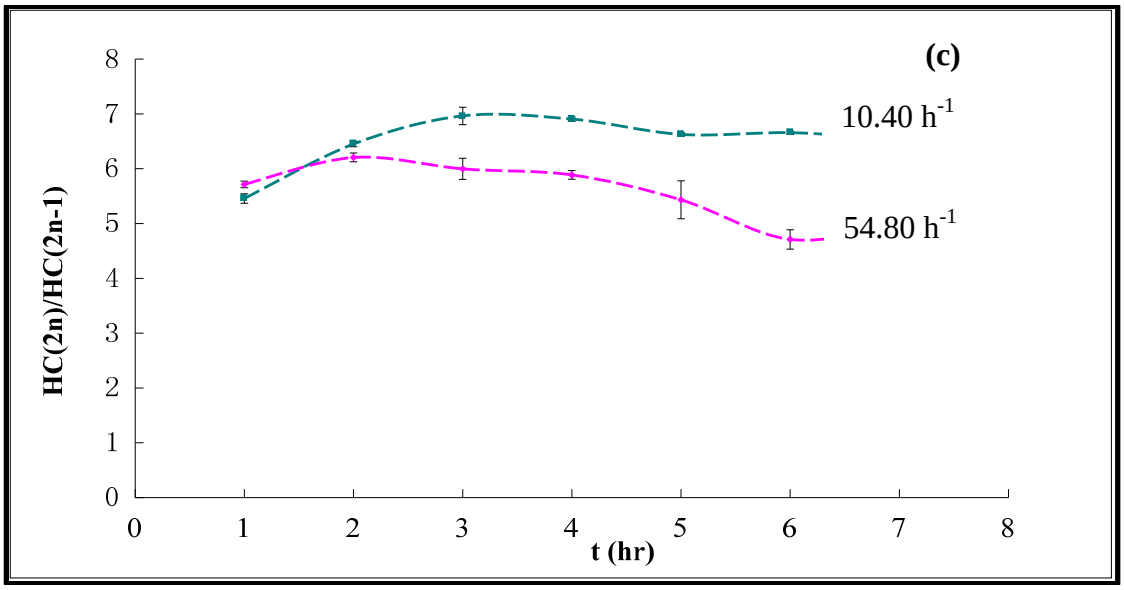

Figure 3.16: Effect of LHSV on (a) carbon yield in hydrocarbon , (b) hydrocarbon yield and (c) ratio of even number carbon hydrocarbons to odd number carbon hydrocarbons (Presulfided NiMo, 1.32wt% Nannochloropsis Salina oil in Dodecane, T=310°C, H_2 pressure=500psig, liquid flow rate=0.05ml/min, GHSV=54,820 h^{-1}).

Figure 3.17 shows the conversion of algae oil at three different LHSV values. During the first 3 hours of the reaction, the conversion is greater at higher LHSV. This indicates that the reaction is not kinetically controlled. The change of conversion from 2nd hour to 3rd hour is the same as the trend observed for hydrocarbon yield. However, less conversion change with time is observed at higher LHSV, which does not correspond with the observation on hydrocarbon yield. It can be concluded that the catalyst selectivity correlates with catalyst activity, but does not change at the same rate. These results are in qualitative agreement with the results of the effect of LHSV on hydrocarbon and carbon yield.

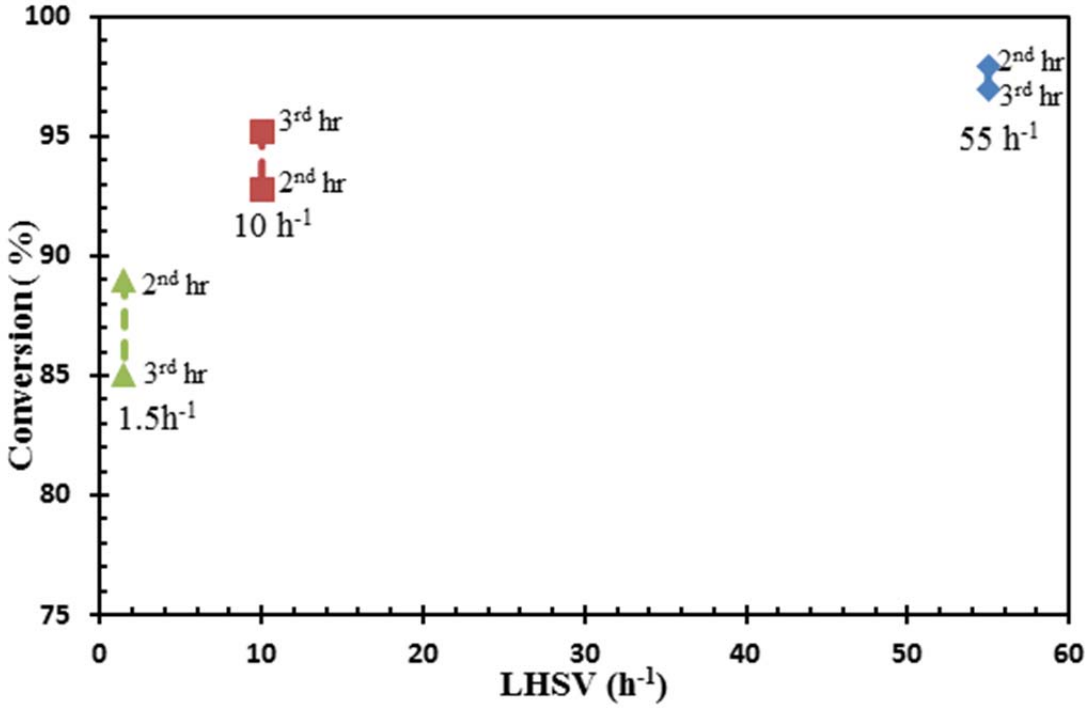

Figure 3.17: Effect of LHSV on microalgae oil conversion based on measured fatty acids (Presulfided NiMo, 1.32wt% Nannochloropsis Salina oil in Dodecane, T=310°C, H_2 pressure=500psig, liquid flow rate=0.05ml/min, GHSV=54,820 h^{-1}).

III.1.4. Gas Hourly Space Velocity (GHSV)

Experiments were performed to study the effect of GHSV on the carbon yield, hydrocarbon yield, ratio of even number carbon hydrocarbon to odd number carbon hydrocarbon and conversion at four values of GHSV, namely ~55,000 hr^{-1}, ~27,500 hr^{-1}, ~11,000 hr^{-1} and ~5,500 hr^{-1} with corresponding gas flow rates of 50 sccm, 25 sccm, 10 sccm and 5 sccm. The liquid flow rate was kept constant at 0.05ml/min and 50mg of NiMo catalyst was used for all reported experiments below.

In prior experiments at low gas flow rates (<10 sccm), it was observed that the liquid slug length in the microreactor was not always stable due to the fluctuation in the readings of the gas mass flow controller. Because the gas flow rate needed to be decreased to as low as 5 sccm to decrease the GHSV by a factor of 10 in this section, the stability and accuracy of the gas mass flow controllers needed to be confirmed as part of the initial preparation for these experiments.

As shown in Fig. 3.18 (a) & (b), for GHSV values of at least 11,000 h^{-1}, during the first 5 hours of reaction, carbon or hydrocarbon yield increase as GHSV increases, which again confirms that the reaction is not kinetically-controlled at high GHSV values, and effort should be focused on enhancing mass transfer to improve the reaction yield. After 5 hours, there is a rapid decrease in yield for the runs at GHSV lower than 27,000h^{-1} apparently because more intermediates are formed than at higher GHSV. Due to the accumulation of oxygenated intermediates on the catalyst bed, the catalyst was, in general, rapidly deactivated. At high GHSV values, catalyst activity seems to decrease with time at a moderate rate. It appears that hydrogen acts not only as reactant, but also serves to protect the hydrotreating catalyst, by preventing the adsorption of the oxygenates. However, there is not much of a difference in product yield for GHSV values of

11,000h^{-1} and 5,500h^{-1}. At the hydrogen flow rates of 10 to 5 sccm which correspond with these GHSV values, it was observed that the liquid slug length was not always stable and usually much longer than that at higher gas flow rates. As a result, mass transfer was inadequate, and in consequence, low yield of product was obtained. In summary, in hydrotreating, high hydrogen flow rate will be preferable not only because it enhances convective mass transfer but also because it protects the catalyst from deactivation. As for the ratio of even number carbon hydrocarbon to odd number carbon hydrocarbon, it ranges from 5.5 to 6.5. At GHSV of 27,500h^{-1}, the rapid decrease of this ratio after 5 hours follows the same trend as the product yield, which indicates that the catalyst selectivity correlates with catalyst activity. Therefore, to keep this ratio constant, catalyst deactivation needs to be avoided.

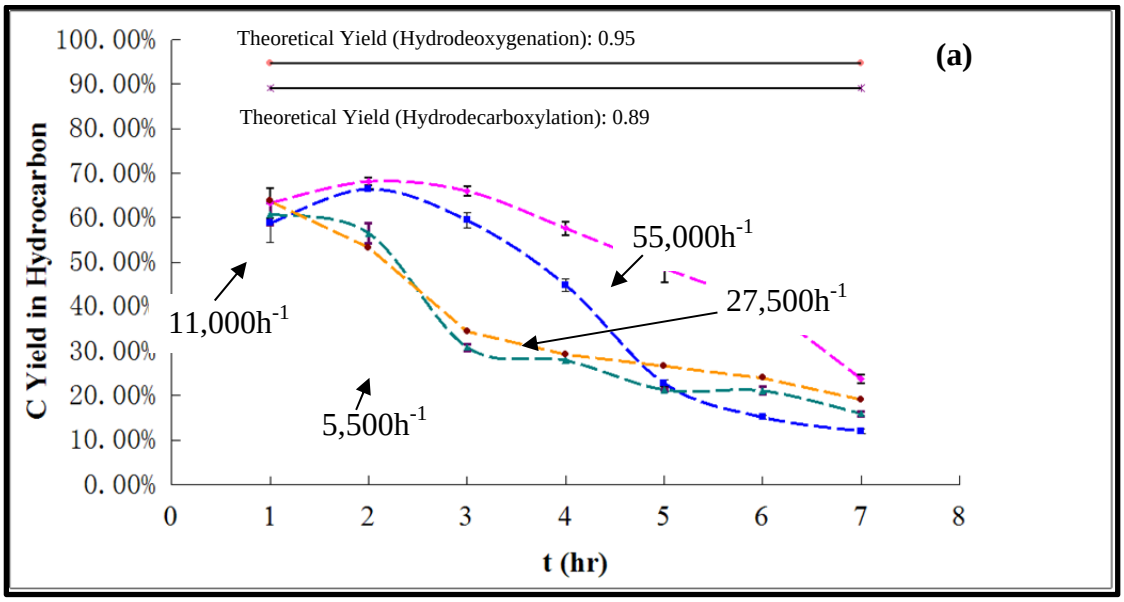

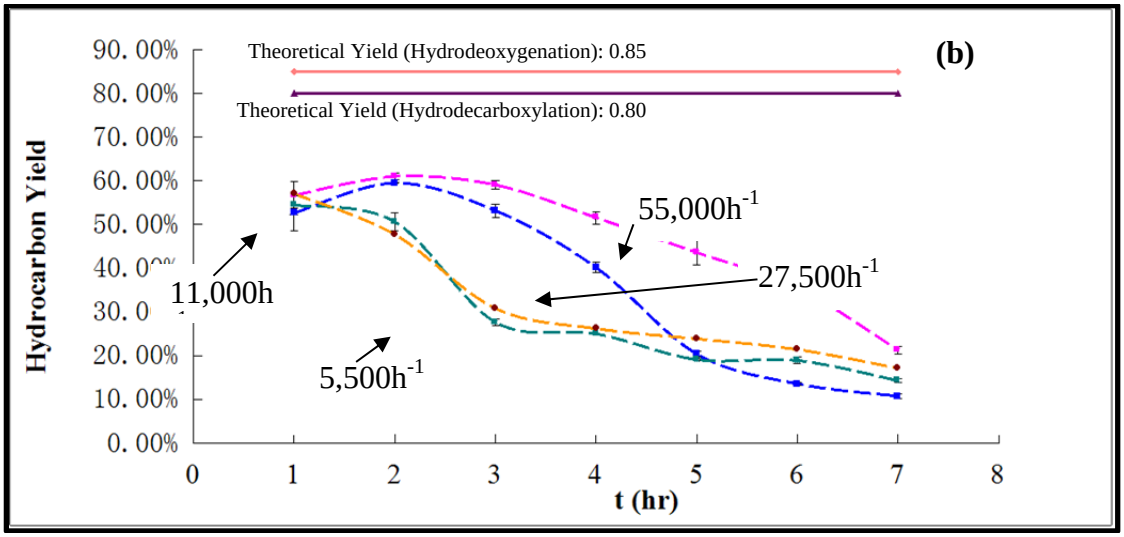

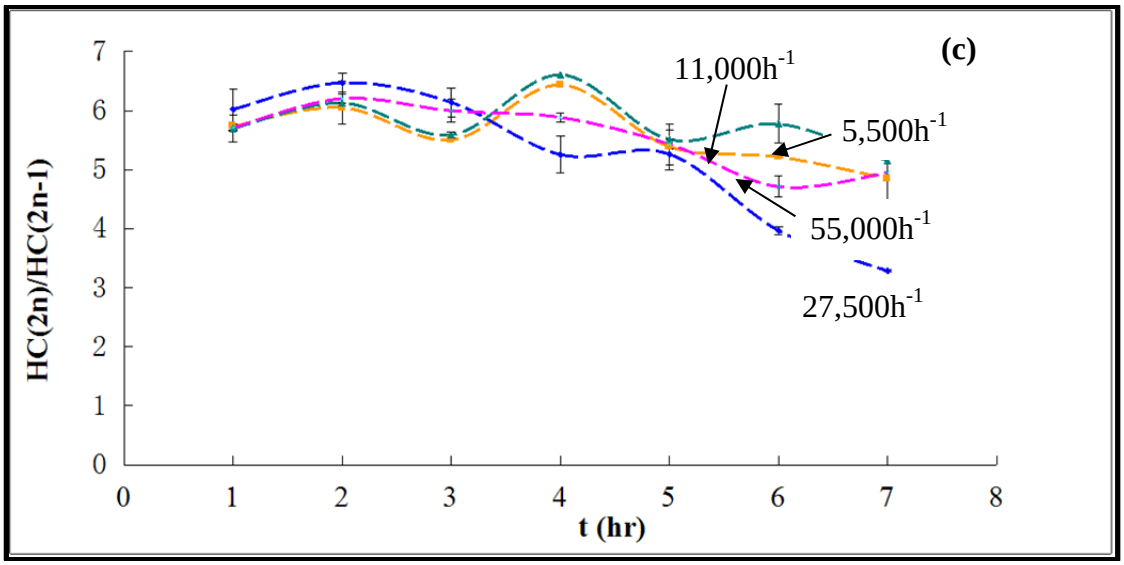

Figure 3.18: Effect of GHSV on (a) carbon yield in hydrocarbon , (b) hydrocarbon yield and (c) ratio of even number carbon hydrocarbon to odd number carbon hydrocarbon (Presulfided NiMo, 1.32wt% Nannochloropsis Salina oil in Dodecane, T=310°C, H_2 pressure=500psig, liquid flow rate=0.05ml/min, LHSV=55 h^{-1}).

As shown in Figure 3.19 for the GHSV of at least 11000h^{-1}, the conversion decreases in the following order: 55000h^{-1}>27500h^{-1} >11000h^{-1}. It proves again that the reaction is not kinetically controlled. Furthermore, it can be seen that the rate at which the conversion declines increases with increase in residence time. This rapid catalyst deactivation at lower GHSV could be due to the accumulation of oxygenates on the catalyst bed. This result agrees qualitatively with that on the effect of GHSV on hydrocarbon yield.

At 5500h^{-1} GHSV, the conversion is initially high and then decreases by 2% within one hour of reaction. However, the hydrocarbon yield (see above) is close to that at 11000h^{-1}, but shows a sharp decrease from the 2nd hour to the 3rd hour. The large difference between conversion and yield is due to the fact that the hydrotreating of fatty acids is the rate-limiting step. This step is not kinetically controlled but limited by mass transfer.

Taking all these observations into consideration, high H_2 flow rate favors hydrotreating as expected. Mass transfer will be enhanced at high gas flow rate due to the high recirculating flow in Taylor slug flow observed in microreactors. In addition, hydrogen serves not only as a reactant, but also as a buffer gas for catalyst protection against deactivating effect of gaseous products especially CO.

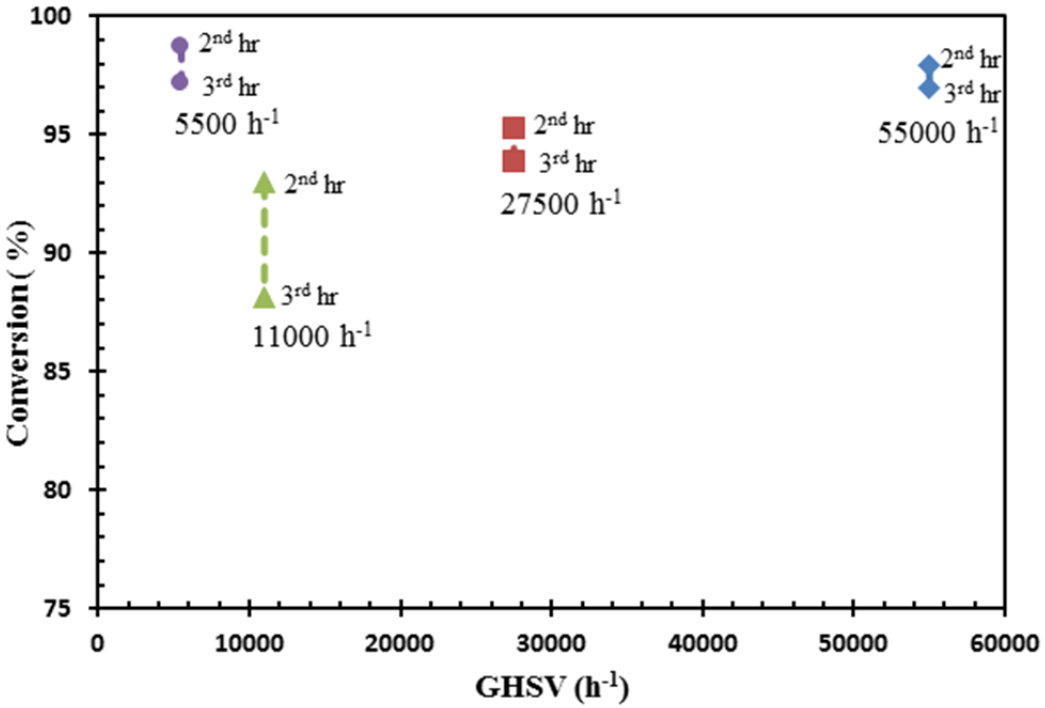

Figure 3.19: Effect of GHSV on microalgae oil conversion based on measured fatty acids (Presulfided NiMo, 1.32wt% Nannochloropsis Salina oil in Dodecane, T=310°C, H_2 pressure=500psig, liquid flow rate=0.05ml/min, LHSV=55 h^{-1}).

III.1.5. Hydrogen to Oil Ratio

The hydrogen to oil ratio is an important process parameter in hydrotreating. The conventional H_2/oil ratio refers to the ratio of hydrogen feed (standard temperature and pressure, STP) to the total liquid feed, solvent included, (Yang et al., 2013). In this project, experiments were conducted to investigate the effect of H_2/oil ratio between 1000 SmL/mL to 385 SmL/mL by adjusting liquid flow rate. Reaction temperature, pressure, GHSV, and catalyst loading were kept constant. Since the actual hydrogen flow rate was at least 24 times higher than the liquid flow rate, the effect of liquid flow rate variation on superficial flow velocity was negligible; hence the residence time remained the same at all studied ratios of H_2/oil.

As shown in Fig. 3.20 (a), during the 7 hour-long reaction, hydrocarbon yield increased with the increase in H_2/oil ratio. For H_2/oil ratio less than 1000 SmL/mL, the yields decreased rapidly after 1 hour reaction and were less than 10% after 3 hours. However, there was no observable change in yield for H_2/oil ratio of 1000 SmL/mL for at least the next 4 hours. The same trend is observed in the microalgae oil conversion results (Fig. 3.20 (b)). During the experiment, it was observed that the liquid slug length decreased with the increase of H_2/oil ratio. Since the gas to liquid mass transfer is a strong function of the liquid slug length (Kreutzer et al., 2001), the increase of H_2/oil ratio will enhance the gas-liquid convective mass transfer, therefore resulting in high yield of product. In contrast, more intermediates were formed at lower H_2/oil ratio because of insufficient amount of hydrogen. As has been stated above, because the conversion of fatty acids is the rate-limiting step, the formed intermediates were mainly fatty acids, which had low solubility in dodecane, and would precipitate on the catalyst surface. Due to the accumulation of oxygenated intermediates on the active sites of the catalyst, the catalyst was, in

general deactivated. However, at elevated H_2/oil ratio, catalyst activity was high and seemed to decrease with time at a moderate rate.

These results show that hydrogen acts not only as reactant, but it also serves to protect the hydrotreating catalyst by preventing the adsorption of the oxygenates on the catalyst surface. The ratio of even number carbon hydrocarbon to odd number carbon hydrocarbon (Fig. 3.20 (c)) changes with on-stream time and follows the same trend as the product yield and reactant conversion, which indicates that the catalyst selectivity correlates with catalyst activity. Therefore, to keep this ratio constant for product quality control, catalyst deactivation needs to be prevented.

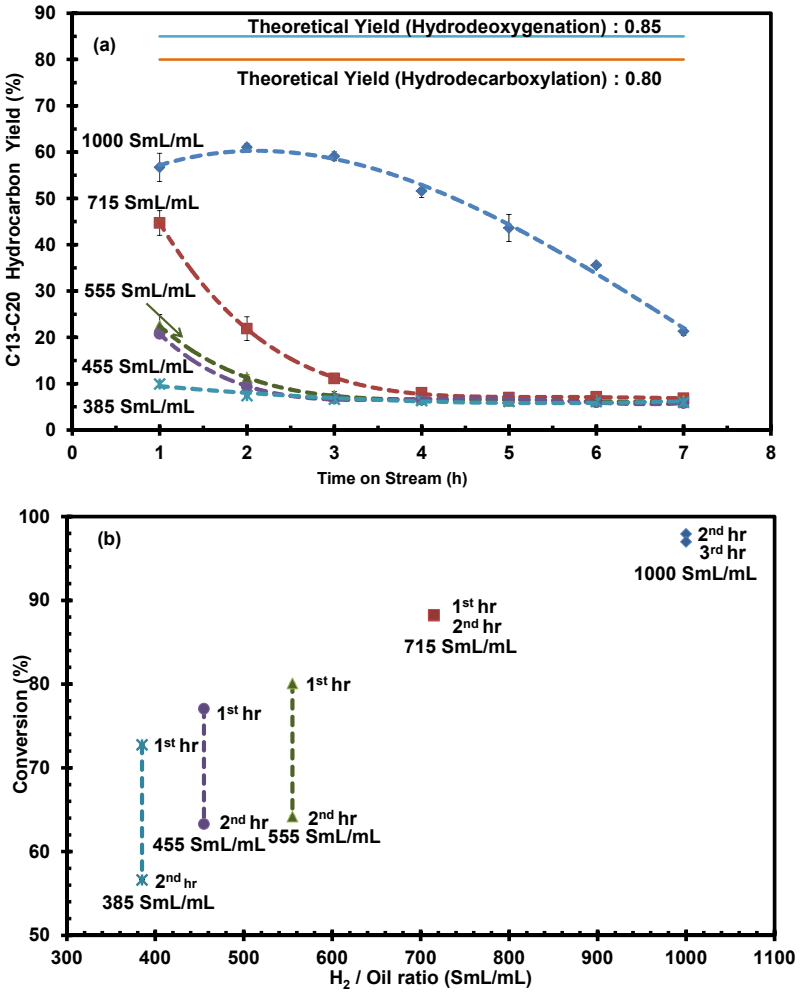

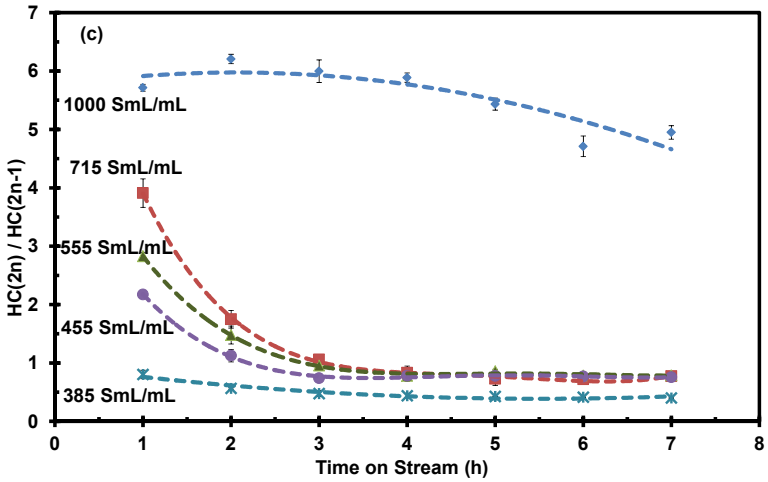

Figure 3.20: Effect of H_2/oil ratio on (a) C13 to C20 hydrocarbon yield, (b) microalgae oil conversion based on measured fatty acids, and (c) ratio of even number carbon hydrocarbon to odd number carbon hydrocarbon (46mg pre-sulfided NiMo, 1.32wt% Nannochloropsis Salina oil in Dodecane, Temperature= 310°C, H_2 pressure=500 psig, residence time= 1s, GHSV=55,000 h^{-1}).

III.1.6. Residence Time

The residence time is defined in this report as the volume of the reactor divided by the superficial volumetric flow rate of the reactants, which is calculated based on the empty bed assumption. The residence time was changed by varying reactor length from 3 cm to 18 cm, as well as the catalyst loading, while keeping all fluid flow rates unchanged. Other experimental conditions, such as temperature, pressure, superficial flow velocity were held constant. The H_2/oil ratio of 1000 SmL/mL was held fixed in all runs to eliminate the convective mass transfer influence. Therefore, weight hourly space velocity (WHSV) was decreased with the increase of residence time. The results in Fig. 3.21 (a)-(c) show that hydrocarbon yield, microalgae oil conversion and ratio of even number carbon hydrocarbon to odd number carbon hydrocarbon increase with the increase of residence time (between 0.25 to 1.5 s) because the catalyst loading increases. Also, all studied performance parameters decline more slowly at longer residence time, which indicates that, per unit mass of catalyst, less oxygenated intermediates were produced and accumulated on catalyst surface. It can be concluded that, when the same amount of reactant is fed into the reactor, the catalyst activity and its stability are a function of catalyst loading. Therefore, decreasing the WHSV is a way to maintain the overall catalyst activity, but productivity will be sacrificed at the same time.

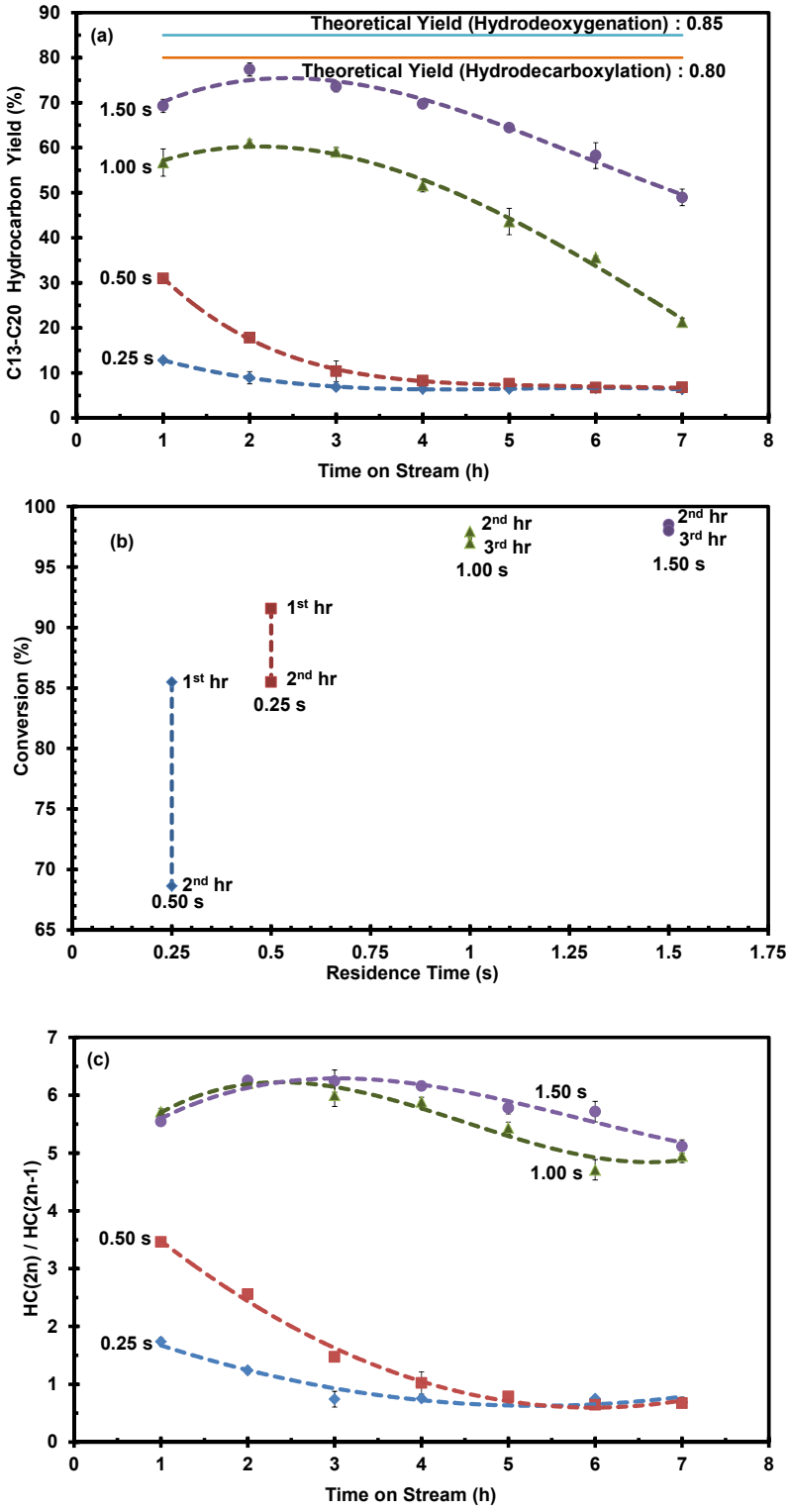

Figure 3.21: Effect of residence time on (a) C13 to C20 hydrocarbon yield, (b) microalgae oil conversion based on measured fatty acids, and (c) ratio of even number carbon hydrocarbon to odd number carbon hydrocarbon (pre-sulfided NiMo

catalyst, 1.32wt% Nannochloropsis Salina oil in Dodecane, Temperature=310°C, H2 pressure=500 psig, superficial flow velocity=0.117 m/s).

III.2. Mass Transfer Analysis

We have examined the effect of reaction temperature, liquid hourly space velocity (LHSV), gas hourly space velocity (GHSV), reaction pressure, hydrogen to oil ratio and residence time on C13 to C20 hydrocarbon yield, carbon yield, ratio of even number carbon hydrocarbon to odd number carbon hydrocarbon, and microalgae oil conversion. Because of the importance of mass transfer in reactor performance, it was important to establish experimental process conditions under which the hydrotreating experiments would not be limited by mass transfer.

III.2.1. Analysis of External Mass Transfer Limitation

According to fluid flow characterization results in the literature (Tadepalli et al., 2007), all the experiments we conducted for catalyst evaluation were performed in Taylor flow regime, comprising of alternating liquid slugs (blank) and gas bubbles (blue), as indicated in Scheme 3.1. Since reaction occurs only at the active sites on the catalyst surface, the hydrodeoxygenation of microalgae oil reaction on NiMo catalyst involves a 3-step external mass transfer as shown in Scheme 3.1: First, the transfer of hydrogen from the bulk gas phase to gas-liquid interface, the cap of the hydrogen bubble; then the diffusion of hydrogen into the bulk liquid phase; finally, the transfer of dissolved hydrogen and microalgae oil to the external surface of the catalyst through the solid-liquid boundary layer.

Since the gas phase is almost pure hydrogen and the gas-liquid interface is saturated with this gaseous reactant, the main mass transfer resistances occur at the gas-liquid and liquid-solid interfaces, with the former being predominant. As the transfer rates through interfaces depend greatly on flow velocity, the overall external mass transfer limitation can be studied experimentally by examining the change of hydrocarbon yield rate at various superficial flow velocities by increasing gas and liquid flow rate but keeping the gas to liquid ratio unchanged, and the residence time constant. The latter is achieved by varying the catalyst loading. The STY of C13 to C20 hydrocarbon at different superficial flow velocities is depicted in Fig. 3.22. The result shows that the reaction rate is independent of the flow velocity within the studied range. This indicates that the reaction is not limited by external mass transfer even at the lowest superficial flow velocity of 0.117 m/s.

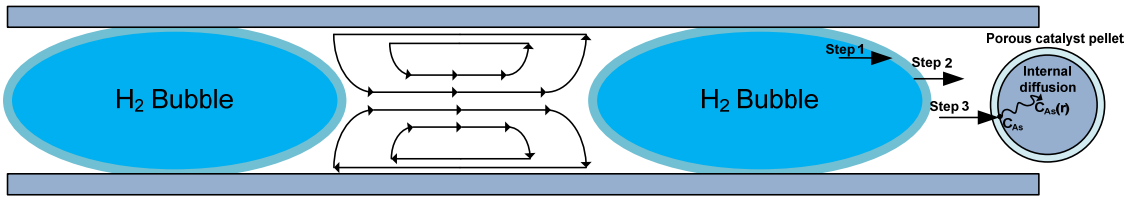

Scheme 3.1: **External and Internal mass transfer analysis for Taylor flow.**

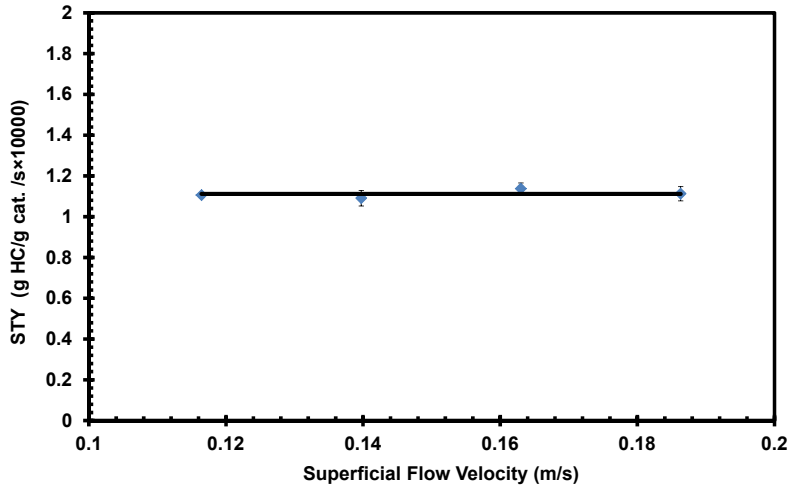

Figure 3.22: Effect of superficial flow velocity on space-time yield of C13 to C20 hydrocarbon. (Pre-sulfided NiMo, 1.32wt% Nannochloropsis Salina oil in Dodecane, Temperature=310°C, H_2 pressure=500 psig, residence time= 1s, H_2/Oil=1000 SmL/mL).

III.2.2. Analysis of Internal Mass Transfer Limitation

As shown in Scheme 3.1, internal mass transfer refers to the diffusion of reactants from the catalyst pellet pore entrance into the pore. The reaction is considered as internal mass transfer limited when the reactants concentration inside the pores is much lower than that at the entrance. This variation in concentration throughout the catalyst pellet can be evaluated by calculating the Weisz-Prater parameter (Fogler, 1999), C_{WP}

$$C_{WP} = \frac{\text{actual reaction rate}}{\text{a diffusion rate}} = \frac{-r'_{A(obs)} \cdot \rho_p \cdot R^2}{D_e \cdot C_{As}} \qquad (3.1)$$

where:

$-r'_{A(obs)}$ = 1.11×10^{-4} g Hydrocarbon / g Cat./s is the observed reaction rate,

ρ_P = 0.29g Cat./cm^3 is the catalyst pellet density,

R = 112.5×10^{-4} cm is the characteristic diameter of the catalyst pellets,

C_{As} = 360 g/m^3 is the hydrogen concentration at the external surface of the catalyst pellet, which can be obtained from the hydrogen solubility data in dodecane, approximately, and D_e is the effective diffusivity of hydrogen in the catalyst pellets, which can be calculated using the equation: $D_e = (D_{AB}\varphi_P\sigma_C)/\tau$, where D_{AB} =1.12 ×10^{-7}m^2/s is the binary diffusivity of H_2 in dodecane; (Matthews et al., 1987) ϕ_p =0.4-0.6 is the porosity of the catalyst pellets; ρ_c = 0.7-0.8 is the catalyst constriction factor; τ =2-8 is the catalyst tortuosity. Therefore, D_e is 3.92×10^{-9} to 2.69×10^{-8} m^2/s.

The Weisz-Prater parameter is calculated to be between 0.042 and 0.289 depending on effective diffusivity value. By the definition, C_{WP} << 1 means reaction rate is much smaller than the diffusion rate, which indicates that hydrogen concentration gradient is negligible inside the catalyst pores and the reaction is not internal-diffusion-limited.

Therefore, at a pressure of 500 psig H_2, temperature of 360°C, H_2/Oil ratio of 1000 SmL/mL, and residence time of 1 s, hydrotreating of algae oil using pre-sulfided NiMo/γ-Al_2O_3 in our microreactor would not be limited by mass transfer.

III.3. Conclusions

Reduced pre-sulfided NiMo/γ-Al_2O_3 catalyst was evaluated for green-diesel production from microalgae (Nannochloropsis Salina) oil via hydrodeoxygenation. Based on the external and internal mass transfer limitation analysis, the catalyst was evaluated by studying changes in the microalgae oil conversion and the product yield and composition as a function of operating conditions: hydrogen to oil ratio, residence time, reaction temperature and pressure. The results revealed that the conventional hydrotreating catalyst, pre-sulfided NiMo/γ-Al_2O_3, was deactivated due to the accumulation of produced oxygenated intermediates in hydrodeoxygenation reaction, and its selectivity to even number carbon hydrocarbon produced from hydrodehydration correlates with the catalyst activity. The catalyst activity and life can be preserved by elevating hydrogen to oil ratio, residence time, reaction temperature, and pressure, which will decrease the adsorption of oxygenates on the catalyst surface. Reaction temperature (in the range of 310 to 360^{o}C) and pressure between 300 and 500 psig have negligible effect on initial catalyst activity. Hydrogen acts not only as a reactant, but it also serves to protect the hydrotreating catalyst. Weight hourly space velocity (WHSV) is reduced when residence time is increased by increasing catalyst loading therefore the packed bed is exposed to decreasing amount of reactant per gram catalyst. It should be noted that the formation of gaseous product, such as CO, CO_2, CH_4, propane, and water vapor, decreases the hydrogen partial pressure which leads to poor catalyst activity. The optimum conditions for hydrotreating of microalgae oil were determined to be 500 psig H_2, 360^{o}C, H_2/Oil ratio of 1000 SmL/mL, and residence time of 1 s. For this set of conditions the initial catalyst activity was maintained without any signs of deactivation for at least 7 hours and the obtained C13 to C20 hydrocarbon yield was 56.2%, with a carbon yield of 62.7%, nearly complete conversion (98.7%) of microalgae oil, and HC(2n)/HC(2n-1) ratio of 6.

III.4. References:

Fogler, H. S., Elements of chemical reaction engineering. 1999.

Kreutzer, M. T.; Du, P.; Heiszwolf, J. J.; Kapteijn, F.; Moulijn, J. A., Mass transfer characteristics of three-phase monolith reactors. *Chemical Engineering Science* 2001, *56* (21), 6015-6023.

Matthews, M. A.; Rodden, J. B.; Akgerman, A., High-temperature diffusion of hydrogen, carbon monoxide, and carbon dioxide in liquid n-heptane, n-dodecane, and n-hexadecane. *Journal of Chemical and Engineering Data* 1987, *32* (3), 319-322.

Tadepalli, S.; Halder, R.; Lawal, A., Catalytic hydrogenation of o-nitroanisole in a microreactor: Reactor performance and kinetic studies. *Chemical Engineering Science* 2007, *62* (10), 2663-2678.

Yang, Y.; Wang, Q.; Zhang, X.; Wang, L.; Li, G., Hydrotreating of C18 fatty acids to hydrocarbons on sulphided NiW/SiO2-Al2O3. *Fuel Processing Technology* 2013, *116*, 165-174.

IV. Hydrotreating of Bio-Oil Feedstocks in High Pressure High Throughput (Pilot Plant) Reactor System

IV.1. Preliminary Evaluation of Reactor System

Upon the completion of the design, fabrication, and assembly of the high flow rate, high pressure pilot plant monolith catalyst HDO reactor system, preliminary experimental runs were carried out. The reactor, which housed the catalyst, was a SS316 tube of outer diameter of 25 mm and inner diameter of 21 mm. The SS316 tube was heated using a three-zone electrical furnace and temperatures in different zones in the furnace were controlled by controllers. Reaction was carried out at a set temperature and pressure. Even though this high flow rate, high pressure monolith catalyst HDO reactor system was capable of handling pressures up to 2500 psig, the experimental runs were limited to pressures lower than 1000 psig. The reason is that during the visit by Marathon Petroleum Corporation (see Task 5 below), we were informed that HDO processes in their refineries are run at 700 psig and not higher. We therefore conducted leakage tests at pressures up to 1000 psig using nitrogen gas. For the trial runs, a packed bed of Co-Mo catalyst supported on γ-alumina was used. 1.2 g of catalyst of particle size 75-150 μm mixed with 90 μm size glass beads to create a bed height of 3.0 cm in the SS316 tube was used. The glass beads were used as inert. Preliminary runs were conducted using as liquid feed, pure canola oil as well as canola oil solution in hexane, and pure hydrogen gas as the gaseous reactant. The reaction pressure used in the runs was 700 psig and the furnace temperature in the reaction zone was varied from 300^{o}C to 350^{o}C. The liquid reactant flow rate was 2.0 ml/min and hydrogen gas flow rate was 1000 sccm. Each experimental run was carried out for a duration of 4-8 hours. After an experimental run, a liquid sample was collected and analyzed in a GC-FID for hydrocarbons.

In all the experimental runs, the pressure across the first HPLC pump gradually increased to a high value. A run was stopped when the pressure drop across HPLC pump increased to more than 3300 psi. This high pressure drop in the pump was due to clogging of the pump filter. The clogging was probably due to formation of coke particles but more likely solid reaction intermediates. Analyses of the liquid products showed that with 300^{o}C furnace temperature the hydrocarbon yields were very low, but increased with increase in furnace temperature. The low hydrocarbon yield could be due to a number of factors, including low activity of the Co-Mo catalyst, low reaction temperature and pressure during the reaction, and low contact time with the catalyst.

IV.2. Evaluation of Catalysts for HDO of Canola Oil and Nannochloropsis Algae Oil

We selected for evaluation in the pilot plant the conventional HDS catalyst, NiMo, and a few of the promising precious metal-based catalysts from the catalyst screening exercise we carried out in Section II. We continued the experiments in the pilot plant using pre-sulfided Ni-Mo catalyst in a packed bed form and Pt-Rh catalyst on γ-alumina washcoated on a monolith. The Ni-Mo packed bed catalyst was used for the hydrodeoxygenation (HDO) of canola oil and Pt-Rh catalyst in a monolith was used for the HDO of Nannochloropsis Salina algae oil and canola oil. Two other catalysts, 0.5wt% Pt/1wt% Rh and 0.5wt% Rh/15wt% Mo, were evaluated in the pilot plant but the results are not presented here because they do not qualitatively differ much from the results in Sections II.2 and II.3 above.

For the packed bed operation, the catalyst pellets were ground and sieved. Catalyst particles in the size range of 75 μm to 150 μm were used for the reaction. The catalyst was placed inside a SS316 sleeve and the sleeve was placed above a blank monolith inside the reactor, a SS316

tube of 2.1 cm inner diameter. The inner diameter of the sleeve was 1.9 cm and total height of the sleeve was 9.5 cm. The catalyst was mixed with inert glass beads 90 μm in size for a total catalyst bed height of 3.7 cm inside the sleeve. The SS316 tube in which the reactor sleeve was placed had a length of 90 cm and was divided into three heating zones. The catalyst bed was located in the first zone. This zone was also used to heat the reactants. The monolith was placed just above the second zone and the third zone is the zone below the monolith. The temperature in each zone was controlled by temperature controllers and the temperatures were measured by thermocouples. The zone 1 thermocouple was inserted through a reactor fitting at the top to measure the temperature inside the catalyst bed. The zone 2 thermocouple was placed on the reactor wall, and zone 3 thermocouple was placed below the monolith through a fitting at the bottom of the reactor. When the reaction was conducted with the monolith catalyst, two pieces of cylindrical monoliths containing Pt-Rh catalyst on γ– Al_2O_3, each of length 7.0 cm and outer diameter 1.9 cm were inserted inside the SS316 tube overlapping zone 1 and zone 2. The monolith was wrapped in glass wool to hold it in place inside the reactor. The zone 1 thermocouple was placed just above the monolith. The flow channels in the monolith were square with side of length of 1.1 mm. The monolith had 400 cells/in^2 of cross sectional area.

In making a run, the catalyst was first reduced with hydrogen at the reaction temperature and pressure for two hours. Hydrogen gas, delivered by a high pressure gas cylinder was metered by a mass flow controller (MFC). The liquid feed was mixed with hydrogen in a T-junction and the mixture flowed to an atomizer where the liquid was atomized to fine droplets and sprayed on the catalyst bed. The inlet and outlet pressures were measured by pressure transducers. From the reactor the product flowed through an in-line filter.

IV.2.1. 8 g Ni-Mo Particulate Catalyst

In all the experimental runs, 8.0 g of Ni-Mo catalyst of 75 to 150 micron size was used. The catalyst was mixed with glass beads of 90 micron size to occupy a height of 3.7 cm in the reactor sleeve. Three concentration levels of canola oil in dodecane solution, namely, 25 wt%, 50wt% and 75wt% were used in the experiments which were conducted at three temperature values, 300^oC, 330^oC and 350^oC. The liquid feed solution flow rate was 0.30 ml/min and the hydrogen gas flow rate was 500 sccm. The reaction pressure was set at 700 psig. A LHSV of 1.72 hr^{-1} (based on bed volume including inert beads) was used in all the runs. Liquid samples were collected from the gas liquid separator. For each experimental run, the first liquid sample was collected 2 -3 hours after the start of reaction and then every hour up to 6-8 hours. Figures 3.23, 3.24 and 3.25 show the data on the hydrocarbon yields obtained at different concentrations of canola oil and different temperatures. The average steady values of the hydrocarbon yields at different temperatures and canola oil concentrations are shown in Table 3.7. It appears from these data that with 25wt% feed canola oil concentration, a maximum hydrocarbon yield of 70 g of hydrocarbon per 100 g of canola oil was attained at 330^oC. Propane and other smaller hydrocarbons were not measured in these experiments. The maximum possible hydrocarbon yield for these liquid hydrocarbons is 86g of hydrocarbon per 100 g of canola oil when all the hydrocarbons are obtained by dehydration route only, and the maximum theoretical yield of liquid hydrocarbon is 81g of hydrocarbon per 100 g of canola oil for the decarboxylation route only. The product analyses with Ni-Mo catalyst showed product hydrocarbons consisting of approximately 70% even number of carbon atoms (mainly octadecane) and 30% odd number of carbon atoms (mainly heptadecane). Thus approximately 70% of the product hydrocarbons were formed by dehydration route and 30% of the hydrocarbons were formed by decarboxylation route. 82% of the theoretically possible hydrocarbon yield was thus obtained in this work. Moreover, some hydrocarbons might have undergone cracking reactions to form smaller hydrocarbons which were not measured. At a

higher temperature of 350°C, the hydrocarbon yield was found to be lower than the yield at 330°C. This might be due to cracking of the hydrocarbons at higher temperature with this Ni-Mo catalyst.

With 50wt% and 75wt% canola oil in the feed, solid was found to form in the product stream, possibly due to insufficient amount of the solvent dodecane. The product hydrocarbon mixture was found to contain around 70wt% n-octadecane. N-Octadecane has a melting point of 28-30°C. The room temperature for the experiment was around 20°C, so the solids could be due to the formation of octadecane. The actual hydrocarbon yields obtained with 50wt% and 75wt% canola oil could be much higher than the hydrocarbon yields shown in Figs 3.23-3.25 and Table 3.7.

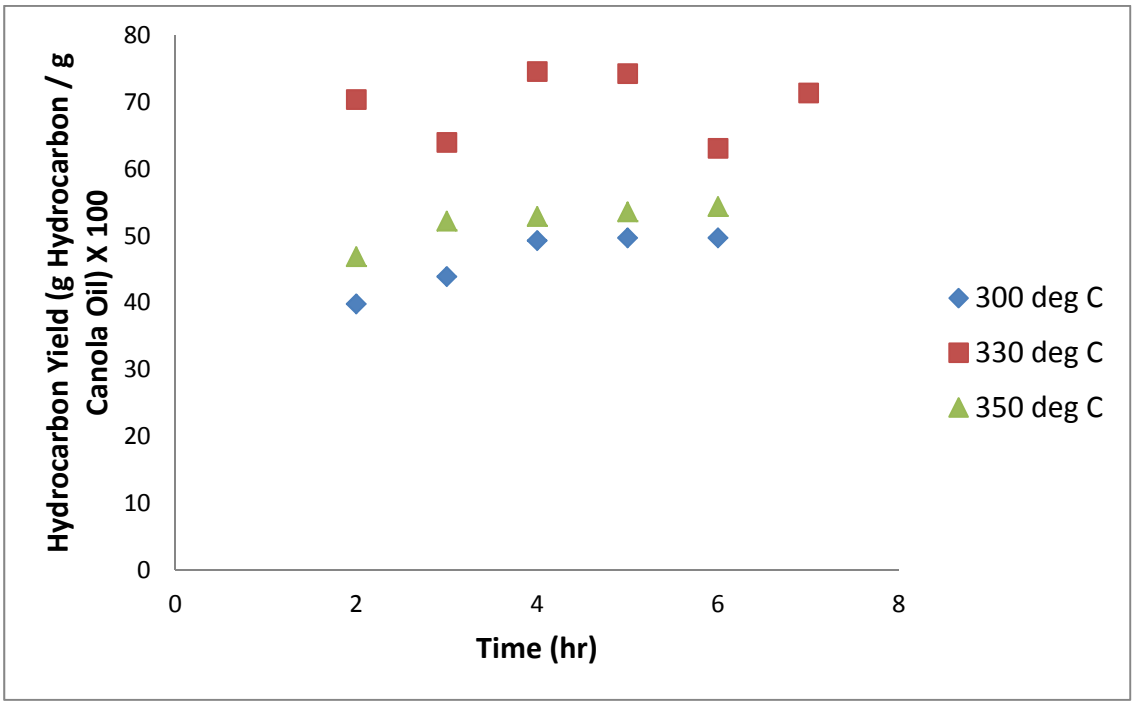

Figure 3.23: Hydrocarbon yield in the hydrodeoxygenation of 25wt% canola oil in dodecane solution at different temperatures (Liquid feed solution flow rate = 0.30 ml/min, H_2 flow rate = 500 sccm, and 8.0 g of Ni-Mo catalyst)

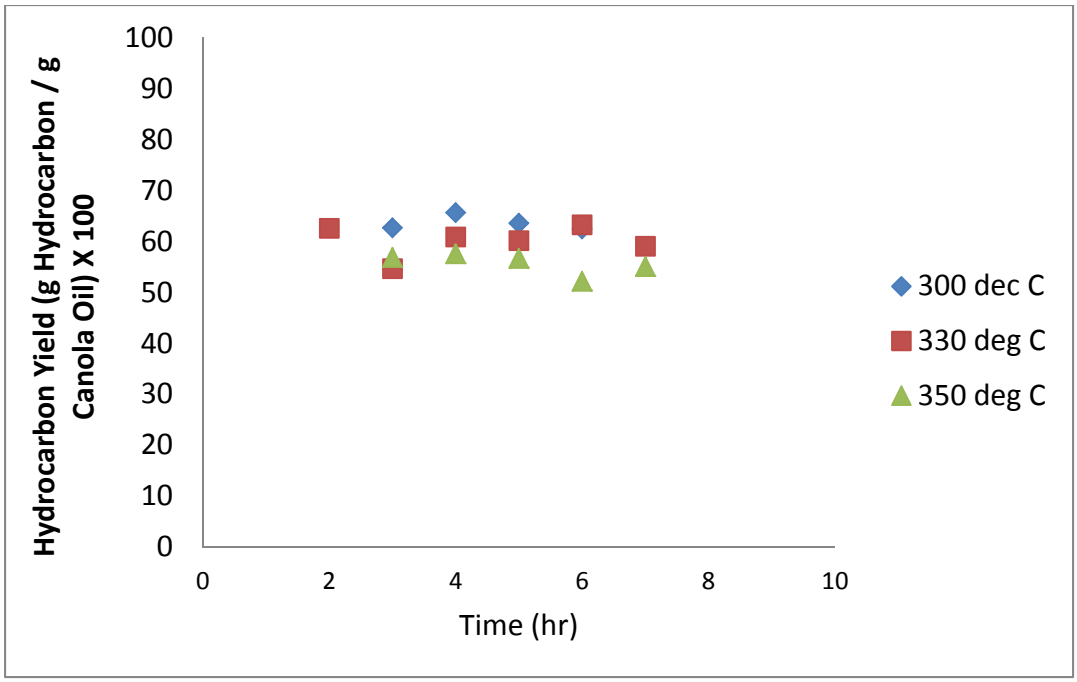

Figure 3.24: Hydrocarbon yield in the hydrodeoxygenation of 50wt% canola oil in dodecane solution at different temperatures (Liquid feed solution flow rate = 0.30 ml/min, H_2 flow rate = 500 sccm, and 8.0 g of Ni-Mo catalyst)

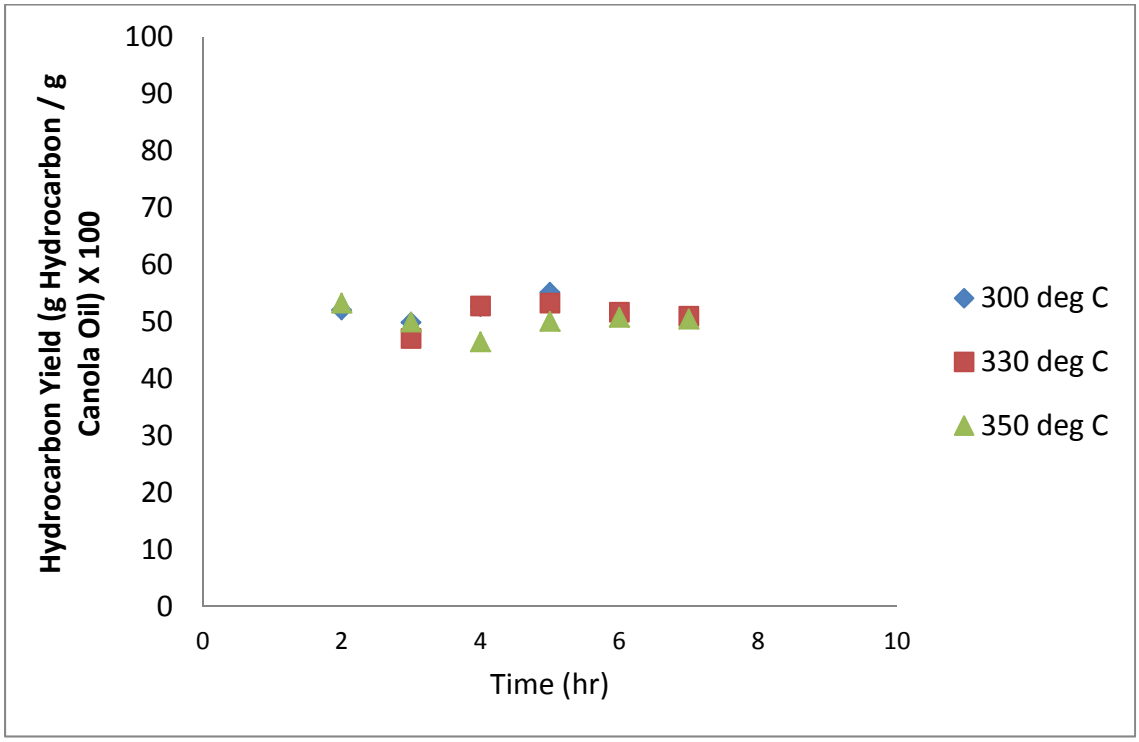

Figure 3.25: Hydrocarbon yield in the hydrodeoxygenation of 75wt% Canola Oil in dodecane solution at different temperatures (Liquid feed solution flow rate = 0.30 ml/min, H_2 flow rate = 500 sccm, and 8.0 g of Ni-Mo catalyst)

Table 3.7: Experimental data on HDO of canola oil in dodecane using Ni-Mo catalyst.

Serial #	Concentration of canola oil in dodecane solution (wt%)	Reaction Temperature (^oC)	Hydrocarbon Yield (g of HC/g of oil) X 100
1	25.0	300	49.7
2	25.0	330	69.6
3	25.0	350	53.2
4	50.0	300	63.6
5	50.0	330	60.1
6	50.0	350	55.7
7	75.0	300	52.5
8	75.0	330	52.2
9	75.0	350	50.2

The hydrocarbon yields given in the table are the average values obtained at steady state which was attained after 2-3 hours of running the reaction.

IV.2.2. 5.2 g Monolith Pt-Rh Catalyst

Hydrodeoxygenation of algae oil (Nannochloropsis Salina) and canola oil was studied in the monolith reactor. In this reactor, a fixed amount of catalyst was used and only the effect of reaction temperature on the hydrocarbon yield was studied. The algae oil feed solution was obtained by dissolving the oil in dodecane and then filtering the solution through VWR 410 filter paper with pore size of 1 micron. The calculation of hydrocarbon yield was based on the oil fed. Figures 3.26 and 3.27 show the hydrocarbon yield obtained with algae oil and canola oil respectively as a function of time on-stream and at two temperatures, 330^{o}C and 350^{o}C. From the data, it appears that with the Pt-Rh catalyst, the hydrocarbon yield obtained at 350^{o}C was slightly higher than that at 330^{o}C. The reverse was the case with the Ni-Mo catalyst as the yield at 330^{o}C was found to be higher than that at 350^{o}C as mentioned above, which was attributed to the cracking of hydrocarbon products at higher temperatures. With the Pt-Rh catalyst and canola oil, more than 95% of hydrocarbons were found to be odd-number-carbon hydrocarbons which suggests that the hydrotreating took place predominantly by the decarboxylation/decarbonylation route. With algae oil also, concentrations of hydrocarbons with odd-number-carbon hydrocarbons were also much higher than hydrocarbons with even number of carbon atoms. As mentioned above, with the Ni-Mo catalyst the hydrodeoxygenation might be mainly by dehydration route. Whereas 82% of the maximum theoretical liquid hydrocarbon yield from canola oil was obtained with packed bed Ni-Mo catalyst, 61% maximum theoretical liquid hydrocarbon yield from canola oil was obtained using Pt-Rh monolith catalyst. Therefore, for these experimental conditions, the monolith catalyst might not be as effective as the packed bed catalyst, noting however the difference in the amounts of catalyst used, 8 g vs. 5.2 g.

Based on these results, it was planned to perform experiments using Pt-Rh catalyst in particulate form to compare its effectiveness with that of Ni-Mo packed bed catalyst. The lower yield of hydrocarbons with algae oil in comparison with canola oil might be due to the lower concentration of fatty acid component in the algae oil. Canola oil virtually contains 100% fatty acid esters whereas the filtered algae oil contains some non-fatty acid components.

Figure 3.28 shows the data of a reproducibility run conducted at 330°C. It appears from the data that the run made with algae oil at 330°C was reproducible. The average values of the hydrocarbon yields obtained with algae oil and canola oil hydrodeoxygenation at 330°C and 350°C are given in Table 3.8.

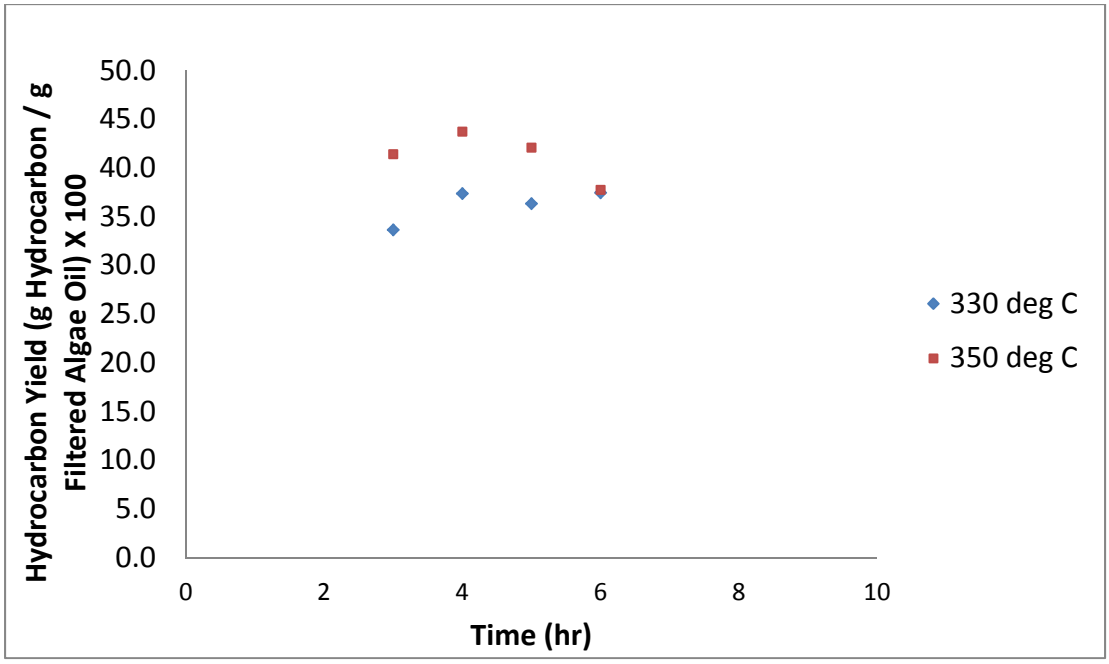

Figure 3.26: Hydrocarbon yield in the hydrodeoxygenation of 20.6% algae oil in dodecane at different temperatures (Liquid feed solution flow rate = 0.30 ml/min, H_2 flow rate = 500 sccm, 5.2 g of Pt-Rh monolith catalyst)

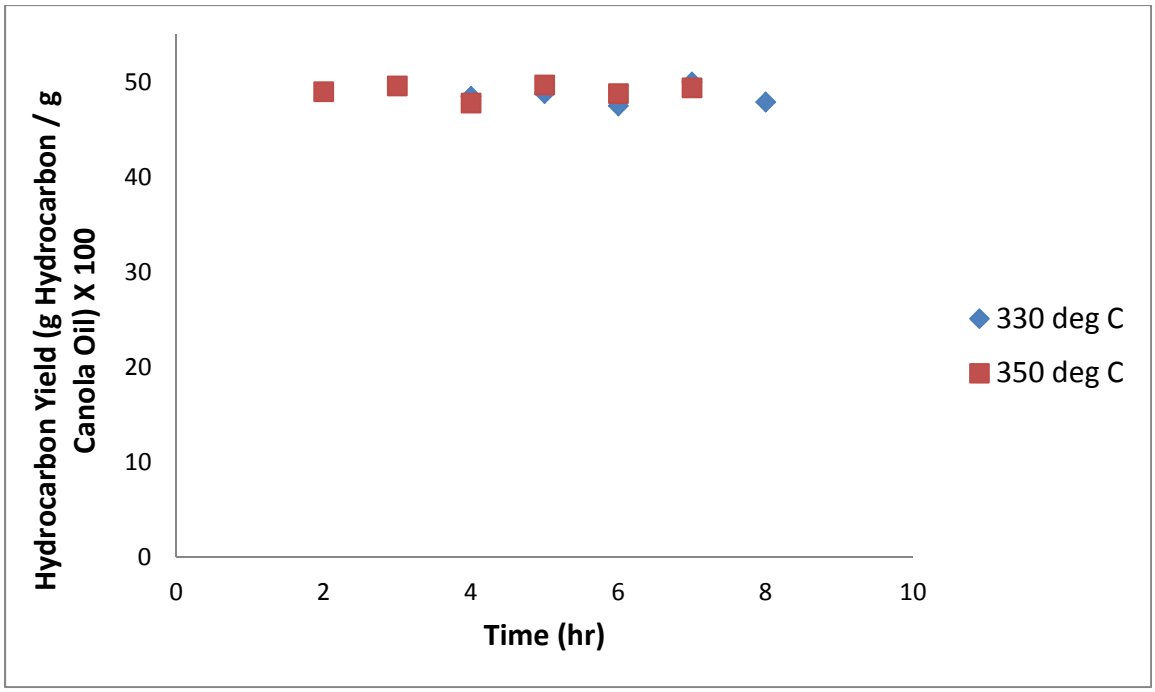

Figure 3.27: Hydrocarbon yield in the hydrodeoxygenation of 25% canola oil in dodecane at different temperatures (Liquid feed solution flow rate = 0.30 ml/min, H_2 flow rate = 500 sccm, 5.2 g of Pt-Rh monolith catalyst)

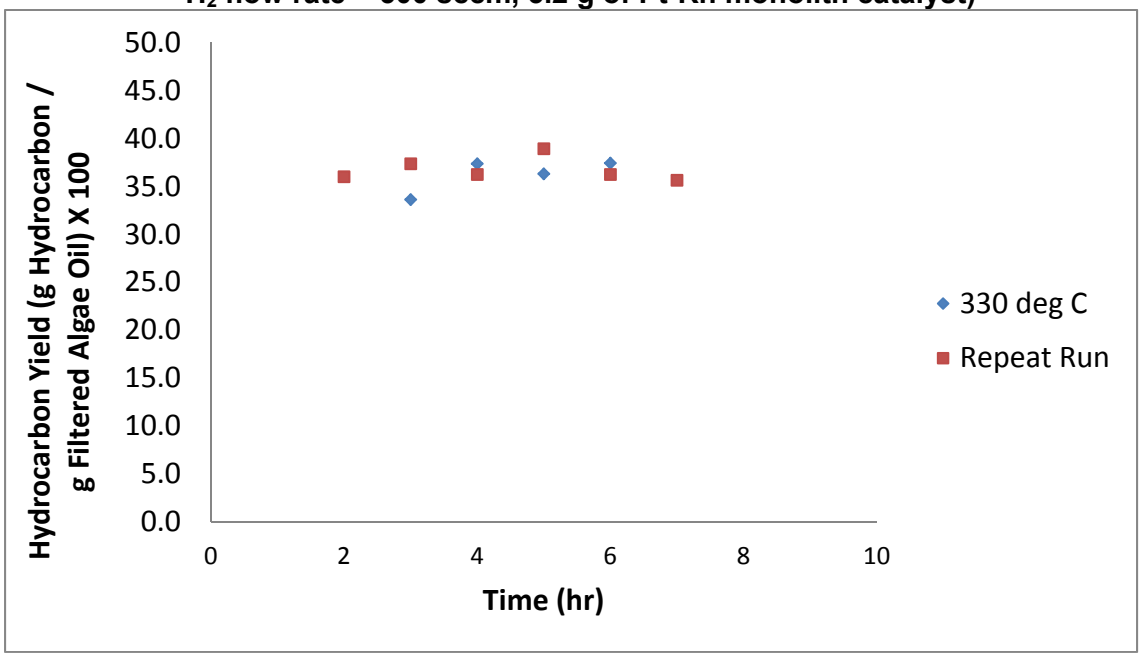

Figure 3.28: Reproducibility of hydrodeoxygenation of 20.6% algae oil in dodecane at 330°C (Liquid feed solution flow rate = 0.30 ml/min, H_2 flow rate = 500 sccm, 5.2 g of Pt-Rh monolith catalyst)

Table 3.8: Experimental data on HDO of canola oil using Pt-Rh monolith catalyst.

Serial #	Concentration of oil in dodecane solution (wt %)	Reaction Temperature (^oC)	Hydrocarbon Yield (g of HC/g of oil) X 100
1	20.6% Algae oil	330	36.2
2	20.6% Algae oil	350	41.2
3	25.0% Canola Oil	330	48.5
4	25.0% Canola Oil	350	49.1

IV.2.3. Analysis of Residual Oxygen Content of Hydrotreated Algae and Canola Oils

Four samples of hydrotreated oil/dodecane mixtures from the high pressure high throughput reactor system were selected for residual oxygen content analysis. The samples were sent to Midwest MicroLab, LLC, and the results of the oxygen content analysis are given in Table 3.9.

Table 3.9: Results of Oxygen Content Analysis in some Product Samples Performed by Midwest MicroLab, LLC.

Catalyst	Oil concentration in solution (with Dodecane as solvent)	Reaction Temperature (^oC)	Liquid HC Yield (g HC/100 g Oil)	Oxygen Content found in Product (%)
8.0 g Ni-Mo in Packed Bed	Canola Oil, 25wt%	330	74	0.41
5.2 g Pt-Rh on Monolith	Nannochloropsis Salina Algae Oil, 15.4wt%	350	60	0.61
5.2 g Pt-Rh on Monolith	Nannochloropsis Salina Algae Oil, 15.4wt%	330	52	Not Detected
16.0 g 1wt% Pt in Packed Bed	Canola Oil, 75wt%	370	51	0.67

The lower detection limit of oxygen in the method developed by Midwest Microlab is 0.5%. The oxygen content in the product samples, as can be seen from the table, was generally very small, indicating that the HDO reaction was nearly complete in removing all the oxygen in the oxygenates.

IV.3. Preparation of Pt-based Bi-metallic Precious Metal Monolith Catalyst at Stevens

In preparation for co-processing of microalgae oil with refinery light atmospheric gas-oil using the monolith catalyst, we developed at Stevens an in-house method for monolith catalyst preparation. The alumina supported Pt-based bi-metallic precious metal monolith catalyst was prepared following the "Double slurry method" provided in Corning Incorporated's patent (US005212130A, Addiego et al., 1993).

As a first step, 190g of Pt-based bi-metallic precious metal catalyst on alumina was prepared in powder form. The catalyst powder was dried in static air for 2 hours at 150 ^{o}C, followed by1^{o}C/min ramping to 550^{o}C, and the catalyst calcined at this temperature for 2 hours.

In the second step, 171.5g (~30wt% with respect to the DI water) of the prepared powder catalyst was mixed with 401.0g of DI water and 8.6g (~5wt% of powder catalyst) of colloidal alumina (nanoparticle), and the entire mixture ball-milled (Labmill-8000, speed 6) for 24 hours. Meanwhile, 10 blank cordierite monolith substrates (0.75" OD, 2.75" length, 400 cpsi (cells per square inch)) from Corning were pretreated to enhance the specific surface area. (Gonzalez et al., 2007) The cordierite substrates were first treated in nitric acid (20 wt%) for 5 hours and washed with water until neutral. Afterward, the substrates were introduced into acetone for 2 hours for aging, dried in an oven at 100^{o}C for 2 hours, and finally calcined under static conditions at 600^{o}C for 2 hours. We also kept one blank substrate untreated for comparison.

In the final step, the in-house-designed "vacuum coating" device (Scheme 3.2 below) was used for coating the 11 monolith substrates with the ball-milled slurry. As shown in Scheme 3.2, the level of the slurry needed to be between 0.5" and 1" from the top edge of the reservoir, and the monolith should be placed at the center of the device. In order to restrict the flow of slurry to only the closed inside channels (and not the outer open channels), in addition to the rubber stopper, putty was also applied to the outside of the monolith some distance from the bottom of the monolith to block the open channels on the outer surface. The distance between the bottom surface of the putty and the top of the monolith was about 1". Each monolith channel is like a capillary, and to enhance the "capillary effect", vacuum was applied to this system. The vacuum pressure needed to be monitored and it was used to control the vacuum coating process in order to achieve reproducibility.

In general, after holding the vacuum pressure at ~21mmHg for about 10 seconds, a "fountain of slurry" would be observed above the monolith indicating a fill-up of the channels The monolith was removed from the device and was air-knifed (7.5 psig compressed air) to remove excess slurry and open any blocked channels. After that, the monolith was dried at 150^{o}C for 2 hours before adding another wash-coat layer. Wash-coating was repeated until the desired wash-coat loading in our case about 2.2 g/in^{3}, was reached. After the last layer was added, the monolith was dried at 150^{o}Cfor 2 hours, and then weighed to ensure that the targeted wash-coat loading had been attained. Since some moisture might be adsorbed during the weighing process, the monolith was dried again at 150^{o}C for 2 hours the temperature ramped to 550^{o}C at 1^{o}C/min, and held for 2 hours for calcination.

We observed that the wash-coat loading (g/in^{3}) value for each layer kept reducing for the first 3 layers, although the mass of adsorbed slurry remained almost the same, which would indicate not much change in pore volume during coating. We also observed visually that the slurry was becoming less viscous gradually. We then decided to ball-mill the slurry for another 11 hours before adding the 4th and 5th layers.

It should also be noted that the untreated monolith had higher g/in^{3} wash-coat loading than the pre-treated monoliths for each wash-coat layer. However, acid pretreatment of the monolith

substrate might still be advantageous for this hydrotreating catalyst because the acidity of the catalyst surface would be increased after pretreatment, and the surface acidity is known to be of vital importance in the hydrodehydration (DHYD) reaction route.

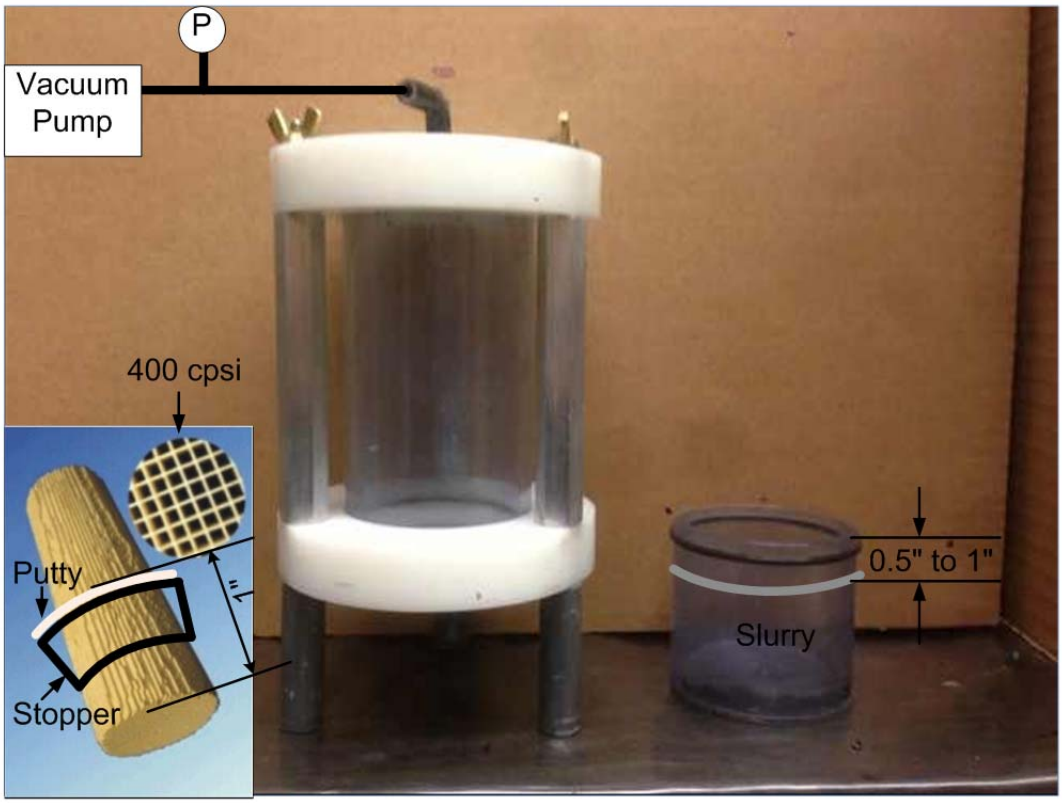

Scheme 3.2: In-house-designed "vacuum coating" device

IV.4. Co-Processing of Refinery Light Atmospheric Gas Oil (LAGO) with Algae Oil

The final phase of the project was the co-processing of mixtures of algae oil and refinery light atmospheric gas oil (LAGO) supplied to us by Marathon Petroleum Corporation (Ohio, USA). LAGO is a middle distillate stream from the atmospheric distillation column of a petroleum refinery. This distillate is hydrotreated in petroleum refining to produce diesel. The successful co-processing of a mixture of LAGO and algae oil will enable integration of algae oil as a refinery feedstock which is one of the goals of DOE-BETO. Our approach will involve the splitting of the LAGO stream from the distillation column into two streams with one stream (of much lower flow rate) being co-processed with the algae oil while the larger flow rate stream will be subjected to normal refinery hydrotreating process. The LAGO/algae oil stream will be processed in a separate Pt-based bi-metallic monolith catalyst reactor system that we have developed in this project to remove primarily the oxygen in the algae oil but also a substantial amount of the sulfur present in the LAGO. The amount of algae oil in the mixture can vary from 5 to 50 wt%, depending on the production capacity of the petroleum refinery and the algae oil plant. The co-processed ***upgraded*** stream will now be similar in physical and chemical properties to the refinery hydrotreated stream. Hence, both streams become compatible and can then be blended to produce low sulfur diesel. The blended mixture can be further hydrotreated to produce ultra low sulfur diesel as required. There are a number of advantages to the proposed approach to co-processing of algae oil and refinery middle distillate. The

petroleum refinery does not require any equipment or process modifications since the LAGO/algae oil mixture is processed in a separate stand-alone reactor system. This reactor system can be modular to accommodate different throughputs. The precious metal-based catalysts in our monolith reactor system, unlike the conventional hydrotreating catalysts (NiMo and CoMo) are not deactivated by water, a by-product of HDO of algae oil. Also, unlike CoMo, these catalysts are capable of removing sulfur and oxygen when both are present in the feed. The CoMo catalyst activity for sulfur (as well as nitrogen) removal has been shown to be inhibited considerably in the presence of CO (carbon monoxide), a product of HDO.

IV.4.1. Initial Evaluation of Co-Processing of Refinery LAGO and Bio-Oil using Canola Oil

IV.4.1.1. Low Pt Loading Bi-metallic Monolith Catalyst

In view of the limited supplies of *N. Salina* algae oil, from time to time we found it expedient during the project to use Canola oil as surrogate for algae oil. For the initial evaluation of the co-processing of refinery LAGO and Canola oil, we selected the low Pt loading bi-metallic monolith catalyst. We varied the concentration of Canola oil in the mixture and for each concentration, the HDO experiments were conducted at different temperatures. The results are presented in Table 3.10. The liquid products from HDO of 75wt% canola oil and 25wt% LAGO contained fatty acids, indicating incomplete HDO treatment of high concentrations of Canola oil at the selected process conditions. However, it was observed that a decrease to 60wt% concentration of Canola oil in LAGO resulted in successful HDO treatment.

Table 3.10: HDO of Canola oil and LAGO HDO conditions: Low Pt loading bimetallic monolith catalyst, Hydrogen flow rate=200sccm, Reaction pressure=700psig.

Catalyst	Feedstock	Reaction temperature (°C)	Observations
Low Pt loading bimetallic monolith catalyst	30wt% Canola oil and 70wt% LAGO	310	Clear, dark yellow liquid product was obtained at 2h. Subsequent liquid products were clear and light yellow.
		330	
		350	
	50wt% Canola oil and 50wt% LAGO	330	
		350	
	75wt% Canola oil and 25wt% LAGO	330	All samples were turbid and yellow. Precipitates settled over time.
		350	

	60wt% Canola oil and 40wt% LAGO		Liquid products were yellow and clear except for 2h sample.

The dark color of the samples at 2h could be explained by the algal oil that remained in the pilot plant system, affecting the initial samples of subsequent experiments.

IV.4.1.2. High Pt Loading Bi-metallic Monolith Catalyst

In order to investigate the effect of Pt loading on the hydroprocessing of the bio-oil/LAGO mixtures, we next conducted the co-processing of mixtures of Canola Oil (used as surrogate for microalgae oil) and LAGO, a high Pt loading bi-metallic monolith catalyst. The experimental procedure and setup were similar to what had been reported elsewhere in this Task. The Pt-based bi-metallic precious metal catalysts were wash-coated on the walls of the monoliths and three of the monoliths (2 ¾" in length and ¾" in diameter) were wrapped with glass wool and placed in series inside the reactor at a predetermined position.

The results from the experiments conducted using the high Pt loading monolith catalysts in the pilot plant are shown in Table 3.11.

Table 3.11: Experiments using high Pt loading monolith catalysts. HDO conditions: 25°C cooling water, inline filter used, Hydrogen flow rate=200sccm, Reaction pressure=700psi.

Feed	Reaction temperature (°C)	Observations
30wt% canola oil/70wt% LAGO	310	Collected samples were yellow and turbid
	330	Samples collected at 2h and 3h were clear and subsequent samples were light yellow in color. All samples were slightly turbid.
	350	Samples collected were observed to be similar to the above but clearer.
50wt% canola oil/50wt% LAGO	330	All samples collected were clear and light yellow in color.
	350	
60wt% canola oil/40wt% LAGO	330	Samples collected were turbid and light yellow.
	350	All samples collected were clear and light yellow in color.

The observations detailed in Table 3.11 indicate that the lower reaction temperature of 310°C was not sufficient for HDO of canola oil/LAGO mixture, particularly at higher concentrations of canola oil; where higher reaction temperature is required for successful HDO.

The liquid product of one of the LAGO/Canola oil mixtures (30wt% Canola Oil/70wt% LAGO) was chosen for further analysis. Table le 3.12 shows the results of the elemental analysis of LAGO, hydrotreated LAGO and hydrotreated 30wt% canola oil & 70wt% LAGO. The elemental analysis was performed by Robertson Microlit Laboratories (Ledgewood, New Jersey, USA). The high Pt loading bimetallic monolith catalyst was able to achieve a twenty-fold reduction of sulfur in LAGO after HDO. This monolith catalyst also achieved significant oxygen reduction in the 30wt% Canola Oil/LAGO mixture (initial oxygen content: 3.6wt%).

Table 3.12: Elemental analysis (High Pt loading monolith catalyst, T=350°C, Hydrogen flow rate=200sccm, Reaction pressure-700psi, Liquid reactant flow rate=0.3ml/min).

Element	Untreated LAGO (wt%)	Hydrotreated LAGO (wt%)	Hydrotreated 30wt% Canola oil and 70wt% LAGO
C	87.31	88.66	88.20
H	12.67	11.33	11.76
N	<0.02	<0.02	<0.02
S	2764ppm	137ppm	202ppm
O*	0	0	0.02

* Oxygen content determined by difference, hence not very accurate.

HDO of mixtures of LAGO and Canola oil was successful at 25wt%, 50wt% and 60wt% concentrations but not at 75wt%, where precipitates of free fatty acids were observed at the experimental process conditions. The high Pt loading bimetallic monolith catalyst was demonstrated to effectively remove a large amount of oxygen as well as sulfur present in LAGO in LAGO/Canola oil mixtures allowing Low Sulfur Diesel Fuel specifications to be met.

IV.4.2. Co-Processing of Refinery LAGO and Nannochloropsis Salina Algae Oil

IV.4.2.1. Low Pt Loading Bi-metallic Monolith Catalyst

The solution of *N. Salina* and LAGO was vacuum filtered. However, unlike *N. Salina* and dodecane, the vacuum filtration of *N. Salina* and LAGO was accomplished much quicker with less retained solids on the filter paper (31.85wt% *N. Salina*-LAGO solution resulted in 30.4wt% after vacuum filtration). Experiments were then conducted using the low Pt loading bimetallic monolith catalyst, with the observations detailed in Table 3.13.

Table 3.13: Experiments using low Pt loading bimetallic monolith catalyst. HDO conditions: Hydrogen flow rate=200sccm, Reaction pressure=700psig.

Catalyst	Feedstock	Reaction temperature (°C)	Observations
Low Pt loading bimetallic monolith catalyst	30.4wt% *N.salina* and 69.6wt% LAGO	330	Dark colored and turbid liquid product was obtained at 2h. Subsequent liquid products were less turbid but maintained the same color.
		350	

Gas chromatography (GC) analysis was not conducted on the liquid products obtained from the HDO of the mixture of *N. Salina* by LAGO due to the fact that LAGO already contains a lot of HCs and GC analysis is unable to determine the HC yield resulting from HDO of N. Salina alone. Based on these initial results, we concluded that *N. Salina* algae oil had been demonstrated to be soluble in LAGO and the HDO of *N. Salina*-light atmospheric gas oil mixture successfully achieved using up to 30.4wt% effective solution over the low Pt loading bimetallic monolith catalyst.

IV.4.2.2. Stevens Pt-based Bi-metallic Monolith Catalyst (see Section IV.3 above)

The ultimate goal of this project was to produce green diesel via the hydro-treating (HDO & HDS) of a mixture of microalgae oil and refinery gas oil in a monolith reactor using a Pt-based bi-metallic catalyst. Based on the successes that had been recorded in the project, in the final phase of the project, we considered it important to produce at least one liter of hydrotreated mixture of algae oil/LAGO which is the minimum amount required for ASTM D975 diesel fuel specification test. The **Nannochloropsis Salina Algae Oil (25.5wt%)/P-LAGO (74.5wt%)** mixture was chosen for this purpose. We also conducted a performance study to see the effect of two important process parameters, namely temperature and H_2 gas to oil ratio on the final product. Comparison with previous experimental results were also made, which could shed some light on the catalyst characteristics in this hydro-treating process.

IV.4.2.2.1. Characterization of process streams

In order to produce green diesel, which is essentially a mixture of hydrocarbons, heteroatoms, mainly oxygen and sulfur, need to be removed from the feed. The oxygen and sulfur contents of all raw materials processed in this section are summarized in Table 3.14. Canola oil was used as a clean and transparent oxygen source. In addition, its fatty acid profile is similar to that of Chlorella oil, with the C18 fatty acids as the predominant lipids therefore, it is also an ideal model feedstock for Chlorella. It can be concluded from Table 3.14 that the oxygen content of algae oil is independent of oil species, while the sulfur content varies for different algae species. The gas oil used for co-processing, the intermediate in the production of diesel in the refinery, has a sulfur content that ranges from around 3000 to 1000 ppm, depending on the source of the oil.

Table 3.14: Oxygen and Sulfur content in feedstock

	Oxygen content (w/w)	Sulfur content (Ion Scan Chromatography, w/w)
Nannochloropsis Salina Oil	12%	2033 ppm

Chlorella Oil	12%	32 ppm
Canola Oil	12%	< 10 ppm
M-LAGO	0	2784 ppm
P-LAGO	0	1647 ppm
P-LVGO	0	1759 ppm

IV.4.2.2.2. Results and Discussion

The objective of this hydro-treating process is to lower both the oxygen and sulfur contents of processed feed through hydro-deoxygenation (HDO) and hydro-desulfurization (HDS), to levels that can be processed further by the conventional hydro-treating unit of the refinery. Gas oil is a complex hydrocarbon mixture which cannot be distinguished from the hydrocarbons produced from algae oil and, hence, making it impossible to quantify the produced hydrocarbons. Therefore, oxygen and sulfur contents of the product were used as criteria for evaluating the hydro-treating process. In this report, all oxygen content analysis was performed by Midwest MicroLab LLC, Indianapolis, IN while all sulfur content measurements were provided by Robertson Microlit Lab, Ledgewood, NJ.

Effect of Hydrogen to oil ratio on oxygen removal

Hydrogen to oil (H_2/Oil) ratio was varied from 333 to 1667 Sml/ml by varying hydrogen flow rate from 100 to 500 sccm at fixed liquid flow rate. All experiments were run for 5 hours and the 5th hour samples were usually sent for oxygen analysis. The initial oxygen content was 3.06% for 25.5 wt% Nannochloropsis Salina oil in P-LAGO. HDO efficiency was based on the following equation:

$$HDO\ Efficiency = \frac{Oxygen\ Content\ in\ Feed - Oxygen\ Content\ in\ Product}{Oxygen\ Content\ in\ Feed} \times 100\%$$

As shown in Figure 3.29, for H_2/Oil ratio > 333 Sml/ml, and residence time > 98 s, the oxygen content of liquid product was below detection limit, which is 0.3 wt%. The HDO efficiency is independent of H_2/Oil ratio at the studied conditions. It should be noted that, because the actual gas flow rate is at least 20 times higher than liquid flow rate, residence time was reduced when increasing H_2/Oil ratio. However, mass transfer was enhanced at elevated H_2/Oil ratios, which might compensate for the decrease of residence time.

The longer residence time was achieved without increasing the size of the reactor at 333 Sml H_2/ ml Oil ratio. Moreover, because the product stream with high concentration of unreacted hydrogen would be treated and recycled in practice, lower gas flow rate is always favored in industry. Therefore, considering only the HDO efficiency, H_2/Oil ratio of 333 Sml/ml should be used for oxygen removal from the 25.5wt% Nannochloropsis Salina oil/74.5wt% P-LAGO.

Effect of temperature on oxygen removal

The hydro-treating experiment was run at three different temperature values with the gas and liquid flow rates kept the same for all the runs. For each set value, the temperature varied within

±10°C, which should have negligible effect on overall superficial flow velocity. Therefore, the residence time was assumed to remain the same at all these three temperatures.

As a rule of thumb, the reaction rate is expected to double for every 10°C increase in reaction temperature, therefore, the HDO efficiency was expected to increase with the increase of reaction temperature, and finally reach 100% and stabilize. However, the results depicted in Figure 3.30 are quite different from the expectation, and no temperature dependence can be established from Figure 3.30. We suspect that this might have resulted from the experimental error considering the order in which the three experiments were performed. The result from the 360°C run was reliable because it was a repeat of previous run, and another subsequent repeat run also showed trace oxygen content in the 360°C product. However, due to the incomplete cleaning of the reactor system, the 350°C product could have been diluted by the previous 360°C product, thus lowering its oxygen content. Similarly, the small amount of oxygenates produced from the 350°C run possibly accumulated in the system, and contaminated the 370°C product, thereby leading to an oxygen content of the 370°C product that was higher than its true value. Some oxygenates produced during hydro-treating, such as fatty acids, have low solubility in the produced hydrocarbons, are solids at room temperature and make the liquid product look turbid. The turbidity observed in the 370°C product showed that the high oxygen content was due to the effect from the 350°C run, and not from the loss of hydrocarbon through cracking at a high temperature of 370°C.

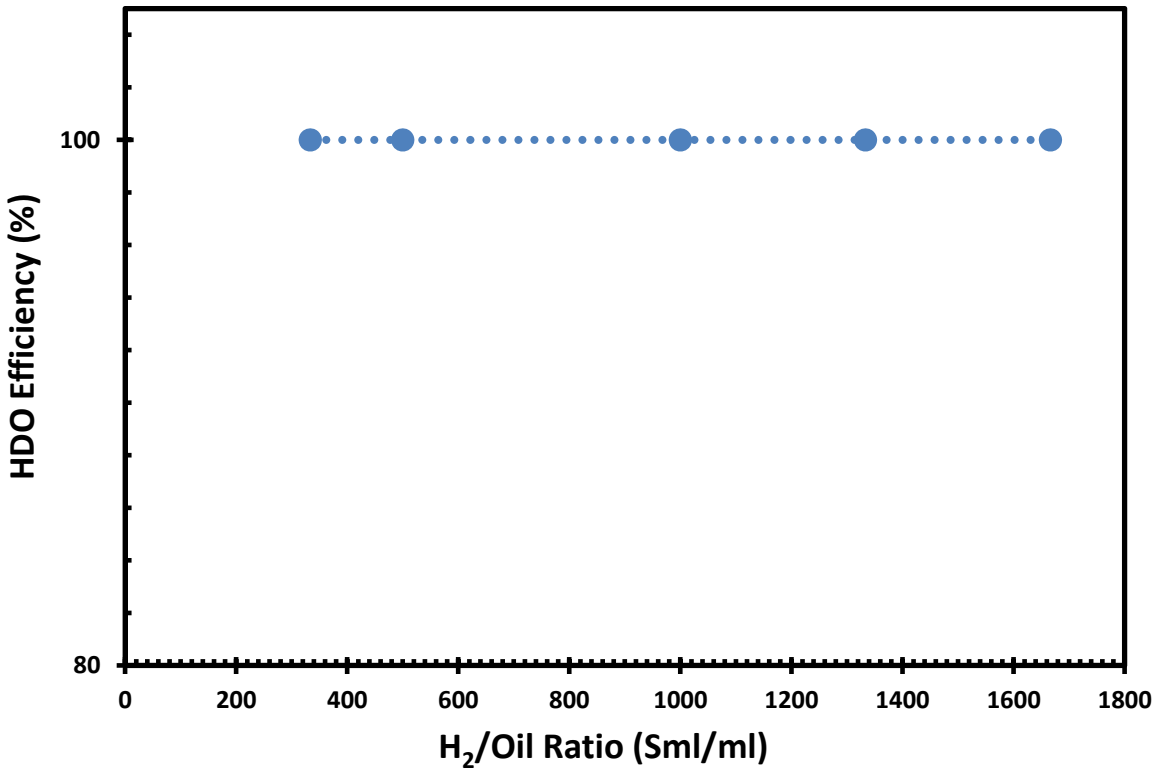

Figure 3.29: Effect of H_2/Oil ratio on Hydro-deoxygenation (Stevens Monolith Catalyst, 25.5 wt % Nannochloropsis Salina oil in P-LAGO, Temperature = 360 °C, H_2 Pressure = 700 psig, Liquid flow rate=0.3 ml/min)

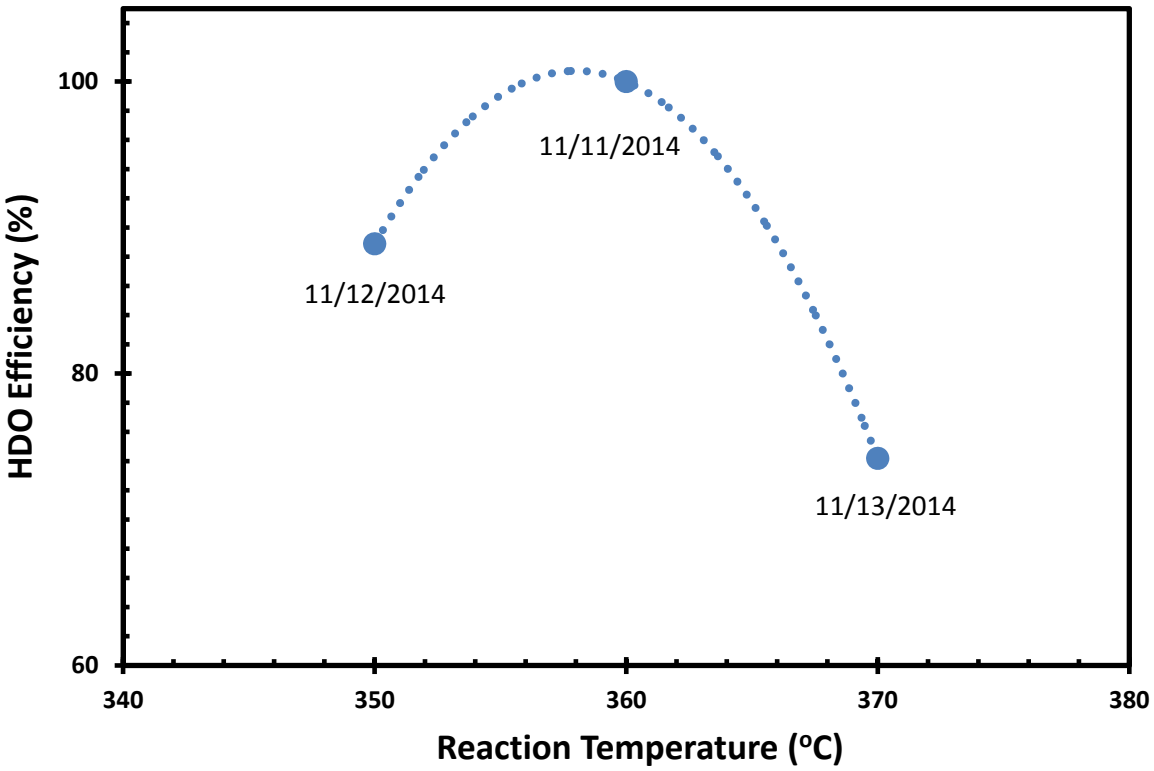

Figure 3.30: Effect of reaction temperature on Hydrodeoxygenation (Stevens Monolith Catalyst), 25.5 wt % Nannochloropsis salina oil in P-LAGO, H_2/Oil ratio=1333 Sml/ml, H_2 pressure = 700 psig, Liquid flow rate=0.15 ml/min)

Evaluation of Stevens Monolith for HDO and HDS

Four different catalysts had been evaluated for the hydro-treating of feedstocks with different oxygen and sulfur contents, and some of the results are summarized in Table 3.15 below. Similar to the HDO efficiency mentioned above, an HDS efficiency is defined as follows:

$$HDS\ Efficiency = \frac{Sulfur\ Content\ in\ Feed - Sulfur\ Content\ in\ Product}{Sulfur\ Content\ in\ Feed} \times 100\%$$

The variables for all the results summarized in Table 3.15 are:

(1) Reaction temperature, which was varied from 330°C to 370°C, and is expected to affect the reaction rate and equilibrium.

(2) H_2/Oil ratio, which was varied by adjusting gas flow rate while keeping liquid flow rate constant at 0.3ml/min. The molar gas flow rate was at least 20 times larger than the liquid flow rate, so the residence time is decreased with the increase of H_2/Oil ratio.

(3) Type of Catalyst: The Stevens Monolith was wash-coated with a Pt-based bimetallic catalyst. The catalyst loading of the Ni/Mo catalyst is the same as the commonly used commercial HDS catalyst, with a typical composition of 4.03wt% NiO and 13.20wt% MoO_3 on a dry basis. The amount of catalyst used is also an important process parameter.

(4) Initial heteroatoms content: We focused mainly on the oxygen and sulfur contents, which are the predominant heteroatoms in the feed.

(5) Source of heteroatoms: Listed in Table 3.14.

(6) Fatty acid profile: As reported previously, the C16 fatty acids are the main lipids in Nannochloropsis Salina oil, while C18 fatty acids predominate in Chlorella and Canola oils. Considering the reaction on molecular level, algae oils or vegetable oils with different molecular weight distributions (fatty acid profiles) should not be compared when studying the effect of other process variables.

Due to the fatty acid profile difference described in (6) above, the 5 experimental runs identified as 3, 4, 5, 7, and 8 (in red) in Table 3.15 should not be compared with the 2 experimental runs 1and 2 (in black), but experimental run 6 (in blue) can be compared with either of the other two groups of experimental runs. It should also be noted that: (1) Experimental runs 3 and 4 are essentially the same except that there is a dilution effect from previous run on run #3. As a result, the actual initial sulfur and oxygen contents may not be the same as the calculated values given in Table 3.15. (2) The discussion on experimental runs 7 and 8 was already included in a previous section of this report, and will not be repeated here.

In the first 5 experimental runs performed with Stevens catalyst, with the exception of run 3, HDO efficiency is always much higher than the HDS efficiency, which shows that the Stevens monolith catalyst has a higher selectivity towards HDO than towards HDS for given experimental conditions. It can be concluded from the first 2 experimental runs that, for the initial oxygen content of 3.06% in feed, the HDO is completed and the efficiency is independent of H_2/Oil ratio; while the HDS efficiency increases with increase of H_2/Oil ratio. For the feeds with predominant C18 fatty acids, the amount of oxygen removed increases with increase in H_2/Oil ratio, but the HDO efficiency remains nearly the same at around 60%. These results indicate that the amount of catalyst was insufficient for the complete removal of oxygen, and 100% HDO efficiency can be achieved by decreasing the Weight hourly space velocity (WHSV) or the Liquid Hourly Space Velocity (LHSV).

The HDS efficiency was not increased as would be expected at high H_2/Oil ratios. This could be attributed to two reasons; higher temperature may help to enhance the HDS process, or the residual oxygen may inhibit the sulfur removal. However, on comparing runs 4 and 6, one observes that the effect of the process variables on HDS efficiency decreases in the order: Initial oxygen content > H_2/Oil ratio > Reaction Temperature for Stevens' monolith Pt-based bi-metallic catalyst.

Of all the experimental runs involving feeds where C18 fatty acids are predominant, the highest HDO efficiency was achieved using 16g 1wt% Pt at 370^{o}C, and H_2/Oil ratio of 1667. Based on the discussion above, further experiments are suggested to have a better understanding of the interaction between different process variables and parameters:

i. Hydrotreating of P-LAGO, using 16g 1wt% Pt, at 370^{o}C, H_2/Oil ratio of 667,
ii. Hydrotreating of 25.5% N.S+ P-LAGO, using 16g 1wt% Pt, at 360^{o}C, H_2/Oil ratio of 1667,
iii. Hydrotreating of 25.5wt% Canola Oil + P-LAGO, using 16g 1wt% Pt, at 360^{o}C, H_2/Oil ratio of 1667.

Table 3.15: Summary of HDO and HDS efficiency under different experimental conditions

			Feed			Temperature	H_2/Oil	Product		HDO		HDS	
			Oxygen (wt%)	Sulfur (ppm, w/w)									
			Algae Oil	Algae Oil	Solvent	°C	(Sml/ml)	Oxygen (wt%)	Sulfur (ppm, w/w)	Amount Removed (wt%)	Efficiency (%)	Amount Removed (ppm, w/w)	Efficiency (%)
8g_Stevens Monolith	1	25.5wt% N.S + P-LAGO	3.06	518	1227	360	333	0	1417	3.06	100	328	19
	2	25.5wt% N.S + P-LAGO	3.06	518	1227	360	1667	0	1100	3.06	100	645	37
	3	30wt% Canola Oil + M-LAGO_1st	3.6	0	1949	370	667	2.59	1284	1.01	28	665	34
	4	30wt% Canola Oil + M-LAGO_2nd	3.6	0	1949	380	667	1.42	1415	2.18	61	534	27
	5	50wt% Chlorella + M-LAGO	6	16	1392	360	1667	2.44	1389	3.56	59	19	1.4
	6	Hydrotreated P-LAGO	\	\	1647	370	667	\	798	\	\	849	52
8g NiMo	7	25wt% Canola Oil + Dodecane	3	\	\	330	1667	0.41	\	2.59	86	\	\
16g 1wt% Pt	8	75wt% Canola Oil + Dodecane	9	\	\	370	1667	0.67	\	8.33	93	\	\

IV.2.2.3. ASTM D975 Analysis of Co-Processed Nannochloropsis Salina Algae Oil (26wt%)/P-LAGO (74wt%) Mixture

In the US, the quality of diesel fuel is evaluated in accordance with the American Society for Testing and Materials Standard D975 (ASTM D975), which describes a limited number of properties that diesel fuels must meet. The green diesel product was obtained by processing 25.5 wt% Nannochloropsis Salina oil in P-LAGO using Stevens Pt-based bi-metallic catalyst wash-coated on a monolith. The processing conditions are: Temperature of 360^{o}C, 700 psig hydrogen pressure, and H_2/oil ratio of 1667 Sml/ml. 120 ml of this green diesel product was collected from each 7-hour experimental run. The catalyst was combusted at 550^{o}C with diluted flowing air, and then reduced at 500^{o}C with pure hydrogen before each run. Altogether, we collected about 1.5 liters of product over a period of two weeks. The collected green diesel was sent to SGS Herguth Laboratories, Inc., Vallejo, California for ASTM D975 analysis, and the results are summarized in Table 3.16. ***The oxygen content was measured by Midwest Microlab LLC and the result was trace to none found.***

The Cetane Index, an inverse function of a fuel's ignition delay, is the most important parameter for evaluating the upgraded microalgae oil/P-LAGO mixture. Generally, diesel engines operate well with a Cetane number from 40 to 55. This green diesel has a very high Cetane Index of 50.5, which means the time period between the start of injection and the first identifiable pressure increase during combustion of this green diesel is very short. It should also be noted that the Cetane Index was obtained through calculation, and is always 2 points lower than the Cetane number obtained from engine test.

Compared with the specification of ASTM D975 for No. 2 Diesel Fuel, Sediment and water, 90% Distillation point, Viscosity at 40^{o}C, and 10% Ramsbottom carbon Residue levels exceed the specification limits. The KF titration result (from Robertson Microlit Lab) shows that the water content of the sample is less than 0.1%, therefore, the high sediment and water level mainly refers to the high sediment content, which might have resulted from the residual solid biomass in the algae oil not removed in pretreatment, rather than the hydro-treating process. According to the ASTM D2709 method, the amount of sediment and water is measured by the volume of sediments that settles to the bottom of a calibrated tube after centrifuge. Therefore, prior to hydro-treating, the feed mixture should be centrifuged to remove the sediment (solid biomass). This pretreatment will help to decrease the sediment content. Also, the viscosity and carbon residue amount could be reduced at the same time.

The 90% 'Distillation Point' of the hydro-treated green diesel is mainly determined by the P-LAGO, the 90% end boiling point of which is higher than specified by ASTM D975. The typical distillation of the P-LAGO used for the co-processing is as follows:

5 wt%	415^{o}F (212.8^{o}C)
50 wt%	575^{o}F (301.7^{o}C)
95 wt%	695^{o}F (368.3^{o}C)

In petroleum refining, this hydro-treated diesel product is usually blended with light components such as kerosene or heavy naphtha to lower the distillation point and meet the ASTM D975 requirement. Taking also the sulfur content into consideration, the produced green diesel should be combined with the LAGO and LVGO stream and subjected to further upgrading process at a higher operating pressure as currently practiced in petroleum refining, to produce ultra low sulfur content diesel fuel.

Table 3:16: Certificate of Diesel Fuel Analysis per ASTM D975

Test Performed	Proc-Rev	Result
Flash Point PMCC (Proc. A) ASTM D93 (Proc. A)	0093-1.7	64.0 Deg. C
Sediment and Water ASTM D2709	2709-1.1	>0.200 % Vol
Distillation of Petroleum ASTM D86	0086-2.6	
Observed Barometric Pressure		767 mm Hg
All results are corrected to 760 mm Hg		
Initial Boiling Point		85.6 Deg. C
5%		246.9 Deg. C
10%		263.0 Deg. C
15%		270.8 Deg. C
20%		276.0 Deg. C
30%		285.1 Deg. C
40%		292.6 Deg. C
50%		298.7 Deg. C
60%		306.0 Deg. C
70%		314.8 Deg. C
80%		326.8 Deg. C
85%		336.0 Deg. C
90%		351.6 Deg. C
95%		368.9 Deg. C
End Point		368.9 Deg. C
Recovery		97.3 % vol.
Viscosity @ 40 Deg C ASTM D445	0445A-2.1	5.00 mm2/s
Ash ASTM D482	0482-2.5	<0.001 mass %
Sulfur by Microcoulometry ASTM D3120	3120-3.1	1100 ug/g
Copper Corrosion @ 50 Deg C ASTM D130	0130-3.4	1A 3 Hours
Cloud Point ASTM D2500	2500-1.4	-8 Deg. C
Ramsbottom Carbon 10% Residue ASTM D524	0524-2.4	1.97 % wt
Cetane Index ASTM D976	0976-1.3	50.5
API Gravity@15.56C ASTM D4052	4052-1.7	33.7 Deg. API
Lubricity of Diesel Fuel by HFRR at 60°C ASTM D6079	6079-1.2	270 um
Conductivity of Distillate Fuels ASTM D2624	1152A-1.3	18800 pS/m
Temperature of sample		20 Deg. C

IV.5. References:

Addiego W P, Lachman I M, Patil M D, et al. High surface area washcoated substrate and method for producing same: U.S. Patent 5,212,130[P]. 1993-5-18.

González C A, Ardila A N, Montes de Correa C, et al. Pd/TiO2 washcoated cordierite minimonoliths for hydrodechlorination of light organochlorinated compounds. Industrial & Engineering Chemistry Research, 2007, 46(24): 7961-7969.

Task 4: Process Analysis, Design & LCA of Integrated System for Production of Partially Upgraded Algal Oil (Stevens, Valicor, Columbia University & Consultants)

I. Summary

The economics of the production of hydrotreated algal oil (HTAO) along with co-production of animal feed and nutraceuticals (omega-3 oils) was explored. Base case calculations were for commercial scale production of 10,000 barrels per day of HTAO with nutraceuticals claiming only 0.05% of the raw algae oil (AO). Sensitivity of economics to critical parameters was studied. Greatest sensitivity of sales price was to the algae doubling time. Doubling time might be reduced by increasing pond velocity or other mixing inducing means. Other important parameters were oil content, CAPEX, and moisture content of post extracted algal residue. Algal area productivity (g/m^2/day) was calculated from four parameters: initial algal concentration, pond depth, residence time in pond, and algae doubling time. Using presently accepted operating parameter values and with co-product credits, the estimated plant gate price was ~$10/gal. However, it was shown that there is significant potential for enhanced economics through moderate improvements in many areas. Credits for coproduction of animal feed and nutraceuticals were $3.24/gal and $0.14/gal, respectively. Hydrotreatment of AO was discussed. Municipal waste water tertiary treatment was briefly discussed but not deemed viable on a large scale. An easy to use Excel spreadsheet for material and energy balances and economics was developed as a flexible scouting tool.

A life cycle assessment for greenhouse gas emission burden was performed for an algae based process to grow, harvest, extract and produce a paraffinic hydrotreated algae oil (HTAO). The process was assumed to produce co-products of animal feed and nutraceuticals. This process was compared to GHG emissions from conventional crude oil production and refining through the middle distillate (MD) of the atmospheric column of a refinery. Both MD and HTAO products were viewed as equivalent. Contributions to CO2 emissions from the HTAO process were tabulated and ranked. The two primary sources of CO2 emission from the HTAO process were from the use of purified CO2 to grow the algae and the drying of high water content animal feed. Ammonia as a nutrient was also a major contributor. On the basis of “well or pond to wheel”, it was found that HTAO contributed 18.7 kg CO2e per MBTU less to the atmosphere than the MD route (67 vs 87 kg CO2e/MBTU). *If algae oil replaced 10% of the US consumption, this would result in a CO2 emission reduction of 210,000 tons per day.*

However if the drying process for animal feed can be made 50% more efficient the reduction of CO2e by the HTAO process would be about 50 kg/MBTU. This represents a more than 50% reduction in CO2e emission compared to the conventional diesel process. It is recommended to explore more energy efficient ways of CO2 capture from flue gas and to reduce the water content of algae residue (use for animal feed) as well as using CO2 generated by the process itself.

II. Techno-economic Analysis of Microalgae Production and Conversion into Refinery Ready Oil with Co-Product Credits

II.1. Introduction

To meet the US mandate for renewable fuels, algal based liquid fuels have been attracting interest [1-12]. Hydrotreating of algal derived oil can produce refinery ready paraffinic oil suitable for insertion in the middle distillate stream of a refinery's atmospheric distillation column [4]. Interest in an algal based biofuel stems from its advantages vis-a-vis other photosynthetic based renewable fuels, such as high area productivity, cultivation of non-arable flat land, ability to use saline water, high CO2 fixation rates, and possible production of by-products such as animal feed and nutraceuticals. However, there are significant challenges to commericializaton which primarily reside in processing demands.

Economic analysis for open ponds and photo bio-reactors which have appeared in prior literature has been well discussed on a harmonized basis in Sun et al [7] which finds a mean of $11.57 per gallon of algal oil, i.e., free fatty acids and acylglycerides. Harmonization was also addressed in ref. [11]. Davis et al [1] did a Aspen Plus techno-economic study of the production of HTAO from algae in open unlined ponds and in photobioreactors with biogas for power generation. Their study concluded that the sale price of HTAO from open ponds would be $9.84/gal and $18.10 for photo bio-reactors for a 10% return. Another study [11] for large scale production of 5 billion gallons of diesel per year with anaerobic digestion of the algae residue put sales price of diesel on the order of $10/gal. When we refer to "sales price" we mean the "plant gate price" or the "minimum fuel selling price" excluding tax. A recent report from NREL [13] examined the economics of a process in which purchased algal biomass was fractionated into carbohydrate values going to ethanol, lipids going to naphtha and diesel products, and residual going to anaerobic digestion to methane and fertilizer.

The chief objective of this paper was to examine the impact and limitation of various parameters on the economics of HTAO.

II.2. Process Description

Since open pond raceways are generally acknowledged to be more economical than photo bio-reactors, e.g., Richardson et al [14] and Davis [1], it is this configuration that forms the basis for this design. The process may be divided into two major sections: (1) algae growth, harvesting, and extraction of the algal oil; and (2) hydrotreating of the algal oil into refinery ready oil. "Refinery ready oil" can be introduced downstream of the atmospheric distillation column of a refinery for further treatment such as hydrocracking or hydroisomerization to obtain the precise desired properties such as freezing point. Hydrotreating removes heteroatoms and converts free fatty acids and acylglycerides into a mixture of paraffinic diesel like hydrocarbons. Block flow diagrams of these two sections, constituting a biorefinery, are shown in Figures 4.1 and 4.2. Figure 4.1 shows the production of animal feed and Figure 4.2 the production of nutraceuticals. Parameters associated with those figures are shown in Tables 4.1 and 4.2. Cells filled in green are input values. Material and energy balances associated with the numbered streams of Figures 4.1 and 4.2 are given in Supplementary Material.

II.2.1 Design Basis and Base Case

The following is assumed:

1. Production rate of 10,000 bbl/d (218 Mgal/yr) of HTAO. For the parameters of this study, this production rate requires ~140,000 acres of ponds.

2. Co-product production of animal feed and nutraceuticals, e.g., omega-3 oils.
3. Production of nutraceuticals is 0.05 % of the AO production. This represents ~25% of the algal omega-3 market. All of the post extracted algal residue goes to animal feed; this being only 1.4% of its market.
4. Capital cost for ponds, harvesting, and extraction is based on Lundquist et al [15]. For 10,000 bbl/day production we estimate CAPEX for ponds, harvesting, extraction, hydrotreating and co-product production to be ~ $B 5.2. This is a unit CAPEX cost of $24/(gal/yr) which compares with an estimate from ref. [12] of $30 to 40/(gal/y) for smaller scale production of ~3 Mgal/y using hydrothermal liquefaction. The effect of CAPEX is discussed in the economics section.
5. Operating and cost parameters are based on current reasonable values rather than future projected improved values. This more readily permits determination of areas of greatest potential improvement.
6. For the parameters chosen, the average annualized area productivity is taken to be 15.2 g (algae dry wt)/m^2/day. This value was computed from eq. (4.4) for 5 day doubling time, 5 day retention time, pond depth of 10 inches, and an initial algal concentration of 0.3 g/L. This value accounts for seasonal variation and is not an unreasonable value based on reported data and estimates refs. [9, 11, 16]. Seasonality will impact economics by virtue, for example, of unemployed CAPEX during winter months [12].
7. AO composed only of acylglycerides and free fatty acids.
8. Hydrotreater efficiency of 90%.
9. A carbon reduction credit of $5/T is taken. This, however, will be shown to have only a small effect being about $0.01/gal.
10. On-stream time of 90%. This is more reflective of a n-th plant, ref. [13].
11. Return on investment of 10%.
12. Income tax rate of 38%.

Figure 4.1: Algae Growth-Harvesting-Extraction Production of Algal Oil and Animal Feed Section 1

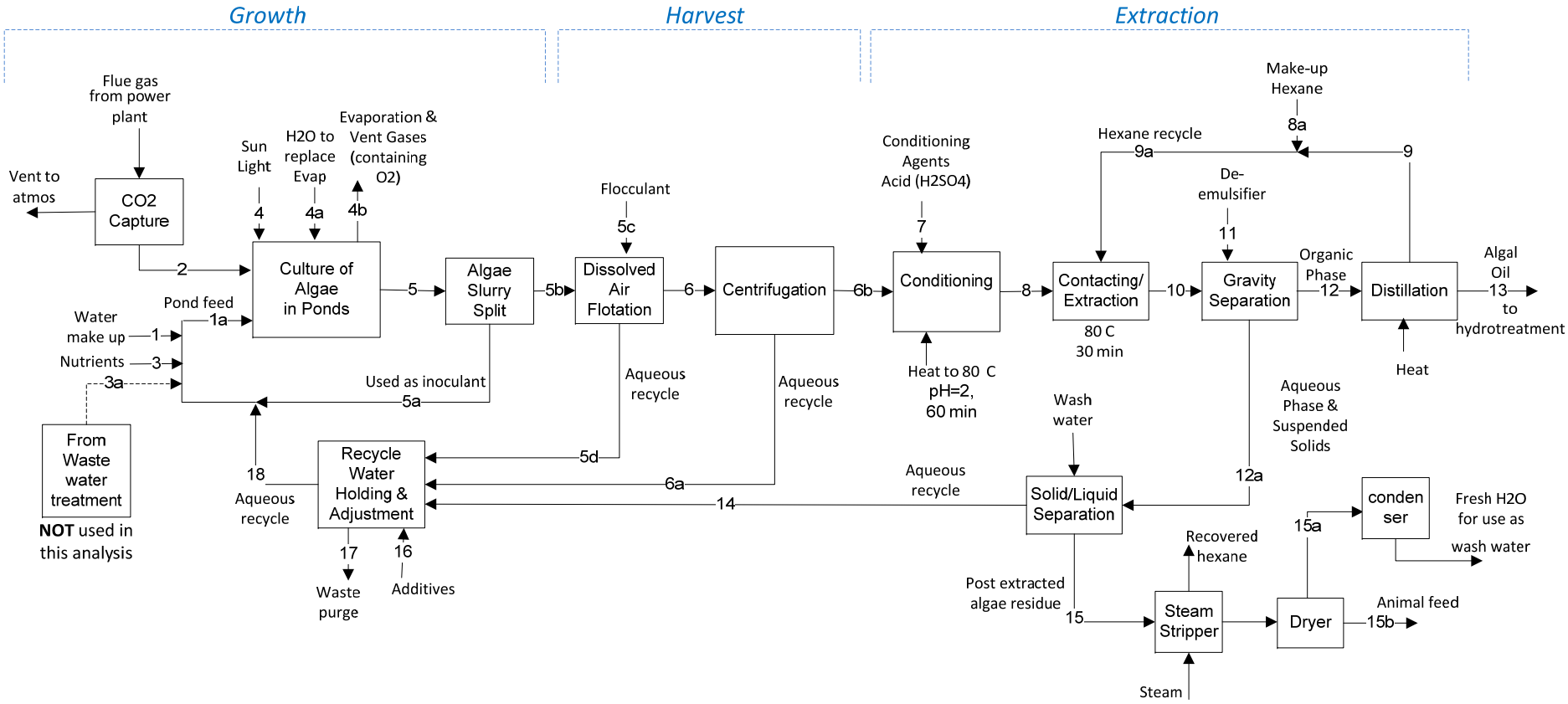

Figure 4.2: Hydrotreating of Algal Oil & Nutraceutical Processing – Section 2

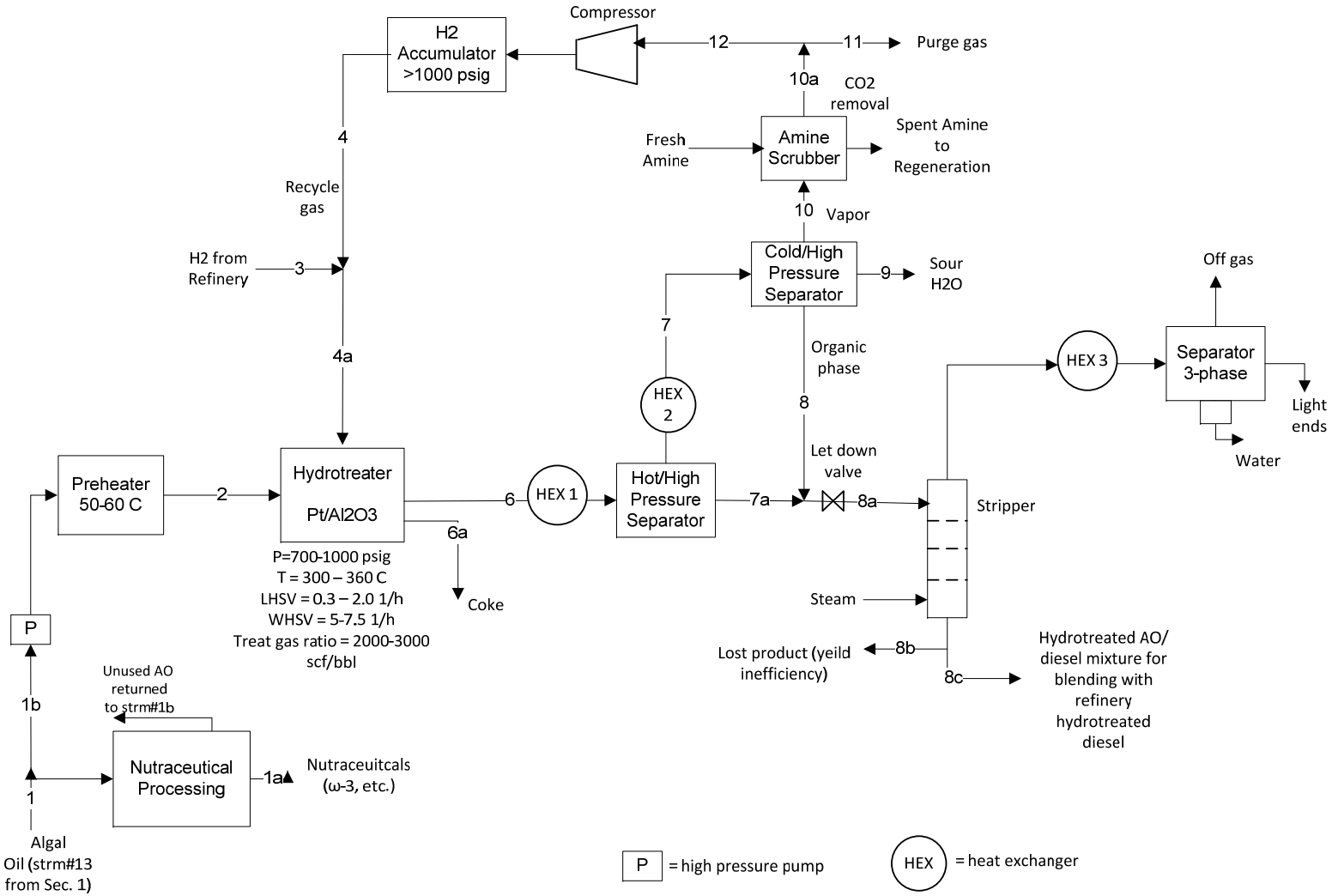

Table 4.1: Section-1 Parameters for Figure 4.1

Algae Growth, Harvesting, & AO Extraction				
Total flow rate thru pond or reactor, gpm	4,729,466		Conditioning H2SO4 dosage, lb 100% acid/lb slurry	0.005
Feed broth algae concentration, g (dry wt)/L	0.300		Wt ratio of hexane to algae (dry wt)	5
Retention time in pond or reactor, hr	120		Efficiency of oil recovery, %	95
Algae doubling time, hr	120		Moisture content of biomass, strm 15, wt%	85
Pond depth, ft	0.83		Moisture content of dryed biomass, strm 15b, wt%	10
Algae gross composition oil, % of dry wt	25		H2O usage, lb H2O/lb algae	0.333
water solubles, % of dry wt	29		Algal Exit conc, g/L	0.60
Insolubles, % dry wt	46		Algal recycle ratio (stm5a/stm5b)	1.00
Efficiency of CO2 utilization, %	95		Fraction of total feed flow that is recycled	0.50
CO2 usage, lb CO2/lb algae	2.0		Total Pond volume, gal	3.405E+10
Oxygen production, lb O2/lb algae(dry)	1.07		Algal area productivity, g(dry wt algae)/m^2/day	15.2
Net Evaportion rate, inch/yr	43		Algal volumetric productivity, g(dry wt algae)/L/day	0.06
Theor N nutrient required, wt% of aglae dry wt	9.2		Total Area of pond, ac	125,915
Theor P nutrient required, wt% of aglae dry wt	1.3		Algae production rate,g/h	321,792,872
% excess nutrient fed to pond	15		Algae production rate, lb/h	708,795
Weight of nitrogen fed to pond as NH3 in pond feed, lb/h	81,496		Algae production rate, lb/day	17,011,077
Weight of phosphorous fed to pond as DAP in pond feed, lb/h	45,121		Annual production, ton algae/ac/y	25
Purge rate (of strm#17) % of strms 5d,6a & 14	10		Algal oil production rate, gal/yr/ac	1,734
Conc of algae in floc thickener exit (strm 6), wt %	2		Algal oil production rate, Mgal/yr	218.3
Conc of algae in centrifuge exit (strm 6b), wt %	12		Algal oil production rate, bbl/day/ac	0.11
Flow rates are "calendar rates". Also, pond size etc. stated for 100% on-stream time.			HTAO oil to refinery rate, bbl/day	10,000

HDCO2 = hydrodecarboxylation; HDO = hydrodeoxygenation; FA = fatty acid moiety; FFA = free fatty acid; AG = acylglyceride

Table 4.2: Parameters for Figure 4.2

Hydrotreatment of Algal Oil				
% of AO to nutraceuticals	0.05		Frac of AGs undergoing hydrogenolysis	1
AO Composition: AGs, wt%	79.0		Frac AGs unreacted (by diff)	0
FFA, wt%	19.0		Frac of CO2 generated that goes to RWGS	0.3
H2O, wt%	1.0		Frac of CO generated that goes to methanation	0.2
inert, wt%	1.0		Frac of CO generated that goes to coke	0.1
ave mol wt of FA	267		Frac of CO generated unreacted(by diff)	0.7
ave moles of double bonds per mole of FA	1.44		Fraction of double bonds hydrogenated	1
ave acyl number of AGs	2.36		Excess H2 over theoretical, %	30
Ave no. of double bonds per molec of AGs	3.40		Efficiency of hydrogenator, %	90
ave mol wt of AGs	679		Gross heating value of purge gas (strm11), MBTU/lb	18,987
Gas purge rate (strm 11), %	10		Wt Ratio of HTAO to AO	0.72
Frac of FA going to HDCO2	0.6		HTAO to refinery rate, gal/day	420,000
Frac of FA going to HDO	0.4		HTAO to refinery rate, Mgal/stream yr	153.3
Frac FA unreacted (by difference)	0		HTAO to refinery rate, bbl/day	10,000
Flow rates are "calendar rates", i.e. 100% on-stream time.			HTAO to refinery rate, bbl/day/acre	0.08
			Nutraceutical oil annual production, Mlb/y	0.7

II.2.2 Section 1- Growth, Harvest, and Extraction

Production of algae and isolation of the algal oil is accomplished as shown in Figure 4.1. This section encompasses the large land area required for algae growth.

Park et al [17] give a typical algal empirical formula as $C_{106}H_{181}O_{45}N_{16}P$. Using this formula to calculate weight percent composition of dry algae, the nutrient requirements per unit weight of dry algae can be estimated, see Table 4.3.

Table 4.3: Estimated Algae Nutrient Requirements

Nutrient	Weight of nutrient per unit weight of dry algae
CO2	1.91
H2O	0.33
N as NH3	0.11
P as P	0.013

II.2.2.1 Pond Configuration

Many pond configurations are possible. Consider that in Figure 4.3. Inoculation ponds which could consist of photobioreactors followed by covered ponds then open plastic-lined ponds [15] are not shown. In pond operation a rather a significant portion of the algal biomass could be retained or recycled to provide the starting biomass for the next batch. This mode of operation raises the concern of increased susceptibility to algal pathogens and possible growth inhibition. Reference [3] notes the possibility of genetic drift of the algal species.

Figure 4.3: High Rate Algal Ponds

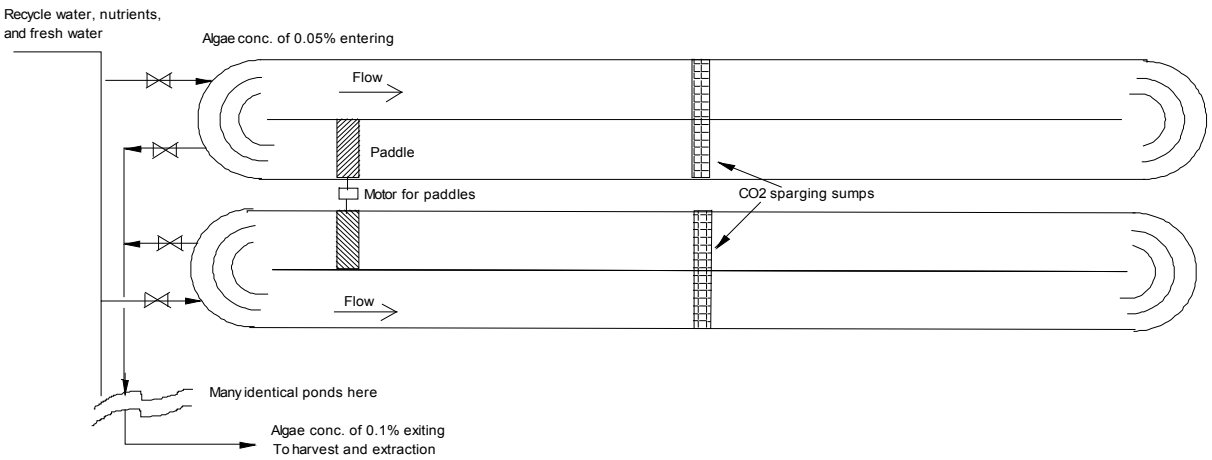

The ponds are raceways in which water flow is induced by paddle wheels and CO2 is sparged into the flowing streams at various points. This design is known as a high rate algal pond. Pond raceways may be designed, as discussed by Lundquist, et al [15], as an elongated loop consisting of a channel 'forward' and a channel 'return', see Figure 4.3, each being on the order of 2300 ft long, 100 ft wide, and ~ 10 inches deep. In our definition, two channels (forward and return) comprise a pond. The flow velocity within the pond is recommended to be about 0.75 ft/sec in order to promote mixing [15]. For the design basis on the order of 140,000 acres of

ponds at 90% on-stream time or ~14,000 ponds of the indicated size would be needed. Pond operation could consist of:

1. Initiate the batch by charging ponds with fresh and recycle water and with partial retention of algae slurry.
2. Operating ponds in batch mode for, say, 5 days.
3. At the end of 5 days, discharging part of the algal slurry sending it forward to harvesting, but retaining a certain portion as inoculant to repeat the sequence.
4. With a multitude of ponds available, it would be possible to stagger charge and discharge to simulate a virtually continuous flow into and out of the pond complex.

II.2.2.2 Calculation of Pond Area Productivity and Production Rate

Under idealized assumptions, algal area productivity can be related to four parameters: (1) initial algal concentration, (2) depth of pond, (3) residence time in pond, and (4) doubling time of algae. The pond area productivity in units of grams of dry algae per square meter per day may be calculated from:

$$P = \frac{454\rho^* c_i q}{4046A}\left[2^{\frac{\theta_r}{\theta_d}} - 1\right] = \frac{0.1122 c_i q}{A}\left[2^{\frac{\theta_r}{\theta_d}} - 1\right] \quad (4.1)$$

Symbol definitions and the required units are given in the Nomenclature. The flow into and out of the pond, q, should not be confused with the flow rate within the raceway which is a completely independent parameter.

The residence time in the pond is given by:

$$\theta_r = Ah / q \quad (4.2)$$

and the density of the algal slurry by:

$$\rho^* = \rho(62.4)(43{,}560) = 2.72 * 10^6 \rho \text{ lb/acre-ft} \quad (4.3)$$

Taking ρ = 1.0 and eliminating 'q' by using equation (4.2), equation (4.1) can be rewritten as:

$$P = \frac{3.05 * 10^5 c_i h}{\theta_r}\left[2^{\frac{\theta_r}{\theta_d}} - 1\right] \quad (4.4)$$

From this equation it is seen that productivity is directly proportional to the inlet algal concentration and to the depth of the pond. *A deeper pond and high inlet concentration are favorable to the extent that light absorption does not overweigh this effect.*

For example, if initial algal concentration expressed as weight fraction is 0.0003 (i.e., 0.3 gram per liter), pond depth h = 0.83 ft, residence time in pond θ_r = 5 days, and doubling time θ_d = 5 days, the area productivity of the pond is calculated from eq. (4.4) to be 15.2 gram dry algae per day per square meter (25 T/acre/yr). Under field conditions the doubling time of 5 days is significantly longer than that experienced for ideal conditions of the laboratory.

In the real world, the doubling time of algae, is linked to the depth. For example, as the depth of the pond increases the doubling time may well increase due to light shading. Also note that 'P' is linearly dependent on the initial concentration of algae going into the pond and, all things constant, linearly dependent on depth, h. Increasing retention time while holding pond depth fixed causes productivity, P, to increase since the exponential factor outweighs the linear factor in the denominator.

Calculation of the production rate of algae, Q = lb algae (dry wt) per day can be made from:

$$Q = \rho^* q c_i \left(2^{Ah/(q\theta_d)} - 1\right) = \rho^* q c_i (2^{\frac{\theta_r}{\theta_d}} - 1) \qquad (4.5)$$

It can be seen from eq (4.5) that as the volumetric flow rate into and out of the pond increases the production rate goes down due to the contrary effects of the linear term and the exponential term. For a fixed pond area and depth, we have the slightly paradoxical situation that if the flow rate into the pond is increased thereby reducing residence time the production rate goes down! Conversely reducing flow rate increases daily production, assuming shading effects don't come into play.

For example, if residence time is reduced from 5 days to 2 by increasing the in and out flow rate, production rate is reduced by ~25%. As great as possible residence time is indicated (compatible with the adverse shading effects) for maximal use of land area. This suggests that it may be beneficial to expend more power to increase pond velocity to reduce the shading effect thereby allowing greater algal density.

II.2.2.3 Harvest

Referring to Figure 4.1, upon completion of the growth phase, a portion of the slurry is retained in the pond to serve as inoculant while the remainder of the slurry is fed to a thickening step where the algae is concentrated by dissolved air flotation or other means to ~ 2%. This thickened algal slurry is then sent to a centrifuge where it can be thickened to 12 - 28%. The figure of 28% solids has been reported by Flottweg SE using a type of solid bowl decanting centrifuge called the "Sedicanter®*". In our subsequent economic analysis was found, for example, that the sale price of HTAO could be reduced by $0.45/gal by being able to go from 12% algal solids to 18% in stream 6b.* This is primarily due to the increase in weight of animal feed due to an increase in its water soluble content. For solids content greater than 18% in the centrifuge exit, moisture content in the animal feed stream to the dryer (stream 15) becomes less than 85% reducing drying expense which can be significant. For example, solids content in stream 6b of 25% would reduce sales price by $1.34/gal.

Water recovered from the thickening and centrifuge steps is sent back to a recycle holding stage where it can be reused in the pond or discharged partially or totally as a purge.

II.2.2.4 Extraction

A variety of ways of extracting algal oil from the thickened slurry have been explored [4]. The method of oil extraction illustrated in Figure 4.1, is based on that pioneered by Valicor Separation Technologies LLC as discussed in ref.[18]. In this method the thickened algal slurry is sent to a "Conditioning" step where pH is reduced by acid addition and temperature is elevated for a period of time. The membrane protecting the cell contents is thus weakened and rendered pervious. From the conditioning step the resulting slurry is then contacted with hexane

in the “Contacting/Extraction” step. Here the lipids from the algae cell are extracted into the solvent hexane. This solution of lipids in hexane is then sent to a “Distillation” step where the more volatile hexane is removed from the lipids and recycled. The resulting bottoms product is the isolated algal oil. The algal oil is next sent to Section-2 (Fig. 4.2), the hydrotreating section.

II.2.2.5 Characterization of AO

To perform the hydrotreatment calculations associated with Table 4.2, the algal oil must be characterized. Algal oil is typically a lipid mixture primarily of acylglycerides (mono-, di- and tri-) and free fatty acids. However, other types of lipids such as glycolipids, phospholipids, lipoproteins, etc may also be present. For the hydrotreater calculations we have idealized AO as being composed exclusively of free fatty acids and acylglycerides. From the analysis by class (ie, % of mono-, di-, tri-glycerides and free fatty acids) and the fatty acid profile we characterize AO in terms of 3 parameters: (1) average molecular weight of the fatty acids, (2) average number of double bonds per fatty acid molecule and (3) average acyl number (i.e., the average number of fatty acid moieties attached to the glycerin backbone) of the acyl glycerides. In our case, based on an analysis of a sample of *Nannochloropsis salina* AO, the three parameters characterizing the AO were taken to be 267, 1.44, and 2.36, respectively.

II.2.2.6 Animal Feed and Nutraceutical Plants

The reader is referred to Sections II.3.1.3 and II.3.1.4.

II.2.2.7 Alternative to Animal Feed Production

An alternative to processing the defatted microalgae (also called post extracted algae residue or “PEAR”) is discussed by Ou et al [19]. This paper shows the possibility of applying hydrothermal liquefaction to the PEAR followed by hydrotreating to convert the waste into additional liquid fuel.

II.2.3 Section 2 – Hydrotreating of Algal Oil

The hydrotreater design of Figure 4.2 is based on refs. [20, 21]. A small portion of the AO is diverted for extraction of nutraceuticals such as omega-3 oils. The preponderance of the AO is delivered to the hydrotreating unit. For improved processability, the AO from section 1 might be diluted with a slip stream from the middle distillate of the atmospheric column of the refinery. This stream is pressurized to system pressure of about 700 psig and heated to ~50-60 C. The feed stream, stream 2 in Figure 4.2, enters the catalytic hydrotreater where contact is made at 300-360 C with a hydrogen rich gas stream which is a mixture of fresh H2 and a H2 bearing recycle, stream 4. The catalyst might be NiMo or Pt on Al2O3.

A hot high pressure separator downstream of the hydrotreater serves to remove the majority of the product hydrocarbons. A cold high pressure separator removes reaction water and remaining product hydrocarbons. The uncondensed gases (CO2, CO, CH4 and propane) are sent to an amine scrubber for removal of CO2. A purge stream is taken and the remaining gases, rich in H2, are boosted in pressure and recycled. This iteration of the design doesn’t provide for recycle of possibly unreacted AO.

Kubicka and Kaluza [22] have outlined a hydrotreatment reaction pathway in which carbon-carbon double bonds are first saturated followed by hydrogenolysis of the acylglycerides to free

fatty acids and propane. The free fatty acids plus the fatty acids resulting from acylglyceride hydrogenolysis then undergo hydrodeoxygenation. In addition, other reactions such as decarboxylation, water gas shift, methanation and the reverse Boudouard reactions simultaneously occur. The independent reactions used to describe hydrotreater chemistry are shown in Table 4.4. Input parameters relative to the hydrotreating reactions are shown in Table 4.2 and have been estimated and bear further definition.

Table 4.4: Hydrotreater Reactions

Rxn	Reactions
1 FFA	Hydrodecarboxylation (HDCO2): RCH2COOH = RCH3 + CO2
2 FFA	Hydrodeoxygenation (HDO): RCH2COOH + 3H2 = RCH2CH3 + 2H2O
3 AGs	Hydrogenolysis: G(OOCCH2R)n(OH)(3-n) + 3H2 = GH3 + nRCH2COOH + (3-n)H2O
4	C=C bond Saturation: RCH=CH2 + H2 = RCH2CH3
5	RWGS: CO2 + H2 = CO + H2O
6	Methanation: CO + 3H2 = CH4 + H2O
7	Reverse Boudouard: 2CO = CO2 + C

where, G = C_3H_5 (i.e., the glycerin backbone); GH_3 = propane; HDCO2 = hydrodecarboxylation; HDO = hydrodeoxygenation; R = fatty acid moiety; FFA = free fatty acid; AG = acylglyceride

II.3. Economics

Detailed economics have been treated in a number of recent studies, notably, refs. [1, 7-9, 11, 14-16, 23]. A recent paper by Davis et al [12] addressed large (national) scale production of diesel from microalgae via hydrothermal liquefaction with a co-product of naptha. This reference shows the impact of seasonality on economics. The reader is referred to these papers for comparative capital and operating inputs and outputs.

II.3.1 Capital Cost

II.3.1.1 Growth-Harvesting-Extraction Step

Lundquist, et al ref [15], give a capital cost estimate for their Case 5 (biofuel-emphasis + oil) in which algae are harvested from 400 ha (~ 1000 acres) of unlined ponds (compacted clay is used instead) and oil is extracted for biofuel production. They estimate a capital cost for the growth-harvest-extraction facility to be $M 100 (in 2010) for the approximately 1000 acre facility. The paper by Jonker and Faaij [16] estimates the cost of lined ponds only (without harvesting equipment) at 157.6 k€/ha or ~$M90/1000 acre. Davis, et al ref.[1] in their Figure 3 and Table 5 estimates $M195 for 4,820 acres (this includes unlined ponds, CO2 delivery harvesting extraction, digestion, inoculum system, hydrotreating, off-sites, and land costs). In any event, the hydrotreating cost is a small fraction of the total cost; estimated to be about 4% of the total cost. Using the data in [12] for diesel production from algae by hydrothermal liquefaction on a scale of 3 Mgal/y CAPEX was estimated at $M85 per 1000 acres. These capital estimates and one from Table 8 of ref. [7] are summarized in Table 4.5.

Table 4.5: Some Literature Capital Cost Estimates

Estimate	Year of Estimate	Pond lined?	Harvest equipment?	Capital Cost $M/1000 acres
Lundquist et al **[15]**	2010	no	yes	100
Davis et al **[1]**	2011	no	yes	40

Sun et al **[7]** NREL	2011	no?	yes	85 (estimated)
Junker & Faaij **[16]**	2013	yes	no	90
Davis et al [12]	2014	yes	yes	88 (estimated)

Capital cost for the growth, harvest and extraction section was estimated from Lundquist et al [15] adjusted to 2014 dollars using a scaling exponent of 0.75. The choice of the 0.75 exponent rather than the more conventional 0.60 acknowledges the fact that ponds number up rather than scale up. Since we are looking at the combination of ponds as well as harvesting and extraction, the latter two benefiting from economy of scale we took a value of 0.75 for the scale up exponent.

II.3.1.2 Hydrotreater Step

The capital cost for this step is estimated from an article by Harwell et al ref. [21] which suggests $M70 for a 30,000 bbl/day capacity. This value is scaled for capacity by the 0.6 exponent. For 10,000 bbl/day the capital cost for the hydrotreater plant is estimated at $M36.2.

II.3.1.3 Animal Feed Plant

Post extracted algae residue can contain very high levels of water having significant cost implications. Also residual hexane in the algal-residue requires steam stripping or the use of a vapor tight dryer. Dewatering equipment to reduce the water content of algal residue and solar drying, see ref. [24], should be studied. Installed capital cost for a drying unit (including off gas scrubbing) of animal feed is estimated to be $M 3 for each 12,000 lb/h of wet cake containing 85% moisture [25]. This would represent 278 drying units. For 10,000 bbl/day production, the CAPEX for animal feed drying is $M 839 which represents about 16% of the total CAPEX.

II.3.1.4 Nutraceutical Plant

An intimation of what could be involved in processing nutraceuticals is afforded by ref. [26]. As a first pass estimate we take its capital to be 30% of the hydrotreater capital.

II.3.2 General Economic Input Parameters

The capital estimates along with those for labor are given in Table 4.6. Estimated total capital cost for a biorefinery to produce 10,000 bbl/day of HTAO is $B 5.2.

Table 4.6: Some Economic Input Parameters.

On-stream time, %	90
Base size for scale factor, acres	1,000
Capital cost for base size, $M	106
Scale exponent on capacity	0.75
Estimated ponds & harvest & extraction capital cost, $M	4,312
Pond operator per 1000 ac, shift-man	0.5
Harvesting, extraction, & distillation operators, shift-man	10
Hydrotreater base capacity, bbl/day	30,000
Hydrotreater base capital cost, $M	70
Estimated hydrotreater capital cost for HTAO to refinery rate, $M	38.6
Hydrotreater operators, shift-man	5
Animal feed & Nutraceutical operators, shift-man	7
Installed CAPEX for animal feed dryer for 12,000 lb/h, $M	3
Factor for capital cost of nutraceutical plant as frac of Hydrotreater cap,fra	0.3
Capital cost of animal feed plant, $M	839
Capital cost of nutraceutal plant, $M	11.6
Total capital cost, M$	5,201

II.3.3 Variable Costs

Variable costs are calculated from usage and price of the raw material and utilities, see Table 4.7. The usages for CO2, NH3 and DAP were derived from Table 4.3. Catalyst cost for hydrotreating was estimated at $0.09/gal. Utility costs for the hydrotreating plant, were regarded as relatively small and were not included.

Table 4.7: Variable Usages and Costs For Sections 1 and 2.

Growth-harvest-extraction:		Price	Usage	Cost	Cost
Raw Materials	Units	$/Unit	Unit/bbl	$/bbl	$/gal
CO2	lb	0.02	3,402	68.0	1.62
nutrient: nitrogen as NH3	lb	0.20	171	34.3	0.82
nutrient: phosphate as DAP	lb	0.22	95	21.0	0.50
make up water (strms 1 & 4a)	k gal	0.05	1.25	0.06	0.00
flocculant	lb			0.0	0.00
H2SO4	lb	0.12	70.9	8.5	0.20
make up hexane	lb			0.0	0.00
deemulsifier	lb			0.0	0.00
TOTAL Raw Mat. Cost				131.9	3.14
Utilities & other costs					
Electric	KWH	0.08	610.5	48.8	1.16
Steam	k lb	8.00	8.8	70.3	1.67
Cooling water	k gal				
TOTAL Utilities cost				119.1	2.84
Hydrotretment:		Price	Usage	Cost	Cost
Raw Materials	Units	$/Unit	Unit/bbl	$/bbl	$/gal
H2	lb	0.68	11.3	7.7	0.18
Catalyst	lb			3.8	0.09
amine solvent	lb			0.0	
TOTAL Raw Mat. Cost				11.5	0.27

CO2 is the major raw material cost contributing $1.62/gal to the sales price. It is remarked however that if a saline aquifer is being used it may contain dissolved sodium bicarbonate which would provide some of the carbon, thereby reducing CO2 cost. Also, not accounted for in this analysis, flue gas from the animal feed dryer could be used to reduce CO2 expense. The sum of nitrogen and phosphorous raw materials, i.e., the nutrients, contribute another $1.32/gal to the sales price. Thus, raw material cost is already at $3.14/gal.

II.3.3.1 Utility Usages

These are shown in Table 4.8 for Section 1 and have been included in Table 4.7. The electric requirement for flow through the ponds and CO2 distribution and sparging is based on Lundquist et al ref. [15], see p. 74 and p. 86, respectively, of that reference. This value of electric consumption for CO2 distribution and sparging is about twice that used in ref. [27] which was 22.2 Wh/kg of CO2. However, Lundquist et al assume use of a flue gas (~12% CO2) whereas we have assumed purified CO2. Therefore, energy usage for CO2 distribution in this analysis is probably on the high side. For electric consumption for the centrifuge we have taken a usage of 1 HP per gpm with 90% motor efficiency [28]. In dissolved air flotation 25% of the total flow is recycled and pressurized to 75 psig. This results in a power requirement for DAF of 0.01219 KW/gpm of total flow at 75% pump efficiency and 90% motor efficiency [25]. The power requirement for compressed air is, comparatively, negligible. A good discussion of utility usage is given in [5]. From Table 4.8, it is seen that drying wet biomass for animal feed contributes $1.15/gal to the sale price of HTAO.

Table 4.8: Utility Usages and Costs for Section 1

Growth-harvest-extraction:					
Electric requirement	unit	value of unit	KWH/bbl	$/bbl	$/gal
Flow thru ponds	KW/ac	0.81	244.8	19.58	0.47
CO2 distribution & sparging	KW/ac	0.415	125.4	10.03	0.24
Dissolved air flotation	KW/gpm	0.012	69.2	5.53	0.13
Centrifuge of algae	KW/gpm	0.84	143.5	11.48	0.27
Contacting/Extraction	KW/gpm	0.15	4.3	0.34	0.01
Centrifuge of biomass (PEAR)	KW/gpm	0.84	23.4	1.87	0.04
		Total	610.5	48.8	1.16
	CO2 foot print, lb CO2/bbl =		1007		
	Energy consumed, MJ/bbl =		5,495		
Steam or Heat Requirment			MBTU/bbl	$/bbl	$/gal
Heat required for conditioning (strm8)			1.41	11.28	0.27
Heat req'ed for hexane distill'n (strm9)			1.34	10.68	0.25
Heat req'ed for drying wet biomass for animal feed(st			6.04	48.34	1.15
		Total	8.79	70.3	1.67
	CO2 foot print, lb CO2/bbl =		1,318		
	Energy consumed, MJ/bbl =		9,270		

II.3.4 Credits

II.3.4.1 Animal Feed

Animal feed is shown as stream 15b of Figure 4.1 and can require washing especially if a saline water source is used to grow the algae. Water condensed from the dryer can be used for washing. Animal feed could be a very interesting co-product in that its market size is large. For example, corn and soybean meal are consumed as livestock feeds at the rate of 158 million tons per in the 2011/2012 market year [23]. The amount of animal feed produced by a 10,000 bbl/day plant is about 2.2 million T/y which is only 1.4% of the market.

Bryant et al [23] have examined the quality of what they refer to as “post-extracted algae residue”, “PEAR”, and have calculated a possible price of this material based on its quality. They show that the high-protein PEAR they studied had total digestible nutrients and crude protein contents of 48% and 36%, respectively, bearing a similarity to distiller dried grains. This compares with high-protein soybean meal having 87% and 54%, respectively. Bryant et al estimate that the value of PEAR could be $100 to $225 per ton as animal feed. They point out that their study is in the early stages, and that other factors such as trace toxins or elements such as sulfur or calcium at unaccustomed levels might influence the price of PEAR. Also the use of saline water in growing algae can impart problematic levels of sodium in the PEAR if not adequately washed out. Current prices for animal feed, due to the recent drought conditions in the Midwest, appear to be in the $350/T range [29]. We take a sale price of $225/T for animal feed.

Our spreadsheet incorporates the drying requirement to remove water from 85% to 10% from the wet biomass in stream 15 of Figure 4.1. As mentioned, this is a utility expense of $1.15/gal as well as a reduction in the CO2 reduction credit. Dewatering equipment should be considered

to reduce the moisture content of the wet cake. For example, if wet cake moisture content could be reduced from 85% to 45% before drying to 10%, a savings of $1.12/gal could be realized when both utility cost and dryer CAPEX are considered. Possibly sun drying may be an option. *We will find that a sales price for animal feed of $225/T will reduce the sales price of HTAO by $3.24 /gal.* CAPEX for drying animal feed adds $0.94/gal; while operating cost adds another $1.15/gal for a total of $2.09/gal cost. This, roughly (excluding labor), yields a net of $3.24 - $2.09 = $1.15/gal for animal feed production. Therefore, production of animal feed, per se, should be beneficial.

It is noted that increasing the oil content of the algae will generally reduce the amount of animal feed produced.

Digestion of PEAR is an alternative to producing animal feed. This would generate methane gas which could be used to dry wet cake or generate electricity. The resulting solids, which are said to be easier to de-water than non-digested solids, could be sold as organic fertilizer.

II.3.4.2 Nutraceuticals

At present, anchovy and tuna are the major sources of omega-3 oils. While the global annual consumption (human consumption and pet foods) of omega-3 oils is around 89,000 metric tons (not including feed for aquaculture and cattle), the consumption of algal omega-3 oils is small, being about 1,500-1,600 metric tons/yr [30]. Average price of algal omega-3 is about $43/lb [30]. In the economic analysis we have taken the price of algal omega-3 as being $30/lb. The price of refined fish oil is about $3.00/lb. Global growth rate of algal omega-3 oils is about ~6%/yr [30].

Algae oil is rich in omega-3 fatty acids which are being increasingly appreciated as being important in building and maintaining human health. Omega-3 fatty acids generally refer to the group of three: eicosapentaenoic (EPA) C20:5(n-3), docosahexaenoic acid (DHA) C22:6 (n-3), and alpha-linolenic acid (ALA) C18:3(n-3). The first two, EPA and DHA, are of marine origin while ALA is of plant origin. Other potential nutraceuticals from algal oil are carotenoids such as astaxanthin. Omega-3 bearing oils are priced according to four qualities: concentration of omega-3s in the oil, ratio of EPA to DHA, environmental source of the oil, and the process to produce the oil. Use of omega-3s in infant formulas, especially in countries like China, is the largest and fastest growing segment of the omega-3 market [31]. Supporting its higher price, there are a number of advantages of algal derived omega-3 compared to fish derived [32].

To produce nutrients for human as well as animal consumption it is essential to prohibit any toxic materials from entering the production system. This means that the water supply and any nutrients, including CO2, must be free of toxic materials. This precludes the use of flue gas directly, but rather requires use of purified CO2 from an absorption-desorption process. Possibly flue gas from a natural gas fired power station might be acceptable, but the operating cost of distribution and compression might equally counterbalance the cost of purified CO2. The present analysis assumes purified CO2 at $40/T.

We assume only 0.05 % of the AO production is diverted to nutraceuticals and an average selling price of $30/lb. This volume would be about 25% of the algal omega-3 market, admittedly a large fraction. As the HTAO plant capacity increases the fraction of AO going to nutraceuticals would have to be further dialed back to suit the market demand so as not to have a disastrous effect on its sale price. The cost of processing from AO into nutraceutical product is assumed to

be 20% of the selling price. *Sale of nutraceuticals under these assumptions lowers the price of HTAO by only $0.14/gal.*

II.3.4.3 Municipal Waste Water Tertiary Treatment

Although not a part of the subsequent analysis, we briefly touch on the economic implications of municipal waste water tertiary treatment here. The idea is that it would be used for its nutrient values and also a credit would be taken for reducing the nitrogen and phosphorous content of the discharged water.

Since there is a tendency for microalgae to accumulate heavy metals there is the obvious concern of mixing nutraceuticals and animal feed production with waste water processing. Use of waste water would preclude simultaneous production of these co-products. Sturm and Lamer [33] have obtained experimental data on algal growth in four 2600 gallon air sparged tanks using nutrients from the secondary effluent from a wastewater treatment plant containing 19.5 mg-N/L and 3.2 mg-P/L. They demonstrated the feasibility of this approach. This area has been explored in a number of other studies, e.g. [17, 34-36].

Metcalf & Eddy, Table 4-5 of ref [37], give the concentrations of TN and TP at various stages in a waste water treatment plant as shown in Table 4.9.

Table 4.9: Concentrations of TN and TP at Various Stages of a Waste Water Treatment Plant

Component	Untreated municipal waste water	Effluent after indicated treatment	
		Conventional activated sludge	Activated sludge with BNR
TN, mg/L	20-70	15-35	5-10
TP, mg/L	4-12	4-10	0.5 – 2.0

TN = total nitrogen, TP = total phosphorous, BNR = biological nutrient removal.

Compare the TN and TP concentrations in: (1) effluent from conventional activated sludge process, (2) algae pond feed requirements, and (3) effluent from the algae pond. The latter two are specific for the given pond operation. This is shown in Table 10. The base case parameters for pond operation show that waste water could provide almost all the nitrogen requirement. However, there appears to be excess phosphorous in the waste water over what is required. This would be a problem. If the productivity of the pond could be increased, this would increase the phosphorous requirement possibly eliminating the excess TP problem and also reduce water demand.

Table 4.10: Concentrations of TN and TP

Component	Conventional activated sludge (secondary) Effluent	Algae Pond Feed with 15% excess nutrients	Algae Pond Effluent with 15% excess nutrients
TN, mg/L	~ 25	28	3.7
TP, mg/L	~ 7	4.5	0.6

Setting aside the issue of excess TP, a charge to a municipality for tertiary treatment of $500/Mgal [38] would reduce the sales price of HTAO by $4.05/gal for treatment plus an additional credit for savings on nutrient cost on the order of $1.20/gal giving a total credit of $5.25/gal if it were used. This is a substantial credit, but for the production of 10,000 bbl/day of

HTAO, waste water from a population of 34 million would be required. Clearly, cities being generally much smaller than 34 million, only a portion of the algal requirement could come from municipal waste water. Nutraceutical and animal feed production would seem to be precluded if waste water treatment was employed.

II.3.4.4 Carbon Dioxide Reduction Credit

The social cost of carbon (SCC) is a measure of the monetary damage that would occur throughout the world for the discharge of a ton of CO2 into the atmosphere. Therefore carbon credit may be given to a process which results in CO2 reduction compared to a standard process. The current value of carbon credits appear to be in the neighborhood of $5/T of CO2 reduction. However, there are estimates of the SCC which put it in the range of $50-100/T.

Partial calculations for CO2 emissions are given in the utility table, Table 4.8. It is mentioned here, that in the capturing of 1 lb of purified CO2 from flue gas, ~0.25 lb of CO2 is emitted to the atmosphere by the capture process due to energy required for heating and cooling of the absorbent. Therefore, only ~75% of the purified CO2 used by the algae can be counted as being removed from the atmosphere.

A life cycle assessment (LCA) comparison of CO2e or greenhouse gas (GHG) emissions between the algae based HTAO process of this report and conventional crude oil to diesel is discussed in ref.[39]. The analysis made in [39] included the emissions from each of the process steps as well as the emissions from raw materials but did not include emissions for infrastructure fabrication and decommissioning. This comparison resulted in an estimate that the HTAO process of this paper saves 20 kg of CO2/MBTU vs the conventional crude to diesel process. This translates to a savings to the environment of 0.121 tons of CO2 per barrel. Assuming the CO2 reduction credit would be on the basis of comparing the conventional process to the algae process and using $5/T of CO2 credit, we find that the CO2 credit would only reduce the price of HTAO by $0.01/gal.

II.3.4.5 Summary of Credits

A summary of usages (a negative usage means production) and credits is given in Table 4.11. It is seen that co-products reduce sale price by $3.37/gal. The main contributor being animal feed, nutraceuticals contributing a reduction of only ~$0.14/gal.

Table 4.11: Summary of Usages and Co-Product Credits

		Price	Usage	Cost	Cost
Credits	Units	$/Unit	Unit/bbl	$/bbl	$/gal
Waste water treatment	Mgal	0	-0.34	0	0.00
Waste biomass (animal feed)	ton	225	-0.60	-136	-3.24
Hydrotreatment Purge gas fuel credit (strm#11, Sec 2)	MBTU	3.5	-0.02	-0.1	-0.002
Nutraceuticals	lb	30	-0.2	-6.1	-0.14
Cost of processing nutraceutical	lb	6	0.2	1.2	0.03
CO2 reduction credit	T	5	-0.12	-0.6	-0.01
TOTAL credits				-141	-3.37

II.3.5 Fixed Costs

These are shown in Table 4.12. We have assumed 0.5 shift-man per 1000 acres, see Table 4.6. Each operator will manage a square ~1.8 mile on a side. For harvesting, extraction and hexane distillation it is estimated that 10 shift operators will be needed. Fixed costs contribute about $ 1.95/gal to the sales price. The estimate (see Table 4.11) of a work force compliment of 605 people is probably on the high side due to the estimate of 0.5 shift-man per 1000 acres.

Table 4.12: Fixed Costs

FIXED COSTS			Cost, $K/	Cost	Cost
A. Labor (incl PAC)	Shift-man	shft-man/y	$/bbl	$/gal	
Operating	85.0	300	6.98	0.17	
Oper Superv	6.2	420	0.71	0.02	
Lab'tory	20.0	280	1.53	0.04	
Yard	30.0	250	2.05	0.05	
Packaging	10.0	320	0.88	0.02	
Maintenance (1.5% of capital)	Tot op labor = 605		21.38	0.51	
B. Supplies					
Operating (10% of total operating labor)			3.35	0.08	
Maintenance (1.5% of capital)			21.38	0.51	
C. Indirect					
Admin (Tech,acc,safety: 40%of tot labor)			13.41	0.32	
Taxes & Ins (1.1% of capital)			15.68	0.37	
TOTAL Fixed Cost			87.36	2.08	

II.3.6 Global Economic Parameters

Economic calculations where made under the global input parameters (in green) shown in Table 4.13.

Table 4.13: Global Economic Parameters

ROR VALUE			10.00%	SALES VOLUME,million bbl per year			0.36
NET PRESENT VALUE,K$			0	SALES PRICE,$/bbl			187.95
DISCOUNTED PAYBACK PERIOD, YRS.			18.50	VARIABLE PLC,$/bbl			-1.62
				FIXED PLC,K$/YEAR			28,361
				STARTUP EXPENSE,K$			2,000
				ADS&R COSTS,K$/YEAR			1,000
				WORKING CAPITAL,% SALES			16%
				DEPL ALLOWANCE,% OF SALES			0%
				DEPL LIMIT,% OF PROFIT			0%
				ESCALATION--		RATES	BASE YR
PRESTARTUP VALUES				SALES PRICE		2.40%	2011
FIRST YEAR OF PROJECT			2014	VARIABLE PLC		2.40%	2011
CAPITAL COST,M$			268	FIXED PLC		2.40%	2011
CONST PERIOD,YRS(3 MAX)			2	ADS&R COSTS		2.40%	2011
FIRST YEAR OF SALES			2016	CAPITAL		2.40%	2011
TOTAL YEARS OF SALES			17	***DISCOUNT FACTOR***			**10.00%**
				*CAPACITY FILLOUTS		1ST YR.	50%
CAPITAL AS M & E,% OF TOT			90%	AS PERCENT		2ND YR.	75%
CAPITAL AS BLDGS,% OF TOT			9%	OF VOLUME		3RD YR.	100%
CAPITAL EXPENSE,% OF TOT			1%	(4 YRS. MAX.)		4TH YR.	100%

ROR = rate of return, PLC = plant level cost, ADS&R = administration sales & research

II.3.7 Base Case HTAO Sales Price

Bear in mind that HTAO is nearly the quality of diesel. The sales price of HTAO for the base case (see Table 4.16) is c*alculated to be $9.89/gal for a 10% return on investment.*

II.3.8 Revenue Streams

The revenue brought in by each of the three products is shown in Table 4.14. Animal feed is seen to contribute a significant portion to the economics, while nutraceuticals are a minor factor.

Table 4.14: Revenue Streams at 10,000 bbl/day Production

Revenue Streams			$M/yr
HTAO	**@ $9.89/gal**		1,516.1
Animal feed			496.2
Nutraceuticals			22.1
		Total=	2,034.5

II.3.9 Economic Case Studies

The effects of various conditions and parameters on the economics of the enterprise are now considered. For some values of the parameters, for example algae doubling time, the pond area requirement for a fixed production will change thereby causing the capital cost to change. This effect is incorporated into the economic calculations.

II.3.9.1 Summary of Base Case Economics

Table 4.15 shows the contribution of each category of the enterprise for the base case parameters (see Table 4.16). It is seen that costs associated with CAPEX is the major contributor to sale price, followed by raw materials and co-product credit.

Table 4.15: Summary of Base Case Economics

Cost Component	$/gal
Raw materials	3.41
Utilities	2.84
Fixed costs	2.08
Capital cost recovery	4.93
Co-product credits	-3.37
Sales Price=	9.89

II.3.9.2 Sensitivity Analysis

The base case values of key parameters, shown in Table 4.16, give rise to a sale price of $9.89/gal. Table 4.16 also shows the change in sales price for a 10% increase in a given parameter, all other parameters remaining fixed. The listing of parameters is in the order of greatest effect, either beneficial or detrimental, to least effect. *The largest effect is from the doubling time of the algae.* A 10% increase in the base case algae doubling time, going from 5 days to 5.5 days, caused the sale price to increase by $0.92/gal. Conversely, a 10% reduction in doubling time would reduce sale price by ~ $0.92/gal. This suggests research into the inhibiting effects on doubling time in the field operation versus the lab would be worthwhile. The next tier of importance includes: % oil content in algae, capital cost and moisture content of stream 15 of Figure 4.1. Next tier of importance are feed broth algae concentration, % return on investment, pond depth, retention time in the pond and sale price of animal feed.

If all of the 10% changes in parameters were made in the right direction a sales price of $4.76/gal could be achieved; indicating a serious beneficial effect on economics could be made by relatively modest improvements in a large number of areas.

Table 4.16: Sensitivity Analysis of Base Case to 10% Increase in Parameter

Production rate, bbl/day	10,000		
On-stream time, %	90		
Base sales price of HTAO, $/gal (ex tax)	9.89		
Base case capital cost, $M	5,201		
	Base Parm	10% increase	Delta SP
PARAMETERS	Value	in Parm Value	$/gal(ex tx)
Algae doubling time, hr	120	132	0.92
Algae gross composition: oil, % of dry wt	25	27.5	-0.69
Capital cost, $M	5,201	5,721	0.64
Moisture in post extracted algae biomass*, %	85	76.5*	-0.63
Feed broth algae concentration, g (dry wt)/L	0.3	0.33	-0.47
Return on investment, %	10.0	11	0.46
Pond depth, ft	0.83	0.91	-0.44
Retention time in pond or reactor, hr	120	132	-0.41
Sale price of animal feed, $/T	225	247.5	-0.33
Conc of algae in centrifuge exit (strm 6b), wt %	12	13.20	-0.09
Conc of algae in DAF floc thickener exit (strm 6), wt %	2.0	2.20	-0.03
Percent of AO going to nutraceuticals,%	0.050	0.055	-0.01
Sale price of nutraceuticals, $/lb	30	33.00	-0.01
CO2 creduction credit, $/T	5.0	5.5	0.00
Delta SP = change in sales price for a 10% change in parameter all other			
parameters remaining fixed, $/gal			
* moisture in post extracted algae residue was reduced by 10%			
note: area of pond and capital cost may change as a function of the changed parameter.			

II.3.9.3 Effect of Capital Cost, Oil Content, and Productivity

The strict effect of capital cost for two combinations of algal oil content and productivity, viz., (a) 25% oil & 15.2 g/m^2/day, and (b) 30% oil & 25.3 g/m^2/day is shown in Figure 4.4. It is seen that at a given capital cost, the difference in sales price between the two cases, (a) and (b), is only $0.69/gal. This is due to the dominate effect of capital. The slope of the lines gives an effect of $1.20/gal per billion dollars of capital cost.

Figure 4.4: Effect of Capital Cost on HTAO Sales Price

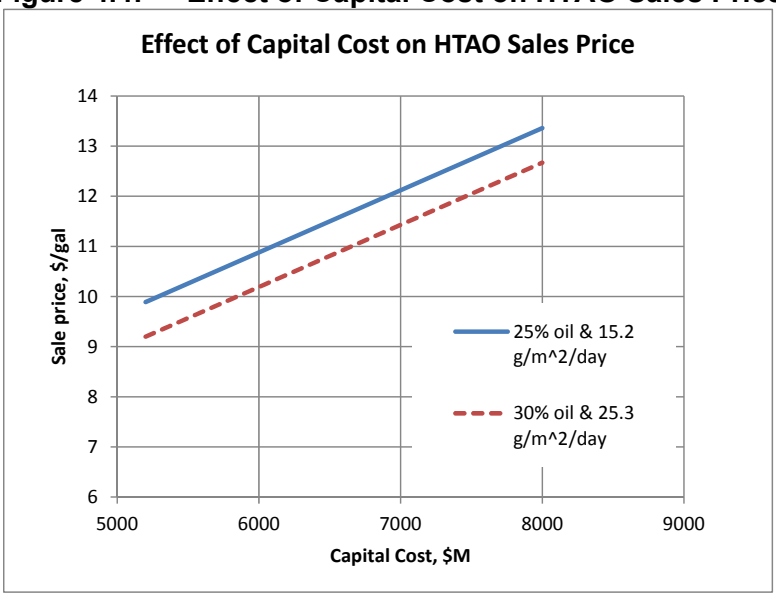

If we let the capital cost be a function of oil content and of productivity, as it in fact will be, then the effect is amplified, see Table 4.17. Variable cost is also given. It is seen that oil content and productivity can have a major effect on sales price by virtue of their impacting capital cost primarily but also variable cost.

Table 4.17 Effect of Oil Content and Productivity on Capital and Sales Price

% Oil	Productivity, g/m^2/d	CAPEX, $M	Variable Cost, $/gal	HTAO Sale Price, $/gal
25	15.2	5,201	2.88	9.89 (base)
25	25.3	3,832	2.54	7.75
30	15.2	4,440	2.60	8.62
30	25.3	3,246	2.31	6.77

If open ponds could be operated at a productivity of 25.3 g/m^2/day rather than 15.2 g/m^2/day with an algal oil content of 30% rather than 25%, then sale price is reduced to $6.77/gal.

II.4. Conclusions

An important conclusion is that if relatively small improvements on the order of 10% in numerous parameters are made, significant reduction in sale price could be achievable. The most impactful parameter on economics was the algae doubling time. The tradeoff between the cost of increased agitation by increased pond flow velocity or installation of turbulence inducing baffles and reduced doubling time merits attention, as does finding an economic means of dewatering algal residue for animal feed. For the parameters assumed, nutraceuticals contributed a reduction of only $0.14/gal to the HTAO selling price. The material balance and economic spreadsheets developed, see Supplemental Material, can be a useful tool in further sharpening economics as more accurate or different data become available.

II.5. Nomenclature

A area of pond(s), acre
c_i initial concentration of algae, wt fraction
h depth of pond, ft
n number of algal doublings in pond, i.e., θ_r/θ_d, or $Ah/(q\theta_d)$, dimensionless
P pond area productivity, gram dry algae per sq meter per day
q volumetric flow rate (time averaged over the duration of the batch) into and out of pond (assumed equal due to replacement of evaporation losses), acre-ft/day
Q production rate of algae, lb(dry wt)/day
θ_d doubling time of algae, day
θ_r residence time in pond, i.e., Ah/q, day
ρ specific gravity (~1.0), dimensionless
ρ^* density of algal slurry, lb/ac-ft

II.6. Acknowledgements

We benefited from discussions with Sam Couture and David Hart of Qualitas-Health; Emilie Slaby of The Scoular Co., David Vaccari Aspasia Kalomoiri, and Lin Zhou, of Stevens Institute of Technology; Robert B. Levine and Kiran Kadam of Valicor Renewables LLC; Philip Pienkos and Ryan Davis of NREL, Warren Seider of UPenn, Adam Ismail of GEOD, and Tom Capehart of the USDA; Jess Ornum and Kerry Kovacs of Komline-Sanderson; Aldo Bernasconi of GOED. We gratefully acknowledge that this work was funded by DOE contract DE-EE0006063.

Supplementary Material
The material and energy balances for Figures 4.1 and 4.2 can be found at the Algal Research web site.

II.7. References

1. Davis, R., A Aden, PT Pienkos, *Techno-economic analysis of autotrophic microalgae for fuel production.* Applied Energy, 2011. **88**: p. 3524-3531.
2. Demirbas, A., MF Demirbas, *Importance of algae oil as a source of biodiesel.* Energy Conversion and Management, 2011. **52**: p. 163-170.
3. Dunlop, E., AK Coaldrake, CS Silva, WD Seider, *An energy-limited model of algal biofuet production: toward the next generation of advanced biofuels.* AIChE Journal, 2013. **59**(12): p. 4641-4654.
4. Ferrell, J., V Sarisky-Reed, *National Algal Biofuels Technology Roadmap*. 2010, US Dept of Energy.
5. Frank, E., J Han, I Palou-Rivera, A Elgowainy, MQ Wang, *Life-cycle analysis of algal lipid fuels with the GREET model, Rpt. No. ANL/ESD/11-5*. 2011, Argonne National Laboratories: Argonne National Laboratories.
6. Stephenson, A., E Kazamia, JS Dennis, CJ Howe, *Life-cycle assessment of potential algal biodiesel production in the United Kingdom: a comparison of raceways and air-lift bioreactors.* Energy Fuels, 2010. **24**(4062-4077).
7. Sun, A., R Davis, M Starbuck, A Ben-Amotz, R Pate, PT Pienkos, *Comparative cost analysis of algal oil production for biofuels.* Energy, 2011. **36**: p. 5169-5179.
8. Benemann, J., WJ Oswald, *Systems and economic analysis of microalgae ponds for conversion of CO2 to biomass Final Rpt. to Dept. of Eng. Pittsburgh Eng. Tech. Center*. 1996.
9. Chisti, Y., *Biodiesel from microalgae.* Biotechnology Advances, 2007. **25**: p. 294-306.

10. Brennan, L., P Owende, *Biofuels from microalgae—a review of technologies for production, processing, and extractions of biofuels and co-products.* Renewable and sustainable energy reviews, 2010. **14**(2): p. 557-577.
11. Davis, R., D Fishman, ED Frank, MS Wigmosta, A Aden, AM Coleman, PT Pienkos, RJ Skaggs, ER Venteris, MQ Wang, *Renewable diesel from algal lipids: An integrated baseline for cost, emission, and resource potential from a harmonized model; Rpt ANL/ESD/12-4*. 2012.
12. Davis, R., DB Fishman, ED Frank, MC Johnson,SB Jones, CM Kinchin, RL Skaggs, ER Venteris,MS Wigmosta,, *Integrated evaluation of cost, emissions, and resource potential for algal biofuels at the National Scale.* Environ. Sci.& Technol., 2014. **48**: p. 6035-6042.
13. Davis, R., C Kinchin, J Markham, ECD Tan, LML Laurens, Dsexton, D Knorr, P Schoen, J Lukas, *Process design and economics for the conversion of algal biomass to biofuels: algal biomass fractionation to lipid- and carbohydrate-derived fuel products Tech. Rpt. NREL/TP-5100-62368, Sept. 2014*. 2014.
14. Richardson, J., JL Outlaw, M Allison, *The economics of microalgae oil.* AgBioForum, 2010. **13**(2): p. 119-130.
15. Lundquist, T., IC Woertz, NWT Quinn, JR Benemann, *A Realistic Technology and Engineering Assessment of Algae Biofuel Production*. Oct. 2010, Energy Bioscience Institute Univ. of California Berkley.
16. Jonker, J., APC Faaij, *Techno-economic assessment of micro-algae as feedstock for renewable bio-energy production.* Applied Energy, 2013. **102**: p. 461-475.
17. Park, J., RJ Craggs, AN Shilton, *Waste Water treatment high rate algal ponds for biofuel production.* Bioresourse Technology, 2011. **102**: p. 35-42.
18. Czartoski, T., R Perkins, JL Villanueva, G Richards, *Algae Biomass Fractionation*, US2011/0086386A1, Editor. 2011.
19. Ou, L., R Thilakaratne, RC Brown, MM Wright, *Techno-economic analysis of transportation fuels from defatted microalgae via hydrothermal liquefactiona dn hydroprocessing.* Biomass and Bioenergy 2015. **72**: p. 45-54.
20. Carlson, L., MY Lee, C A E Oje, A Xu, *Algae to alkanes (Senior design report)*. 2010: University of Pennsylvania.
21. Harwell, L., S Thakkar, S Polcar,R Palmer, P Desai, *Study outlines optimum ULSD hydrotreater design.* Gas&Oil Journal July 28 and August 4, 2003, 2003.
22. Kubicka, D., L Kaluza, *Deoxygenation of vegetable oils over sulfided Ni, Mo and NiMo catalystss.* Applied Catalyusis A: General, 2010. **372**: p. 199-208.
23. Bryant, H., I Gogichaishvili, D Anderson, JW Richardson, J Sawyer, T Wickersham, ML Drewery, *The value of post-extracted algae residue.* Algal Research, 2012 **1**(2): p. 185.
24. Kadam, K., *Environmental implications of power generation via coal-microalgae cofiring.* Energy, 2002. **27**: p. 905-922.
25. Komline-Sanderson, *Personal communication*. 2014.
26. *The production and processing of marine oils* AOCS, Editor.
27. Kadam, K., *Microalgae Production from Power Plant Flue Gas: Environmental Implications on a Life Cycle Basis Rpt. NREL/TP-510-29417*. June 2001, NREL.
28. Inc., D.M., *Personal communication*. 2013.
29. Slaby, E., M Cici, J Messerich, *Algae as nutrition: needs of the feed markets*, in *ABO Summit*. 2012, Scoular Co.
30. *Global Market for EPA/DHA Omega-3 Products*, R. Packaged Facts, MD, Editor. 2012.
31. Report, *Global Market for EPA/DHA Omega-3 Products*. September 2012, Packaged Facts, 11200 Rockville Pike, Rockville, Maryland 20852.
32. http://www.algaeindustrymagazine.com/aim-interview-dr-isaac-berzin/.

33. Sturm, B., SL Lamer, *An energy evaluation of coupling nutrient removal from wastewater with algal biomass production.* Applied Energy, 2011. **88**: p. 3499-3506.
34. Pittman, J., AP Dean, O Osundeko, *The potential of sustainable algal biouel production using wastewater resources.* Bioresource Technology, 2011. **102**: p. 17-25.
35. Roberts, G., MP Fortier, BSM Sturm, SM Stagg-Williams, *Promising pathway for algal biofuels through wastewater cultivation and hydrothermal conversion.* Energy & Fuels, 2013. **27**: p. 857-867.
36. Olguín, E.J., *Dual purpose microalgae–bacteria-based systems that treat wastewater and produce biodiesel and chemical products within a Biorefinery.* Biotechnology Advances, 2012. **30**: p. 1031-1046.
37. Metcalf&Eddy, *Wastewater Engineering Treatment and Resource Recovery, Fithe Edition*, ed. G. Tcholbanoglous, HD Stensel, R Tsuchilhashi, F Burton: McGraw Hill.
38. *City of Sunnyvale California Waste Water Treatment Plant, personal communication*. 2012.
39. Manganaro, J., A Lawal, *Life-Cycle assessment of the production of algae based liquid fuel compared to crude oil to diesel process (to be submitted for publication).*

III. Life-Cycle Assessment of the Production of Algae Based Liquid Fuel Compared to Crude Oil to Diesel

III.1. Introduction

A major motivation, if not the central one, in considering renewables such as algae for liquid transportation fuels is reduction of greenhouse gas emissions, primarily CO2. The LCA provides a systematic approach for process evaluation. A good review, to which the reader is referred, of a number of prior LCAs of algae based processes is found in ref. [5]. LCA methodology as applied to biofuels is discussed in ref. [36]. An LCA analysis of an algae based process, more specific to Australia, for production of biodiesel rather than HTAO is given in ref. [37]. The present LCA, as contrasted with prior studies, is for production of a paraffinic hydrotreated algal oil with co-products and is highly focused only on CO2 emissions.

The methodology for LCA analysis has been outlined in International Standards Series ISO 14040. It consists of the following parts, ref. [38]:

1. Definition of goal and system boundaries
2. Life cycle inventory (LCI) analysis
3. Life cycle impact assessment (LCIA), and
4. Interpretation and improvement recommendations

III.2. Goal

The goal of this assessment is to compare the greenhouse gas emission from conventionally producing middle distillate (MD) from the atmospheric column of a refinery to producing an energetically equivalent quantity of hydrotreated algae oil (HTAO) by the process outlined in ref. [39]. Acknowledging that diesel fuel represents a further, but less than major, refinement to MD and HTAO, we make the assumption that MD and HTAO are essentially equivalent to diesel.

III.3. Scope

The scope of this analysis is limited to greenhouse gas (GHG) emissions from the two processes for MD and HTAO. Therefore, the inventory will be limited to CO2e emissions.

III.3.1. System Boundaries

Two processes are to be compared, namely: (1) the process to produce MD oil from conventional crude and (2) the process to produce HTAO. The process for MD would encompass extraction of crude oil from the ground or sea, transportation to the refinery, followed by upgrading in the refinery's atmospheric distillation column resulting in the middle distillate stream, see Figure 4.5a. The system boundary for production of HTAO is more complex and is shown in Figure 1b and given in more detail in ref.[39]. Both systems assume that the equipment for production of both MD and HTAO is already in place. Thus, the streams for fabricating the infrastructure are excluded from the analysis. The system end-points for MD is from well-to-tank, and that for HTAO is from pond-to-tank.

Figure 4.5a: System Boundary for Middle Distillate (diesel) Production

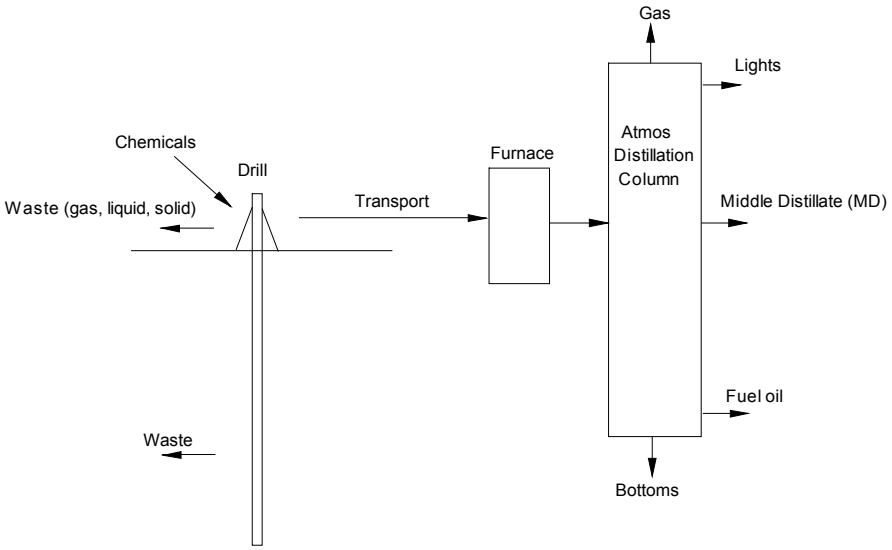

Figure 4.5b System Boundary for HTAO Production

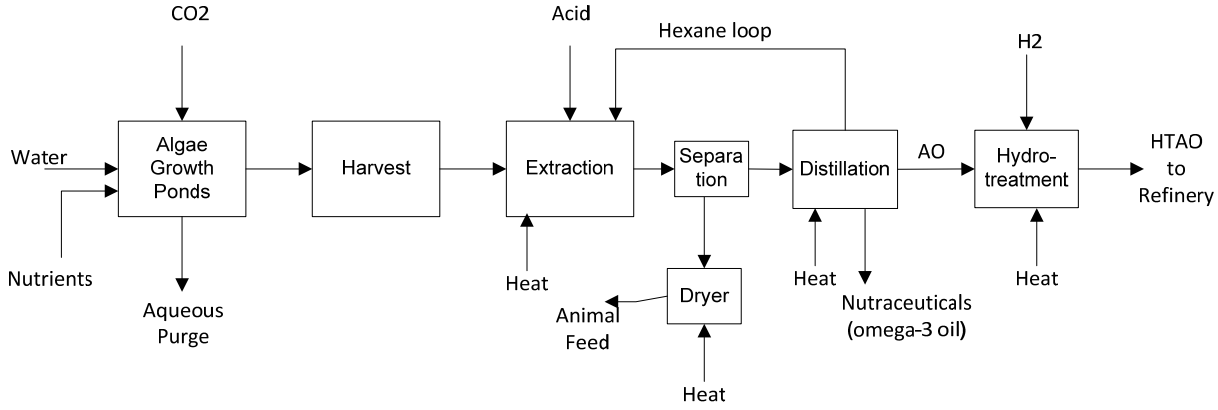

The process to produce HTAO, as discussed in ref. [39] and illustrated in abbreviated form in Figure 4.5b, consists of growing microalgae in ponds, harvesting the algae, extracting the algae oil (AO) with hexane, recycling hexane by distillation, followed by hydrotreating the extracted algae oil. The resultant HTAO is a paraffinic mixture of hydrocarbons which can be upgraded by blending with the middle distillate stream from the atmospheric column of a refinery. Refinery upgrading of MD and HTAO includes hydroisomerization and cracking to render the product more usable at cold temperatures. The algae process also produces co-products of animal feed and nutraceuticals.

III.3.2. Functional Unit

For direct comparison of the two processes, the functional unit is taken to be 1 MBTU (MBTU = million BTU) of energy value in the fuel oil. It is assumed that the heating value of MD and HTAO are equal. Thus, 1 bbl of either MD or HTAO contains 5.512 MBTU. In comparing HTAO to MD we have to account for HTAO co-products. From ref. [39] we have that the production of a quantity of HTAO equivalent to 1 MBTU will produce as co-products:

animal feed, T/MBTU 0.078

nutraceuticals, lb/MBTU 0.762

It will be seen later that a CO2 credit can be taken for not having to produce conventional animal feed.

III.3.3. Design Basis for HTAO Process

The design basis and assumptions for this discussion are:

1. Production rate of 1000 bbl/d of HTAO.
2. Land on which algae is grown is arid so that no adverse impact of CO2 uptake occurs by displacing existing vegetation.
3. Production of animal feed from post extracted algae residue (PEAR). All PEAR goes to animal feed.
4. Animal feed co-product of the HTAO process and soy meal feed are assumed equivalent
5. Production of nutraceuticals from a small portion of AO produced. This amount is taken to be 1.1% of the total AO stream. Emissions from the nutraceutical process are ignored as being equal to a conventional process.
6. On-stream time of 100%
7. CO2 for growth of algae is "pure" coming from a flue gas absorption/stripping process.
8. Utilities of the hydrotreater section are assumed negligible in comparison to the growth-harvest-extraction section.
9. Production of greenhouse gases other than CO2 is assumed negligible in the HTAO process, so that CO2 emission from the HTAO process can be compared with CO2 equivalent emissions (CO2e) from the MD process.
10. MD and HTAO are equivalent to diesel oil.
11. In the process to produce HTAO, we site the value of CO2e for raw materials such as H2, NH3, etc. as these are readily available from GREET. However, emissions for utilities (i.e., heat and electric) and also for the CO2 purification process we approximate CO2e with the CO2 value. Generally, the difference between CO2 and CO2e is on the order of 10%.

The greenhouse gases (GHG) are usually considered to be CO2, CH4 and N2O as well as "Criteria pollutants" which include VOC, CO, NOx, PM_{10}, $PM_{2.5}$, and SOx. When weighted by their respective contribution to global warming in aggregate are given the designation "CO2e", i.e., carbon dioxide equivalent or "GHG". The terms GHG and CO2e are synonymous and will be used interchangeably.

The GHG emissions from the production of MD have been rather extensively studied and therefore will produce a firmer estimate of CO2e as contrasted to the developing information on HTAO.

III.3.4. Green House Gas Emissions for producing MD

Reference [40] gives an estimate of GHG emissions reported as CO2e for producing diesel. The system boundary is from 'well-to-tank' which excludes the final actual use or burning of the MD. Reference [40] reports the following for the production of diesel for well-to-tank:

Table 4.18: Life Cycle GHG Emissions for Diesel (US 2005) from Figure ES-2 of ref. [40]

Life Cycle Stage	kg CO2e/MBTU
Raw material acquisition	6.6

Raw material transport	**1.3**
Liquid fuels production (refinery)	**9.5**
Product transport & refueling	**0.9**
Total	**18.3**

El-Houjeiri, et al [41] have shown that due to wide variability in field conditions, there can be considerable variation in the GHG emissions in the production of crude oil ranging from 3 to 17 kg CO2/MBTU. Their value doesn't include the refinery and product transport stages. The value in Table 4.18 for raw material acquisition and transport is 6.6 + 1.3 = 7.9 kg CO2/MBTU which is a median value compared to ref. [41].

Thus, to produce a quantity of MD from well to tank containing 1 MBTU, about 18.3 kg CO2e would be released to the atmosphere. This value is in rough agreement with the GHG value for conventional diesel from crude oil of 21.2 kg/MBTU given by the GREET model [42].

III.3.5. CO2 Emissions from HTAO Process

The calculation of CO2 emission from production of HTAO requires estimation of:
1. CO2 removed from atmosphere to grow the algae at the required high rates
2. CO2 emitted directly by the process (i.e., utilities- electric and heat)
3. CO2 emitted indirectly from purchased raw materials, such as CO2, H2 and nutrients, minus the CO2 credit that could be taken by displacing a certain amount of animal feed (soy meal) from external production.

III.3.5.1. CO2 Removal from the Atmosphere to Grow Algae

We first estimate the amount of CO2 removed from the atmosphere to grow enough algae to produce 1 MBTU worth of HTAO. This is calculated in a straight forward way from ref. [39] to be:

$$\text{Amount of CO2 removed from atmosphere by HTAO Process} = 224.4 \text{ kg / MBTU} \quad (4.6)$$

III.3.5.2. CO2 Direct Emission from HTAO Process

The amount of CO2 released directly to the atmosphere by the algal process to produce HTAO is estimated from the utility requirements (electric and heat) for the process. To do this calculation, estimates have to be made of the amount of CO2 released by electric and heat generation. For production of electricity the following CO2 emission rates are reported for different fuels [43], see Table 4.19a. We take an *average of ~ 0.75 kg CO2/KWH.* This value may be too high, as electricity is generated by other means beside fossil fuels, e.g., nuclear and hydroelectric.

Table 4.19a: CO2 Emissions for Electricity Generation

Fuel	kg of CO2 per KWHe
Coal	**~ 0.97**
Oil	**~ 0.77**
Natural Gas	**~ 0.55**

Where KWHe = KWH "electric" as distinguished from "KWHt" which is KWH "thermal".

Next, for burning fuels to produce heat we have the values listed in Table 4.19b, which suggests an approximate average *CO2 emission for burning fuel of 68.2 kg CO2/MBTU.*

Table 4.19b: CO2 Emission for Heat Generation

Fuel	kg CO2 per MBTU
Coal	~ 97.7
Oil	~ 72.7
Natural Gas	53.2

Detailed material and energy balances have been presented in ref. [39]. The data of that reference are used here to determine CO2 emissions. As mentioned, we have excluded the utility requirements of the hydrotreating section as being small compared to the utilities requirement of the algae growth, harvest and extraction section. An estimate of the utility usages for the growth-harvest-extraction section along with animal feed production is given in Table 4.20a. From Table 4.20a it is seen that 303.6 KWH of electric and 6.41 MBTU are required to produce 1.0 bbl of HTAO and co-products of animal feed and nutraceuticals.

Table 4.20a: Utility Usages and Direct CO2 Emissions for HTAO Production

Growth-harvest-extraction:			per MBTU of HTAO	
Electric requirement	KWH/bbl	KWH	kg CO2
Flow thru ponds	123.7	22.4	16.8
CO2 distribution & sparging	63.4	11.5	8.6
Dissolved air flotation	35.0	6.3	4.8
Centrifuge of algae	120.9	21.9	16.4
Contacting/Extraction	3.6	0.7	0.5
Centrifuge of biomass (PEAR)	19.6	3.5	2.7
Total	366.1	66.4	49.8
		per MBTU of HTAO	
Steam or Heat Requirment	MBTU/bbl	MBTU	kg CO2
Heat required for conditioning (strm8)	1.19	0.22	14.7
Heat req'ed for hexane distill'n (strm9)	1.12	0.20	13.9
Heat req'ed for wet biomass solids for animal feed(strm15b)	4.60	0.83	56.9
Total	6.91	1.25	85.5
Grand total direct kg CO2 emissions per MBTU for HTAO Process =			135.3

Putting the CO2 emissions on the basis of 1.0 MBTU of HTAO fuel, it is seen that total direct CO2 emissions are 135.3kg CO2 per MBTU of HTAO fuel.

II.3.5.3. Indirect CO2 Emissions

By "indirect" emissions we mean the emissions from the processes to produce the purchased raw materials or not produced directly but by associated processes. We group indirect CO2 emissions into two categories: (a) indirect emissions from purchased CO2, H2SO4 and H2 raw materials, and (b) indirect emissions from nutrients minus the CO2 credit for displaced animal feed (which is the ultimate fate of the nutrients).

Indirect CO2 Emissions from CO2, H2SO4 and H2 Raw Materials

Carbon dioxide is the major raw material for growing algae and will be found to constitute a significant CO2 emission. An estimate is now made of the emission factor for CO2, i.e., the amount of CO2 emitted to the atmosphere in manufacturing purified CO2. Two major processes for capture and recovery of CO2 appear in the literature, namely amines (chemical) and physical solvents. Selexol (UPO LLC) employs a physical process and is used at relatively high partial pressures of CO2 (>50 psig). The amines, such as monoethanolamine, are utilized at flue gas pressures. We assume the amine process. In this process CO2 is absorbed from the flue gas in monoethanolamine. The amine is then regenerated by heating to release the CO2. UPO LLC gives an approximate energy requirement, primarily for solvent regeneration, of 70,000 BTU per lb-mol of CO2 captured or 1590 BTU per lb of CO2 captured. Using 68.2 kg CO2 emission per MBTU of heat (see Table 4.19b) we have that:

$$\text{kg of CO2 Emission per lb CO2 Produced} = 68.2 * 0.00159 = 0.109 \text{ kg/lb} \quad (4.7)$$

This means that for 1 lb of CO2 captured, 0.24 lb of CO2 is emitted by the capture process. Or, in other words, the capture process for CO2 removes only 76% of the captured amount from the atmosphere.

Sulfuric acid is used in the conditioning step prior to hexane extraction of the AO. Hydrogen is used in the hydrotreating to remove oxygen from the AO, see Figure 4.5b. The usages, from ref. [39], and emission factors from the CO2 calculation above and from GREET are shown in Table 4.20b.

Table 4.20b: Raw Material Usages and their Indirect CO2 Emissions

					Emission	
			Usage		Factor	kg CO2e
Raw Materials		Units	Unit/bbl	lb/MBTU	kg CO2e/lb	per MBTU
CO2		lb	2865	519.8	0.109	56.4
H2SO4		lb	60	10.8	0.023	0.2
H2		lb	11	2.1	5.1	10.5
					Total =	67.1

For example, the GREET 2014 program indicates that the amount of CO2e produced from H2SO4 manufacture is 0.023 kg per lb of H2SO4 and for H2, the value is ~5.1 kg/lb of H2. The total CO2e indirect emissions from CO2, H2SO4 and H2 is estimated to be 67.1 kg CO2/MBTU of HTAO. The major contributor by far being the CO2 raw material.

Indirect CO2 Emissions from Nutrients minus CO2 Credit for Displaced Animal Feed

The nutrients used to grow algae are primarily nitrogen and phosphorous containing compounds, specifically NH3 and diammonium phosphate (DAP). Their usages have been calculated in ref. [39], see Table 4.20c.

Table 4.20c: Nutrient Usages and their Indirect CO2 Emissions

					Emission	
			Usage		Factor	kg CO2e
Nutrient Raw Materials		Units	Unit/bbl	lb/MBTU	kg CO2e/lb	per MBTU
neutrient: nitrogen as NH3		lb	154	28.0	1.23	34.5
neutrient: phosphate as DAP		lb	85	15.5	0.59	9.2
						43.6

For example, it is found from the GREET model that production of 1.0 lb of NH3 will generate 1.23 kg of GHG. Thus, NH3 will cause the emission of 26*1.23 = 31.9 kg of GHG per MBTU, etc. Therefore, *the total GHG indirect emissions from the use of the nutrients NH3 and DAP is 43.6 kg CO2e/MBTU contained in HTAO.*

Since animal feed is being made as co-product to the HTAO, it will displace such feeds as soy meal. Now, we determine how much CO2e is being saved by the co-production of animal feed in the algae process. From GREET 2014, it is found that 0.132 kg of GHG are generated per 1 lb of soy meal. From ref. [39], the amount of animal feed produced by the algae process is 0.46 T/bbl or 167 lb/MBTU. Therefore, the amount of GHG that would be displaced by the algae process is 167*0.132 = 22.0 kg of CO2e/MBTU.

Therefore, the net CO2e emissions due to the combination of nutrient use and soy meal displacement is about one-half of what the nutrient emission would have been without the co-product CO2 (animal feed) credit:

$$\text{Net CO2e emissions (nutrient\&animal feed)} = 43.6 - 22.0 = 21.6 \text{ kg CO2e / MBTU} \qquad (4.8)$$

The tacit assumption in this calculation is that the animal feed is not ultimately a source of biogenic CO2 emission, which after an indeterminate length of time it would be. However, biogenic CO2 from externally produced animal feed would anyway cancel that from the algae process.

The final calculation for the net emission of CO2 to the atmosphere of the HTAO process is shown in Table 4.21.

Table 4.21: CO2 Emission from the HTAO Process (Pond to Tank)

Item	Process Stage	Amount, kg CO2/MBTU
1	**CO2 removal from atmos. by algae growth**	**224.4**
2	**CO2 direct emission from HTAO process (utilities)**	**135.3**
3	**CO2 indirect emission from CO2, H2SO4 and H2**	**67.1**
4	**Net CO2 indirect emission from nutrients and animal feed co-product**	**21.6**
5	**Net emissions of CO2 from atmos. (items 2, 3 & 4 minus item 1)**	**-0.4**

From Table 4.21 it is seen that for the HTAO process, on a pond to tank basis, the net emissions of CO2 to the atmosphere is negative 0.3 kg CO2 per MBTU of HTAO produced, i.e. there is net consumption of CO2.

III.3.6. Summary of CO2 Emissions from HTAO Process

Table 4.22 gives a summary, in order of greatest to least, of contributors to CO2 emission from the HTAO process on a pond to tank basis. It is seen that purified CO2 and drying of animal feed are the greatest contributors to greenhouse gas emission, followed by ammonia as nutrient. Then follows a series of other smaller but significant contributors mostly but not entirely related to utilities. It is seen, as already shown, that this process emits -0.3 kg/CO2 per MBTU of HTAO produced.

Table 4.22: Summary of Contributors to CO2 Emissions from HTAO Process

Contributors in order of importance	kg CO2e per MBTU of HTAO
Heat req'ed for drying wet biomass solids for animal feed	56.9
CO2 (as raw material)	56.4
Nutrient: nitrogen as NH3 (raw material)	34.5
Flow thru ponds	16.8
Centrifuging of algae (harvest step)	16.4
Heat required for conditioning	14.7
Heat req'ed for hexane distill'n	13.9
H2 (raw material)	10.5
Nutrient: phosphate as DAP (raw material)	9.2
CO2 distribution & sparging	8.6
Disolved air flotation	4.8
Centrifuging of biomass (extraction step)	2.7
Contacting/Extraction	0.5
H2SO4 (raw material)	0.2
Hexane make up	*
Hydrogenation catalyst	*
Hydrotreatment utilities	*
* not included in calculation — sub tot.=	246.1
Credit for CO2 removed from atmosphere by algae	-224.5
CO2 credit for displacing animal feed	-22.0
Net CO2 emissions (pond to tank) =	-0.4

It is interesting to note that if 10% improvement is made in each of the myriad of contributors, CO2 emissions can be reduced by 24.6 kg CO2e/MBTU. This is a substantial improvement.

III.4. Comparison HTAO to Conventional Crude Oil Middle Distillate Process

The well or pond to wheels environmental impact of HTAO and MD produced from conventional crude oil refining are compared in Table 4.23 which shows the 'well or pond to wheels' values. By way of comparison to prior algae work, ref. [5] estimates WTW of 55.5 kg CO2e/MBTU for production of biodiesel from an algae route as compared to our estimate of 67.8 kg CO2/MBTU

for the HTAO process. Reference [5] also estimates WTW emission of 101 kg CO2e/MBTU for conventional low sulfur diesel as compared to our value in Table 6 of 86.5 for MD. Reference [37] estimates CO2e emissions of 18.2 g CO2e/ton-km which translates to 21.3 kg CO2e/MBTU, significantly less than our estimate for HTAO.

Table 4.23: Comparison of Emissions (WTW) from HTAO and Conventional Crude MD Processes

	Emission to Atmosphere, kg CO2e/MBTU	
Step	**HTAO Process**	**Conventional Crude to MD**
Process Emissions	**-0.4**	**18.3**
Burning fuel	**68.2**	**68.2**
Total, "well to wheels"	**67.8**	**86.5**

It is seen from Table 4.23 that the conventional crude oil to middle distillate process emits about 1.3 times more CO2e than the algae process. Or, we can say that HTAO will contribute to the atmosphere 18.7 kg CO2 per MBTU less than crude oil. If 10% of the US petroleum demand were replaced by algae oil, *this would cause a reduction of 210,000 tons per day of CO2 emissions.*

We believe the number quoted above for the HTAO process represent a worst case scenario. Clearly the drying of animal feed must be vastly improved. Also GREET 2014 quotes a WTP for conventional diesel of 21.3 rather than 18.3 kg CO2e/MBTU. If we say that animal feed drying can be improved to reduce CO2e emissions by half and use the GREET 2014 number for conventional diesel we are looking at a comparison of CO2e emissions from HTAO and conventional diesel of 39.4 and 89.4 kg/MBTU, respectively. *This implies a 56% reduction in CO2e emissions for the HTAO process.* Improvement in the recovery of purified CO2 will further accentuate the value of the HTAO process.

We must bear in mind that production of renewable fuels and most particularly algae derived fuel is in its very infancy. Comparing renewables to an industry which is well more than a century old is unfair. The HTAO process is at the threshold of a long development program.

III.5. Conclusions and Recommendations

1. The two major contributors to CO2 emissions from the HTAO process are animal feed drying and CO2 raw material.
2. HTAO contributes to the atmosphere 18.7 kg CO2 per MBTU less than crude oil. However if the drying process for animal feed can be made 50% more efficient the reduction of CO2e by the HTAO process would be about 50 kg/MBTU. This represents a more than 50% reduction in CO2e emission compared to the conventional diesel process.
3. Opportunities for major reduction of CO2e emissions in the algae to fuel process reside in:
    a. Moisture reduction of algae residue
    b. More efficient means of capturing purified CO2.
    c. Use of CO2 generated by the process itself.
    d. Possible solar drying of animal feed or fertilizer
    e. Consider anaerobic digestion of PEAR to generate methane and electricity with capture of CO2.
4. Explore more energy efficient ways of CO2 capture from flue gas or use of clean flue gas directly.

5. Do full LCA which would include the accounting for GHG emissions from the construction of equipment and ultimate decommissioning.
6. The process to produce HTAO is a complex one involving a myriad of steps. If each of the steps was improved by only 10% over present technology, CO2 emissions from the process would be reduced drastically.

III.6. Acknowledgements

A.Kalomoiri of Stevens Institute of Technology; D. Dieffenthaler, E. Frank, J Han, A.Elgowainy, J. Dunn of Argonne Nat. Lab; and D. Birkett of US EPA Region-2 Air Programs. We gratefully acknowledge that this work was funded by DOE contract DE-EE0006063.

III.7. References

1. Davis, R., A Aden, PT Pienkos, *Techno-economic analysis of autotrophic microalgae for fuel production.* Applied Energy, 2011. **88**: p. 3524-3531.
2. Demirbas, A., MF Demirbas, *Importance of algae oil as a source of biodiesel.* Energy Conversion and Management, 2011. **52**: p. 163-170.
3. Dunlop, E., AK Coaldrake, CS Silva, WD Seider, *An energy-limited model of algal biofuet production: toward the next generation of advanced biofuels.* AIChE Journal, 2013. **59**(12): p. 4641-4654.
4. Ferrell, J., V Sarisky-Reed, *National Algal Biofuels Technology Roadmap*. 2010, US Dept of Energy.
5. Frank, E., J Han, I Palou-Rivera, A Elgowainy, MQ Wang, *Life-cycle analysis of algal lipid fuels with the GREET model, Rpt. No. ANL/ESD/11-5*. 2011, Argonne National Laboratories: Argonne National Laboratories.
6. Stephenson, A., E Kazamia, JS Dennis, CJ Howe, *Life-cycle assessment of potential algal biodiesel production in the United Kingdom: a comparison of raceways and air-lift bioreactors.* Energy Fuels, 2010. **24**(4062-4077).
7. Sun, A., R Davis, M Starbuck, A Ben-Amotz, R Pate, PT Pienkos, *Comparative cost analysis of algal oil production for biofuels.* Energy, 2011. **36**: p. 5169-5179.
8. Benemann, J., WJ Oswald, *Systems and economic analysis of microalgae ponds for conversion of CO2 to biomass Final Rpt. to Dept. of Eng. Pittsburgh Eng. Tech. Center*. 1996.
9. Christi, Y., *Biodiesel from microalgae.* Biotechnology Advances, 2007. **25**: p. 294-306.
10. Brennan, L., P Owende, *Biofuels from microalgae—a review of technologies for production, processing, and extractions of biofuels and co-products.* Renewable and sustainable energy reviews, 2010. **14**(2): p. 557-577.
11. Davis, R., D Fishman, ED Frank, MS Wigmosta, A Aden, AM Coleman, PT Pienkos, RJ Skaggs, ER Venteris, MQ Wang, *Renewable diesel from algal lipids: An integrated baseline for cost, emission, and resource potential from a harmonized model; Rpt ANL/ESD/12-4*. 2012.
12. Richardson, J., JL Outlaw, M Allison, *The economics of microalgae oil.* AgBioForum, 2010. **13**(2): p. 119-130.
13. Park, J., RJ Craggs, AN Shilton, *Waste Water treatment high rate algal ponds for biofuel production.* Bioresourse Technology, 2011. **102**: p. 35-42.
14. Lundquist, T., IC Woertz, NWT Quinn, JR Benemann, *A Realistic Technology and Engineering Assessment of Algae Biofuel Production*. Oct. 2010, Energy Bioscience Institute Univ. of California Berkley.

15. Czartoski, T., R Perkins, JL Villanueva, G Richards, *Algae Biomass Fractionation*, US2011/0086386A1, Editor. 2011.
16. Ou, L., R Thilakaratne, RC Brown, MM Wright, *Techno-economic analysis of transportation fuels from defatted microalgae via hydrothermal liquefactiona dn hydroprocessing.* Biomass and Bioenergy 2015. **72**: p. 45-54.
17. Carlson, L., MY Lee, C A E Oje, A Xu, *Algae to alkanes (Senior design report)*. 2010: University of Pennsylvania.
18. Harwell, L., S Thakkar, S Polcar,R Palmer, P Desai, *Study outlines optimum ULSD hydrotreater design.* Gas&Oil Journal July 28 and August 4, 2003, 2003.
19. Kubicka, D., L Kaluza, *Deoxygenation of vegetable oils over sulfided Ni, Mo and NiMo catalystss.* Applied Catalyusis A: General, 2010. **372**: p. 199-208.
20. Bryant, H., I Gogichaishvili, D Anderson, JW Richardson, J Sawyer, T Wickersham, ML Drewery, *The value of post-extracted algae residue.* Algal Research, 2012 **1**(2): p. 185.
21. Jonker, J., APC Faaij, *Techno-economic assessment of micro-algae as feedstock for renewable bio-energy production.* Applied Energy, 2013. **102**: p. 461-475.
22. Kadam, K., *Environmental implications of power generation via coal-microalgae cofiring.* Energy, 2002. **27**: p. 905-922.
23. *The production and processing of marine oils* AOCS, Editor.
24. Levine, R., T Pinnarat, PE Savage, *Biodisel production from wet algal biomass through in situ lipid hydrolysis and supercritical transesterification.* Energy & Fuels, 2010. **24**: p. 5235-5243.
25. Levine, R., CO Sambolin Sierra, R Hockstad, W Obeid, PG Hatcher, PE Savage, *The use of hydrothermal carbonization to recycle nutrients in algal biofuel production.* Environ. Prog. & Sustainable Energy, 2013. **32**(4): p. 962-975.
26. Kadam, K., *Microalgae Production from Power Plant Flue Gas: Environmental Implications on a Life Cycle Basis Rpt. NREL/TP-510-29417*. June 2001, NREL.
27. Slaby, E., M Cici, J Messerich, *Algae as nutrition: needs of the feed markets*, in *ABO Summit*. 2012, Scoular Co.
28. Report, *Global Market for EPA/DHA Omega-3 Products*. September 2012, Packaged Facts, 11200 Rockville Pike, Rockville, Maryland 20852.
29. *Global Market for EPA/DHA Omega-3 Products*, R. Packaged Facts, MD, Editor. 2012.
30. Sturm, B., SL Lamer, *An energy evaluation of coupling nutrient removal from wastewater with algal biomass production.* Applied Energy, 2011. **88**: p. 3499-3506.
31. Pittman, J., AP Dean, O Osundeko, *The potential of sustainable algal biouel production using wastewater resources.* Bioresource Technology, 2011. **102**: p. 17-25.
32. Roberts, G., MP Fortier, BSM Sturm, SM Stagg-Williams, *Promising pathway for algal biofuels through wastewater cultivation and hydrothermal conversion.* Energy & Fuels, 2013. **27**: p. 857-867.
33. Olguín, E.J., *Dual purpose microalgae–bacteria-based systems that treat wastewater and produce biodiesel and chemical products within a Biorefinery.* Biotechnology Advances, 2012. **30**: p. 1031-1046.
34. Metcalf&Eddy, *Wastewater Engineering Treatment and Resource Recovery, Fithe Edition*, ed. G. Tcholbanoglous, HD Stensel, R Tsuchilhashi, F Burton: McGraw Hill.
35. Manganaro, J., A Lawal, *Life-Cycle assessment of the production of algae based liquid fuel compared to crude oil to diesel process (to be submitted for publication).*
36. Gnansounou, E., et al., *Life cycle assessment of biofuels: energy and greenhouse gas balances.* Bioresource technology, 2009. **100**(21): p. 4919-4930.
37. Campbell, P.K., T. Beer, and D. Batten, *Life cycle assessment of biodiesel production from microalgae in ponds.* Bioresource technology, 2011. **102**(1): p. 50-56.

38. Koroneos, C., EA Nanaki, *Life cycle environmental impact assessment of a solar water heater.* J. of Cleaner Production, 2012. **37**: p. 154-161.
39. Manganaro, J., A Lawal, B Goodall, *Techno-economic analysis of microalgae production and conversion into refinery ready oil with co-product credits.* submitted to Enviromental Science and Technology.
40. Skone, T., K Gerdes, *Development of Baseline Data and Analysis of Life Cycle Greenhouse Gas Emissions of Petroleum-Based Fuels Report DOE/NETL-2009/1346*. November 26, 2008.
41. El-Houjeiri, H., AR Brandt, JE Duffy, *Open-source LCA tool; for estimating greenhouse gas emissions from crude oil proudction using field characteristics.* Environ. Sci. Technology, 2013. **47**: p. 5998-6006.
42. v1.2.0.10917, G., Argonne National Lab.
43. *US Energy Information Admin.*, in http://www.eia.gov/tools/faqs/faq.cfm?id=74&t=11.

Task 5: Engaging & Securing a Petroleum Refinery Partner (Valicor & Stevens)

An important requirement by BETO for our award was the securing of a refinery partner by the end of project execution. From the onset of the project, Dr. Brian Goodall of Valicor began an effort to meet this requirement by engaging in preliminary discussions with a number of petroleum refiners. The most promising of this discussion occurred with Marathon Petroleum Corporation (MPC). Hence, it was followed up with three separate face-to-face meetings:

1. The first meeting took place in Dexter, MI at the headquarters of Valicor Renewables. In this meeting the project was presented and it received a high level of interest from the two MPC representatives (the two Commercial Development Managers of Biofuels and Emerging Technology). As a result of this meeting, MPC requested two further meetings involving visits to Valicor's algae cultivation partner (Qualitas Health) in Imperial, TX where they were growing Nannochloropsis Oculata and expanding to 64 acres of commercial production Q1 2014, and to the Stevens Institute of Technology in Hoboken, NJ to meet the PI, Prof. Adeniyi Lawal, and his team as well as to view Stevens facilities.
2. A full day visit (8/29/13) to the new algae farm in Imperial, TX where we viewed algae under active cultivation and harvesting as well as earthmoving and pond construction as the farm was being expanded to full commercial scale (64 acres of ponds under cultivation) of Nanno production for EPA (omega-3) in Q1 2014. They also got to spend 3 hours with the Founder and CTO of Qualitas Health, Isaac Berzin – one of the fathers of the current fuels from algae initiatives (he was a co-founder of Green Fuels in 2001 (http://web.mit.edu/erc/spotlights/alg.html), and in Time Magazine's Top 100 most influential people in 2008 (http://content.time.com/time/specials/2007/article/0,28804,1733748_1733754_1735703,00.html)). After the tour and discussions with our partner Isaac, the executives (having visited 14 other algae farms previously) stated that "for the first time" they "can visualize algae cultivation at scale" and "see algae oil being produced at cost-parity with fossil crude."
3. A full day visit on September 16, 2013 to the Stevens Institute of Technology in Hoboken, NJ where the two executives, and Valicor led by Brian Goodall (Co-PI) met with PI Prof. Adeniyi Lawal and his graduate students, a research associate, Dr. Jim Manganaro, Prof. Robert Farrauto (Co-PI, formerly of BASF Catalysts, LLC now a professor at Columbia), and Prof. George Korfiatis, Stevens Provost and University Vice President. In his opening welcome remark to the visitors, Prof. Korfiatis stressed that 'energy' is one of the focus areas that have been identified in the research component of the ten-year Strategic Plan of Stevens, and the algae-to-fuel project is recognized by Stevens as one of the key research initiatives on energy being undertaken at Stevens. There was also a tour of the lab featuring hydrotreating facilities, and analytical capabilities. The discussions centered around the project plan for a potential phase 2 collaboration, the collaborative structure of the project and identifying the best person at MPC for the technical interface.

As a result of all the foregoing effort, MPC began working on a letter expressing both their interest in the collaboration and the goal of testing the products coming out of the project to establish where best they could be inserted in their existing refinery infrastructure. Having both this letter, and guidance from MPC as to how to guide our future collaborative R&D initiatives on algae-to-fuel would be invaluable and would greatly increase the relevance of what we were doing as well as the chances of commercial success going forward.

By the end of the first quarter of FY2014, Marathon Petroleum Corporation (MPC) had officially agreed to become a partner on the project. Towards this end, a letter of commitment was secured from MPC and was appended to the quarterly report for first quarter of FY2014. MPC is the fourth largest refining company in the USA after ConocoPhillips, ExxonMobil, and Valero with 7 refineries and a capacity of 1,690,000 barrels-per-calendar-day (http://www.marathonpetroleum.com/About_MPC/).

To ensure that we would have sufficient quantities of algal oil for the next phase of the project, (Phase 2), we needed a guaranteed source of large volumes of biomass. To this end we secured a letter of commitment from a trusted algae cultivator (Valicor partner), Qualitas Health who would be producing roughly 4 tons of algae biomass per day starting Q3 2014, and was then producing 100 Kg's per week) (http://www.qualitas-health.com).

In the third quarter of FY2014, Marathon Petroleum Corporation (MPC) provided Stevens with about 5 gallons of unhydrotreated light atmospheric gas oil (LAGO) from their refinery distillation column. In the refinery, this stream upon hydrotreating (using conventional NiMo or CoMo catalyst) becomes the diesel product hence it is the most suitable stream for co-processing with algae oil, since the chemical species in this gas oil are similar to those present in algae oil. Also, the viscosity, and other physical properties are compatible with those of algae oil. This gas oil is miscible with algae oil as well as vegetable oils in practically relevant proportions. Mixtures of this gas oil and algae oil were successfully hydrotreated in the high throughput reactor system and the results are presented in details in Task 3 above.

6. Products Developed and Technology Transfer Activities

a. Publications

L. Zhou, and A. Lawal, "Evaluation of Presulfided NiMo/γ-Al_2O_3 for Hydrodeoxygenation of Microalgae Oil to Produce Green Diesel," *Energy & Fuels*, 29 (2014) 262 – 272.

L. Zhou, and A. Lawal, "Hydrodeoxygenation of Microalgae Oil to Green Diesel over Pt, Rh and NiMo," to be submitted April 2015.

Manganaro, J., A. Lawal, and B. Goodall, "Techno-economic Analysis of Microalgae Production and Conversion into Refinery Ready Oil with Co-Product Credits," Algal Research, revised version under review 2015.

Manganaro, J., and A. Lawal, "Life-Cycle Assessment of the Production of Algae Based Liquid Fuel Compared to Crude Oil to Diesel," to be submitted 2015

b. Web site or other Internet sites that reflect the results of this project

Not Applicable

c. Networks or collaborations fostered

This project has provided us the opportunity to develop important relationships that will be beneficial to the development of the next phase of the technology reported herein, a prelude to its eventual commercialization. By the first quarter of FY2014, we had secured a 'letter of intent' from Marathon Petroleum Corporation (MPC), the fourth largest petroleum refiner in the US, stating their intention to partner with us on this project and all subsequent phases until commercialization. This was a significant accomplishment in many ways. Most importantly, it has provided us access to a company with extensive practical experience in petroleum refining in general, and hydrotreating of petroleum distillates in particular. MPC supplied us with several gallons of light atmospheric gas oil (LAGO) which enabled us to co-process it with our algae oil. They also helped us in the selection of process parameters for the co-processing of the mixtures. Valicor and Stevens held a series of meetings with MPC personnel, and throughout the project we kept them apprised of the progress of the project.

In realization of the need for access to commercial quantities of algae oil for the future phases of our project, we forged a relationship with Qualitas Health Inc., a company heavily involved in commercial scale growth and harvesting of microalgae for production of nutraceuticals. Like MPC, Qualitas has also assured us of their commitment to this partnership and this was expressed in a 'letter of intent.' In addition to supplying microalgae biomass for oil extraction, discussions were regularly held with research staff (Sam Couture and David Hart) of Qualitas on microalgae growth. Our techno-economic analysis, especially those aspects pertaining to microalgae growth and harvesting, benefited tremendously from these discussions. Their contribution was reflected in the quality of our manuscripts on TEA and LCA of hydrotreating of algae oils.

Numerous studies have indicated that the economic viability of microalgae to biofuel will depend on the production of valuable co-products. Apart from nutraceuticals, animal feed is another important co-product of the algae to biofuel route and this is produced from the post extracted

algae residue (PEAR). In order for the PEAR to be competitive as a feedstock for animal feed, it has to meet some stringent requirements. In recognition of this important challenge, we approached Scoular Company, a company leader in the provision of diverse supply chain solutions for end-users and suppliers of grain, feed ingredients, and food ingredients to solicit their partnership in the next phase of our project, and they consented. Ms. Emilie Slaby is our contact person.

Our economic analysis of the hydrotreating of microalgae oils enabled us to identify parameters that are critical to the success of the enterprise. One of these parameters is the amount of energy that is required in de-watering of algae biomass. In an effort to minimize this energy, we investigated other options beside flocculation and centrifugation. We found out that Komline-Sanderson has extensive experience in the processing of biosolids, sludge, etc., experience that may be relevant to algae processing. Discussions were held with the company, principally with Jess Ornum and Kerry Kovacs, which culminated in a preliminary evaluation of one of their systems for de-watering of algae biomass. The results were promising. The microalgae biomass was provided by Dr. Jennifer Stewart, a Scientist at the College of Earth, Ocean and Environment, University of Delaware, DE, USA. Dr. Stewart was invited by Prof. Lawal, the project PI, as a seminar speaker at the Dept. of Chemical Engineering and Materials Science, Stevens Institute of Technology, Hoboken NJ. Dr. Stewart is a marine biologist with research interest in the development of commercial platforms for cultivating algal biomass based on understanding their unique biologies. This is a relationship that will further grow to collaboration between Delaware and Stevens. Another marine biologist, Prof. Paul Falkowski of Rutgers University, New Brunswick, NJ has agreed to work with us on the next phase of the project, bringing to bear his expertise on microalgae cultivation. Dr. Manganaro and the PI held a productive meeting with Prof. Falkowski at Rutgers on October 30, 2014.

d. Technologies/Techniques

Production of ‘green diesel’ via hydrotreating of microalgae oil

e. Inventions/Patent Applications, licensing agreements

Patent disclosure on the Pt-based bi-metallic catalyst under preparation

f. Other products –

Not Applicable